

ABSTRACT

Title of Dissertation: THE DYNAMICS OF DIUBIQUITIN
REVEALED BY NMR: WHAT IS THE
DRIVING FORCE BETWEEN THE OPEN
AND CLOSED STATES?

Ming-Yih Lai, Doctor of Philosophy, 2012

Directed By: Prof. David Fushman
Department of Chemistry and Biochemistry

The K48-linked polyubiquitin chains are important signals for proteasomal degradation and other biological processes. Their recognition of ubiquitin binding partners such as the UBA2 (ubiquitin associated domain 2) domain of hHR23a is via the canonical hydrophobic patch formed by L8, I44, and V70. In near physiological pH (pH 6.8), the K48-linked diubiquitin predominantly adopts the closed conformation in which the binding sites for ubiquitin-binding partners are buried in the inter-domain interface, and therefore are not available for binding. The K48-

linked diubiquitin also can adopt an open conformation at acidic pH. However, the mechanism of the transition between the open and closed states is poorly understood. This study is aimed at elucidating the driving force for the exchange between the open and closed conformations of K48-linked diubiquitin. Using different mutations of H68 in diubiquitin and NMR methods, I found that the protonation state of the histidine side chain is crucial for controlling the equilibrium between open and closed conformations. I also found that H68 is essential for maintaining the integrity of the inter-domain interface. I concluded that there are at least four interactions involved in controlling the transitions between open and closed states. These are point-to-point repulsion (strongest), point-to-bulk repulsion (medium), bulk-to-bulk repulsion (weakest), and hydrophobic interaction. Based on these results, I also proposed a pre-open state model for K48-linked diubiquitin which assumes that the closed conformation of Ub₂ opens by twisting instead of directly pulling two domains away from each other.

THE DYNAMICS OF DIUBIQUITIN REVEALED BY NMR: WHAT IS THE
DRIVING FORCE BETWEEN THE OPEN AND CLOSED STATES?

By

Ming-Yih Lai

Dissertation submitted to the Faculty of the Graduate School of the
University of Maryland, College Park, in partial fulfillment
of the requirements for the degree of
Doctor of Philosophy

2012

Advisory Committee:

Professor David Fushman, Chair

Professor Dorothy Beckett

Professor George Lorimer

Professor Nicole LaRonde-LeBlanc

Professor Jonathan D. Dinman

© Copyright by

[Ming-Yih Lai]

Acknowledgements

I would never have been able to finish my dissertation without the guidance of my committee members, help from lab members, and support from my family and wife.

I would like to express my deepest gratitude to my advisor, Prof. David Fushman, for his excellent guidance, caring, patience, and providing me with an excellent atmosphere for doing research.

I would like to deeply thank Mark Nakasone who patiently corrected my writing. He is always willing to help and give his best suggestions.

I would like to thank Daoning Zhang who helped me to set-up and troubleshooting the NMR experiments.

I would also like to thank Professor Dorothy Beckett, Professor George Lorimer, Professor Nicole LaRonde-LeBlanc, Professor Jonathan D. Dinman for being my committee members.

I would also like to thank my wife, parents and two daughters. They were always supporting me and encouraging me with their best wishes.

Finally, I would like to thank my wife, Chen-Yu Chen. She was always there cheering me up and stood by me through the good times and bad.

Table of Contents

Acknowledgements.....	ii
List of Abbreviations	v
List of Figures	vii
Chapter 1: Introduction	1
1.1 A brief history of ubiquitin	1
1.2 The ubiquitination process and its outcomes	1
1.3 Ubiquitination process	2
1.4 The Proteasome.....	3
1.4.1 The proteasome and its function	3
1.4.2 19S and 20S subunits of proteasome	4
1.4.3 The recognition of polyubiquitin by the proteasome.....	6
1.5 Functions related to proteasomal degradation	6
1.5.1 Cell cycle	6
1.5.2 ERAD (endoplasmic reticulum associated degradation) pathway.....	7
1.5.3 Control of transcription.....	8
1.6 Non-proteolytic roles of Ubiquitin.....	8
1.6.1 DNA Repair	9
1.7 Biological NMR techniques.....	11
1.7.1 The advantages of NMR techniques for biology studies	11
1.7.2 The need for stable isotope labeling of protein for NMR studies.....	12
1.7.3 Applications of NMR methods to my research.....	13
1.8 Specific aims	14
Chapter 2: Literature Review	16
2.1 Structures of Ub ₁ and K48-linked Ub ₂	16
2.1.1 Structures of Ub ₁	16
2.1.2 Structures of K48-linked Ub ₂	17
2.2 The interaction of K48-linked Ub ₂ and UBA2 at pH 6.8	19
Chapter 3: Methods.....	20
3.1 Protein expression and purification	20
3.1.1 Plasmid constructs, growth media and conditions.....	20
3.1.2 Purification of Ubiquitin	21
3.1.3 Synthesis and separation of Ub ₂ chains	22
3.1.4 Purification of UBA2 of hHR23a and E2-25K.....	23
3.1.5 Expression and Purification of E1	24
3.2 NMR Methods	25
3.2.1 Chemical shift perturbation (CSP) surface mapping	25
3.2.2 NMR pH titration experiments	26
3.2.3 NMR titration of UBA2 (hHR23a) with Ub ₁ and Ub ₂	28
3.3 Introduction to RDC and Relaxation NMR experiments.....	30
3.3.1 Residual Dipolar Coupling (RDC).....	31
3.3.2 NMR Spin relaxation experiments (R ₁ , R ₂).....	32
Chapter 4: Interaction between open state of Ub ₂ and UBA2	35
4.1 Introduction.....	35
4.2 Interaction of UBA2 and Ub ₁ at pH 4.5.....	37

4.3 Interaction of UBA2 and Ub ₂ at pH 4.5.....	38
4.4 Discussion.....	43
Chapter 5: Roles of H68 in conformation exchange in Ub ₂	46
5.1 Introduction.....	46
5.2 Monitoring the pKa of H68 and distribution of open and closed states in Ub ₁ and Ub ₂	47
5.2.1 Motivations.....	47
5.2.2 The distribution of open and closed states of Ub ₂ and the pKa of H68 in Ub ₁ and Ub ₂	48
5.2.3 Discussion.....	49
5.3 The effect of H68 mutations on open and closed states of Ub ₂	51
5.3.1 Introduction.....	51
5.3.2 H68A double mutant.....	52
5.3.3 H68V and H68L double mutants.....	53
5.3.4 H68F and H68Y double mutant.....	55
5.3.5 Relaxation data of H68Y double mutant.....	57
5.3.6 Interaction of H68Y and H68F double mutants with UBA2.....	58
5.4 The single-charge effect on open and closed conformations of Ub ₂	60
5.4.1 Introduction.....	60
5.4.2 Half H68Y mutants and the point-to-bulk charge repulsion.....	60
5.5 Exploring the salt effects on the half H68Y mutant and wild type of Ub ₂	63
5.5.1 Introduction.....	63
5.5.2 The salt effects on half H68Y mutant and wild type at 0.5 M and 1 M NaCl.....	63
5.6 The structure of half H68Y mutant Ub ₂ at pH 4.5 with 0.5 M NaCl.....	65
5.7 Summary.....	68
Chapter 6: The hydrogen-deuterium (H-D) exchange studies of Ub ₂ and Ub ₁ at pH5.5.....	70
6.1 Introduction.....	70
6.2 The results of H-D exchange at pH 5.5.....	71
Chapter 7: The dynamics of K48-linked Ub ₂ in an anchored form.....	73
7.1 Introduction.....	73
7.2 The results.....	74
Chapter 8: Studies of the most proximal domain in K48-linked Ub ₅ and of OTU1's binding surface on Ub ₂	78
8.1 The penta-ubiquitin (Ub ₅).....	78
8.2 Elucidating the OTU1 binding surface on Ub ₂	79
Chapter 9: Summary of my studies and future directions.....	80
Appendix.....	83
References.....	87

List of Abbreviations

Abbreviation	Full name	Page
ATP	Adenosine-5'-triphosphate	1
C12E5	Pentaethylene Glycol Monododecyl Ether	31
CDKs	Cyclin-Dependent Kinases	7
CP	Catalytic/Core Particle	3
CSP	Chemical shift perturbation	25
DNA	Deoxyribonucleic Acid	2
DNaseI	Deoxyribonuclease I	21
DUBs	Deubiquitining enzyme	1
E1	Ubiquitin-activating enzyme	1
E2	Ubiquitin-conjugating enzyme	1
E3	Ubiquitin-protein ligase	1
EGF	Epidermal Growth Factor	10
ER	Endoplasmic Reticulum	7
ERAD	Endoplasmic Reticulum Associated Degradation	7
GST	Glutathione S-transferase	23
HADDOCK	High Ambiguity Driven protein-protein DOCKing	32
HECT	Homologous to E6AP C-terminus	2
HMQC	Heteronuclear Multiple Quantum Coherence	24
HSQC	Heteronuclear Single Quantum Coherence	13
K _d	Disassociation Constants	12
MHC	Major-Histo-Compatibility	4

MW	Molecular weight	33
MWCO	Molecular Weight Cut Off	21
NMR	Nuclear Magnetic Resonance	11
NOE	Nuclear Overhauser Effect	30
PBDM	Protein Break Down Mix	22
PCNA	Proliferating Cell Nuclear Antigen	9
PDB	Protein Data Bank	16
PMSF	PhenylMethylSulfonyl Fluoride	21
Pru	Pleckstrin-like Receptor for Ubiquitin	6
RDC	Residual Dipolar Coupling	14
RP	Regulatory Particle	3
SOFAST	band-Selective Optimized Flip-Angle Short-Transient	24
ssDNA	Single Strand DNA	9
SDS-PAGE	Sodium Dodecyl Sulfate PolyacrylAmide Gel Electrophoresis	22
TCEP	3,3',3"-Phosphanetriyltripropanoic acid	22
TLCK	TosylLysine Chloromethyl Ketone Hydrochloride	21
Tris	2-Amino-2-hydroxymethyl-propane-1,3-diol	23
UBA	Ubiquitin-associated	6
UBL	Ubiquitin-like proteins	6
UIMs	Ubiquitin-interacting motifs	6
UPS	Ubiquitin-proteasome system	3

List of Figures

Fig 1.3.1 Ubiquitination of substrate	2
Fig 1.4.1 Structure of the 26S proteasome	5
Fig 1.7.1 The time scale of motions in proteins	12
Fig 2.1 The structure of monoubiquitin (PDB:1D3Z)	16
Fig 2.2 The CSPs in WT Ub ₂ compared to Ub ₁ at pH 4.5	17
Fig 2.3 The Ub ₂ structure of closed (PDB:1AAR) and open (3NS8)	17
Fig 2.4 (A) NMR model (PDB: 1ZO6) with the sandwich like binding mode	19
Fig 2.4 (B) The binding of Ub ₁ and UBA2	19
Fig 3.1.3 The scheme how the selective labeling on Ub ₂ is achieved	21
Fig 4.1(A) The structure of closed state Ub ₂ (PDB:1AAR)	36
Fig 4.1(B) The structure of open state Ub ₂ (PDB:3NS8)	36
Fig 4.1(C) The cartoon presentation of hHR23a	37
Fig 4.1(D) The sandwich binding mode PDB:1ZO6	37
Fig 4.2 NMR studies of the interaction of Ub ₁ and UBA2 at pH 4.5	38
Fig 4.3(A)-(F) NMR analysis of K48-linked Ub ₂ binding to UBA2 at pH 4.5	41
Fig 4.3 (G)(H) NMR analysis of UBA2 binding to K48-linked Ub ₂ at pH 4.5	42
Fig 5.1 The diagram of the side chain of histidine and its charge state	47
Fig 5.2.2 NMR of the signals of H68's side chain	49
Fig 5.3.2 The CSPs of Ub ₁ /Ub ₂ of H68A double mutant	53
Fig 5.3.3 The CSPs of Ub ₁ /Ub ₂ of H68V and H68L double mutant	54
Fig 5.3.4 The CSPs of Ub ₁ /Ub ₂ of H68F double mutant	56
Fig 5.3.5 The CSPs of Ub ₁ /Ub ₂ of H68Y double mutant in proximal	56

Fig 5.3.6 The CSPs of Ub ₁ /Ub ₂ of H68A double mutant in distal	57
Fig 5.3.7 R1 and R2 between H68Y double mutant and wild type Ub ₂	58
Fig 5.3.8 Titration results of H68F and H68Y double mutant	59
Fig 5.4.1 The CSP of Ub ₁ /Ub ₂ of distal half H68Y mutant (¹⁵ N proximal)	61
Fig 5.4.2 The CSP of Ub ₁ /Ub ₂ of distal half H68Y mutant (¹⁵ N distal)	61
Fig 5.4.3 The CSP of Ub ₁ /Ub ₂ of proximal half H68Y mutant (¹⁵ N proximal)	62
Fig 5.4.4 The CSP of Ub ₁ /Ub ₂ of proximal half H68Y mutant (¹⁵ N distal)	62
Fig 5.5.2 The CSP of Ub ₁ /Ub ₂ of proximal half H68Y mutant at high salt (¹⁵ N distal)	64
Fig 5.5.3 The CSP of Ub ₁ /Ub ₂ of proximal wild type Ub ₂ at high salt (¹⁵ N distal)	65
Fig 5.6.1 The NMR model of pre-open state	67
Fig 5.6.2 The proposed mechanism of opening the closed conformation of Ub ₂	67
Fig 6.1 The K48-linked Ub ₂ can be used as mimic of mono-ubiquitinated substrate (ubiquitin)	71
Fig 6.2 The result of H-D exchange	71
Fig 6.3 The residues affected by ubiquitination	72
Fig 7.2.1 The CSP of Ub ₁ /Ub ₃ -Distal labeled	74
Fig 7.2.2 The CSP of Ub ₂ /Ub ₃ Distal labeled	75
Fig 7.2.3 The CSP of Ub ₁ /Ub ₃ Proximal labeled	75
Fig 7.2.4 The CSP of Ub ₂ /Ub ₃ Proximal labeled	76
Fig 7.2.5 The CSP of Ub ₁ /Ub ₃ substrate labeled	76
Fig 7.2.6 Titration result between K48-linked Ub ₂ in an anchored form with UBA2	77

Fig 8.1 The CSP of Ub₁/Ub₅ at pH 6.8 79

Fig 8.2 NMR CSP maps of the human Otu1 binding interface on the two domains in
K48-linked Ub₂ 80

Chapter 1: Introduction

1.1 A brief history of ubiquitin

The concept of protein turnover in cells was originally discovered by Schoenheimer and coworkers in 1942 about 70 years ago [7]. However, the ubiquitin proteasome system underlying this process remained unknown until 1978 when Hershko and coworkers studied a heat-stable protein (APF-1) required for an ATP-dependent proteolytic system [8]. Ubiquitin, named after its nearly universal biological presence, is an 8.5 kDa protein originally identified as a thymus hormone in 1975. In 1980 Hershko and Irwin Rose verified that ubiquitin is covalently ligated to protein substrates in an ATP-dependent reaction [9, 10]. For “the discovery of ubiquitin-mediated protein degradation,” Hershko, Ciechanover, and Rose were awarded the 2004 Nobel Prize in chemistry. Since its discovery, the field of ubiquitin biology has grown considerably mainly due to the multiple signaling properties of ubiquitin.

1.2 The ubiquitination process and its outcomes

Ubiquitin (Ub) is a 76 residue protein that is highly conserved across all eukaryotes from yeast to humans with over 95% sequence identity. At some point in their life time most cellular proteins in eukaryotes are post-translationally modified by the addition of one or more ubiquitin(s) by the action of the E1, E2, and E3 enzyme cascade [11-14] (discussed in the next section). It is also important to note that ubiquitination is reversible and a special class of enzymes, the deubiquitinases

(DUBs) [15-17], can remove all or part of the ubiquitin modification. The ubiquitin modification is essential for cell survival and has been found in many important biological pathways, such as heat-shock response, DNA repair, mitosis, histone modification, and the immune system. Disruptions in ubiquitination have been implicated in many major human diseases. The most notable diseases are the neurodegenerative diseases (Alzheimer's & Parkinson's) and cancers.

1.3 Ubiquitination process

Ubiquitination results in the formation of an isopeptide bond between the carboxylic group of Gly76 and the ϵ -amino group of a Lys residue. This reaction is completed by the sequential actions of three enzymes (shown in **Fig 1.3.1**). First, ubiquitin-activating enzymes (E1s) use energy from ATP hydrolysis to form a thioester between the thiol group of the E1 active site cysteine and the carboxyl group of ubiquitin's G76. Second, ubiquitin is transferred to the ubiquitin-conjugating enzyme (E2) from E1 by transacylation to an active site cysteine in the E2 [11-14]. Last, ubiquitin ligase (E3) transfers the activated ubiquitin from the E2 to the substrate's lysine residue [18]. Once one ubiquitin is added to the lysine of a "substrate" protein, subsequent ubiquitins can be added at one of eight positions on the previously ligated ubiquitin.

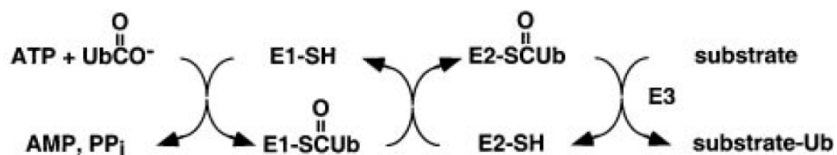


Fig 1.3.1 Ubiquitination of substrate occurs in a series of transthioesterification reactions. For HECT E3s, the final step involves an E3-ubiquitin thioester intermediate. (Ub=ubiquitin). The figure is from[5]

It has been shown that different ubiquitin-ubiquitin linkages in polyubiquitin chains produce distinct signaling outcomes, mainly attributed to the different conformations the chains can adopt. Eight ubiquitin-ubiquitin linkages through K6, K11, K27, K29, K33, K48, K63, and the N-terminal amine group of M1 [19, 20] have been found in nature. Depending on the linkage, the signaling outcome can be very different. For example, the K48-linked polyubiquitin chains are involved in proteasomal degradation; while the K63-linked polyubiquitin chains are involved in DNA repair [21-27].

1.4 The Proteasome

1.4.1 The proteasome and its function

The K48-linked polyubiquitinated substrates are recognized by receptors on the regulatory particle (RP) in proteasome and degraded by catalytic/core particle (CP) in the proteasome. The proteasome is a giant multi-subunit complex (over 2.5 MDa) for degrading proteins, such as misfolded proteins. The proteasome is an ATP-dependent and ubiquitin-dependent protease found in eukaryotic cytoplasm and nuclei. Its primary function is to degrade proteins that have been ubiquitinated by a cascade of enzymes known as E1, E2, and E3 enzymes [11-14]. The polyubiquitin chain is attached to a substrate via its carboxyl group of C-terminal glycine to an amine group of lysine side chain of the target protein. The ubiquitin-proteasome system (UPS) is the major cytosolic proteolytic system in eukaryotes. Unlike typical proteases which cleave randomly, the proteasome degrades substrates processively. This unique

feature results from its compartmentalized structure and substrate translocation mechanism. Processive protein degradation avoids generating truncated products which may compromise important cell functions. The proteasome does not degrade proteins to single amino acid [28]. Actually, the substrates are degraded into a heterogeneous mixture of peptides [29] which also can be used as raw material for adaptive cell-mediated immunity. For example, the degraded peptide products can be docked onto the major histo-compatibility (MHC) class I molecule, routed to the cell surface and recognized by cytotoxic T lymphocytes through epitope-specific T cell receptors. The UPS is involved in many critical functions in the cell such as cell cycle control, apoptosis, inflammation, transcription, signal transduction, and many other processes.

1.4.2 19S and 20S subunits of proteasome

The proteasome is composed of two major assemblies, the 20S and 19S subunits. The 20S subunit, also known as core or catalytic particle (CP), is a barrel-like structure whose 28 subunits are arranged in four heteroheptameric rings [30] (as shown in **Fig1.4.1**). Each inner ring is formed by β -type subunits. Three of them are proteolytic ($\beta 1$, $\beta 2$, and $\beta 5$) which can cleave a broad range of peptide sequences. Because the active sites face the interior space of the CP, the substrates must be directed into this space for degradation. Each outer ring is composed of 7 α -type subunits which create a series of seven pockets on the regulatory particle (RP). These pockets provide binding sites for the RP [31-33].

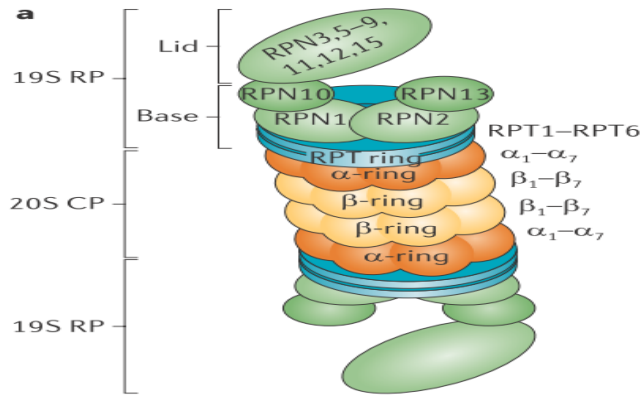


Fig 1.4.1 Structure of the 26S proteasome. The 26S proteasome composed of the core 20S catalytic particle (CP) and the 19S regulatory particle (RP). The substrate is bound via its polyubiquitin tag, to specific subunits in the 19S RP. The substrate is unfolded by ATPases in the base of the RP (the RPT ring) and then inserted its unfolded C-terminus via an open channel in the α -ring of the 20S CP into the proteolytic chamber. The RP also contains deubiquitylating enzymes that recycle ubiquitin. Figure from [2]

The substrate entry is controlled by the 19S subunit, also known as RP, which consists of 19 subunits. The 19S is docked on the cylinder end of the 20S [34] and creates a channel located centrally within the cylinder end. The 19S subunit not only opens a substrate translocation channel into the 20S but also guides substrates into this channel. The RP has also been further subdivided into the lid and base assemblies [35].

The ten components of the base are six ATPases, two scaffolding proteins (Rpn1 and Rpn2) and two polyubiquitin receptors (Rpn10 and Rpn13) [36-44]. The base is critical for RP-CP complex formation, as the C-termini of the base insert into the above-described α -subunit pockets on the CP [31-33]. The hexameric ATPase ring directs substrate unfolding and translocation into the CP [31-33, 45-48]. In addition, this ring also mediates opening of the CP gate.

There are 9 subunits in the RP lid. Rpn11 has DUB (deubiquitinating enzyme) activity which is critical for proteasome function [49-52]. Before being degraded, the

polyubiquitin chain is removed from substrates. This step in degradation is mediated primarily by Rpn11. Rpn11 removes polyubiquitin chains by cleaving the chains from proximal end of polyubiquitin chain [52]. The DUB activity of Rpn11 is ATP dependent and is coupled to substrate degradation. The proteasome also can recruit two nonessential DUBs, Uch37 and Usp14 (Ubp6 in yeast).

1.4.3 The recognition of polyubiquitin by the proteasome

There are five currently known conserved ubiquitin receptors associated with the proteasome. Rpn10 and Rpn13 are components of the proteasome. Rpn10 (22) recognizes ubiquitin through ubiquitin-interacting motifs (UIMs) consisting of a single α -helix [53]. Rpn13 binds ubiquitin via a pleckstrin homology domain known as the pleckstrin-like receptor for ubiquitin (Pru) domain. On the other hand, Rad23, Dsk2, and Ddi1 are “shuttle proteins” which are not subunits of the proteasome. The shuttle proteins bind the proteasome through their UBL (ubiquitin-like) domain and simultaneously interact with ubiquitin through an UBA (ubiquitin-associated) domain containing a bundle of three α -helices.

1.5 Functions related to proteasomal degradation

1.5.1 Cell cycle

As a molecular signal, ubiquitin is involved in many biological events, such as cell-cycle regulation, inflammatory response, and endocytosis. The positive and

negative regulators of the cell cycle, such as cyclins and inhibitors of cyclin-dependent kinases (CDKs), are crucial during cell cycle transitions. These regulators are also controlled by ubiquitination-induced degradation [54]. The eukaryotic cell cycle is driven by the various CDKs. The activities of CDKs are regulated by production and degradation of positive (cyclin) and negative (CDK inhibitors) regulatory subunits and by reversible phosphorylation. For example, the cyclins, which are specific for the G1 phase of the cell cycle, could accumulate and activate the corresponding CDKs during G1 phase. During the transition from G1 to S phase, the G1-specific cyclins will be targeted by their corresponding E3 ubiquitin ligases for degradation.

1.5.2 ERAD (endoplasmic reticulum associated degradation) pathway

The endoplasmic reticulum (ER) has two parts. The rough ER has many ribosomes to create proteins for the cell which are either used in the ER or sent to the Golgi apparatus for transportation. One of the functions of smooth ER is to remove toxins from the cell. In the ER quality control, the mutated proteins that misfold are targeted for degradation. A K48-linked polyUb chain will be attached to these abnormal proteins by the corresponding E3 ubiquitin ligase so that they can be degraded by proteasome. Not only abnormal proteins but also normal proteins such as 3-hydroxy-3-methylglutaryl-coenzyme A (HMG-CoA) reductase, which catalyzes the committed step in cholesterol biosynthesis, in the ER are also degraded via ERAD pathway in response to levels of metabolites of sterol synthesis. [55, 56]

1.5.3 Control of transcription

The UPS regulates transcription in different ways (reviewed in [57]) which can be categorized into degradative and nondegradative mechanisms. Although proteasomal degradation is largely distinct from transcription, the two processes are closely connected. Ubiquitin or small Ub-like modifier (SUMO) regulates transcription by controlling the nuclear localization and levels of transcriptional activators such as NF- κ B and p53. The NF- κ B (nuclear factor κ B) transcription factor functions as a dimer of NF- κ B proteins. Under the non-stimulated condition, NF- κ B proteins are hetero-dimerized into an inactive form by their inhibitor I κ B (inhibitory κ B). I κ B holds NF- κ B proteins in the cytoplasm. Cell stimulation can activate IKK (I κ B kinase). Once I κ B is phosphorylated by IKK, the phosphorylated I κ B can then be ubiquitinated by an E3 ubiquitin ligase and degraded by proteasome. In this way, NF- κ B is released and can enter the nucleus where it regulates the transcription of different classes of genes.

1.6 Non-proteolytic roles of Ubiquitin

The proteolytic roles of K48-linked polyUb chains are described in section 1.5. There are several new non-proteolytic roles of Ub that have been discovered. Non-proteolytic pathways are signaled by modification of a protein with a mono-Ub or K63-linked polyUb chain. This suggests that the fates of the substrate protein are dictated by the various linkages of polyUb chain.

1.6.1 DNA Repair

It is essential for cell to control DNA damage caused by endogenous and environmental agents to maintain the integrity of genome. Most DNA lesions can be removed by base excision repair and nucleotide excision repair mechanisms before DNA replication. If these pathways fail to remove the lesion before the S phase (DNA synthesis phase), replication forks accumulating at the sites of DNA damage will activate post-replication DNA repair pathways which allow DNA synthesis to restart without removing the lesion. Post-replicative repair pathways can occur through either 'error-free' mode that continues by a template switching process involving the undamaged sister chromatid, or by 'error prone' mode that proceeds by recruiting specialized DNA polymerases that read through the site of DNA lesion [58]. There are several genes required for post-replicative repair pathways such as Rad6, Rad18, Rad5, MMS2, and UBC13. Rad6 itself is an ubiquitin E2 conjugating enzyme whereas Mms2 and Ubc13 function as an E2 in a heterodimer to synthesize of K63-linked polyUb chains. Rad18 and Rad5 are ssDNA (single strand DNA) binding proteins proposed to function as E3 ligases because of the presence of signature RING finger domains. Ubiquitination of proliferating cell nuclear antigen (PCNA) is shown to be induced by DNA damage. PCNA is a trimeric ring-shaped complex that encircles DNA and functions as a sliding clamp and interacting factor for DNA polymerases. The 'error-free' mode is initiated by K63-linked polyubiquitination of PCNA via K164 of PCNA. On the other hand, the 'error-prone' mode initiated by monoubiquitination of PCNA is less efficient than K63-linked polyubiquitination of PCNA.

Protein trafficking: Ub is involved in several protein trafficking systems such as transporting proteins from the plasma membrane and the trans-Golgi network to the endosomal compartments [59]. Ub was also found to play an important role in sorting proteins to multivesicular bodies and the lysosomal compartments. Furthermore, the receptors on plasma membranes such as the G-protein coupled receptors and the epidermal growth factor (EGF) receptor require ubiquitination of these receptors for internalization. Although the role of Ub in the endocytic pathway is not yet fully understood, it has been suggested that the ubiquitinated transporting proteins could bind epsins (one of ubiquitin-binding proteins) through their UIM (Ub-interacting motif) and UBA (Ub-associated) domains. Epsins subsequently interact with the components of the endocytic machinery such as clathrin which would lead to the formation of multi-protein complexes required for efficient internalization of the membrane receptors.

Histone ubiquitination [22, 60-63]: Although core histones (such as H2A, H2B, and H3) and the linker histone (H1) were found to be monoubiquitylated, studies of histone ubiquitination were not prevailing because of the irrelevance to protein degradation. The finding that H2B is the only ubiquitinated histone in budding yeast made studies of genetics on histone ubiquitination more tractable. The C-terminus of H2B has been found to be monoubiquitylated at K123 residue. This part of C-terminus of H2B in yeast sticking out from the nucleosome makes it accessible for DNA and regulatory factors. The ubiquitination of H2A and H2B has been found to have a positive role in transcription. Along this line, the methylations of histone H3 is

also dependent on ubiquitination of H2B. Although the mechanism of ubiquitination-induced gene expression is not yet clearly understood, the methylations of histone H3 at K4 and K79 residues have been shown to play key roles in the regulation of gene expression.

1.7 Biological NMR techniques

1.7.1 The advantages of NMR techniques for biology studies

Nuclear magnetic resonance (NMR) spectroscopy is a very powerful technique that can be used for structure determination, molecular dynamics, and chemical kinetics. NMR can also be used to determine the structures of proteins in solution at atomic resolution that are as accurate as those determined by X-ray diffraction. Although protein structure determination by NMR is generally limited by size (to molecular weights less than 40-60 kDa) due to the spectral overcrowding and the intrinsically slow tumbling rate of large proteins, NMR techniques provide an alternative method for structure determination, which can help overcome some of common limitations of X-ray crystallography such as that the protein cannot be crystallized, or that there is concern that crystal packing has distorted the true structure in solution.

NMR spectroscopy can also be used to detect motion and dynamics in proteins. Other methods, like fluorescence spectroscopy, are restricted by the number of sites that can be probed and the limited time scale. The NMR resonance signals from individual observable nuclei provide a great amount of information on protein

dynamics. Furthermore, it is possible to characterize the dynamic properties over a wide range of time scales (from seconds to picoseconds) as illustrated in **Fig 1.7.1**. NMR is also useful in probing molecular interactions, such as protein-drug or protein-protein interactions. The binding site can be mapped by monitoring changes in NMR signals that occur for atoms involved in the interaction. In addition, the equilibrium dissociation constants (K_d) quantifying the strength of binding can also be measured.

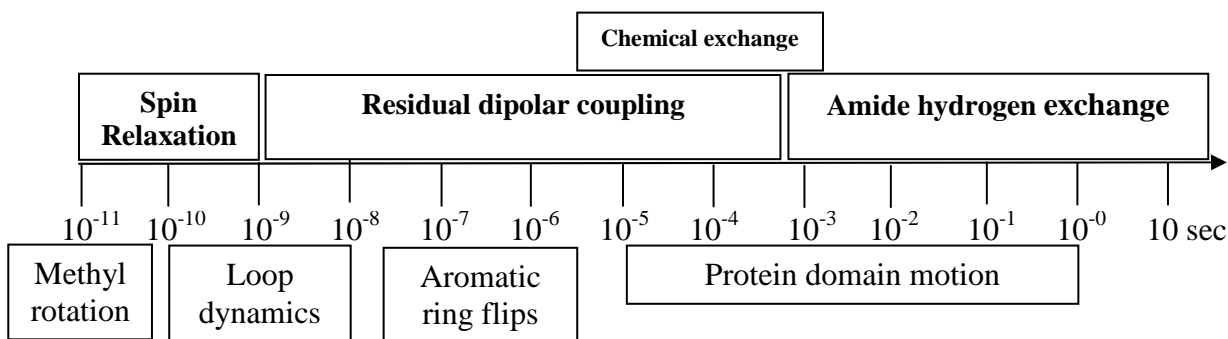


Fig 1.7.1 The time scale of motions in proteins are indicated below the axis and NMR techniques that can be used to characterize motion on the various time scales are shown above the axis.

1.7.2 The need for stable isotope labeling of protein for NMR studies

Proteins are mainly composed of hydrogen, carbon, nitrogen, oxygen, and sulfur atoms. In general, the useful NMR nuclei have spin quantum number $I = 1/2$ such as ^{15}N , ^{13}C , and ^1H , however the natural abundance of these isotope are 0.37%, 1.108% and 99.985% respectively. Although ^{14}N (natural abundance ~99%) and ^2H are NMR-active, they are quadrupolar nuclei ($I = 1$) and need to be treated differently from spin $1/2$ nuclei. Multi-dimensional NMR was a new major development of NMR techniques recently. There are thousands of hydrogens in an average protein and their signals span a relatively small range of about 12 ppm. In order to distinguish

signals from individual protons, multidimensional NMR experiments have to be introduced such as ^{15}N - ^1H HSQC (Heteronuclear Single Quantum Coherence) experiment. In order to acquire heteronuclear multi-dimensional NMR spectrum, proteins need to be ^{15}N and/or ^{13}C enriched by growing cells in minimal medium with corresponding isotope source. In this way, the protein can be uniformly labeled with ^{15}N (using $^{15}\text{NH}_4\text{Cl}$ as the sole source of nitrogen) and/or ^{13}C (using ^{13}C labeled glucose as the sole source of carbon).

1.7.3 Applications of NMR methods to my research

Each signal in ^1H - ^{15}N HSQC spectrum is a probe of N-H functional group in a protein. Every residue in a protein shows as a single signal in HSQC spectrum except prolines (no amide proton in the backbone for proline) and the first N-terminal residue (the amide proton exchanges rapidly with solvent). These amide signals are so sensitive to changes in local environment (such as hydrogen bonding, structural rearrangements, protein-ligand binding) around their nuclei that they can be used as reporters to pin-point the affected residues. In my research, I mapped the perturbations in chemical shift for each amide residue between the spectrum of ^{15}N -labeled Ub₁ and half-labeled Ub₂ (only one of the two domains is ^{15}N -labeled at a time). The hydrophobic patch on ubiquitin surface is composed of L8, I44, and V70. Almost all ubiquitin binding partners bind ubiquitin through this canonical hydrophobic patch. If the Ub₂ adopts closed conformation in which there is an inter-domain interface, the hydrophobic patch residues in the inter-domain interface will show perturbations in spectra of Ub₂ when compared to the spectra of Ub₁. On the

other hand, if the Ub₂ adopts an open conformation in which there is no inter-domain interface, the spectra of Ub₂ will show no perturbations for those inter-domain residues when compared to the spectra of Ub₁.

I also performed spin relaxation NMR experiments (R_1 , R_2) to study the dynamics of each residue in Ub₂ H68Y mutant at pH 6.8 (at this condition wild type Ub₂ adopts the closed conformation) and 4.5 (at this condition the wild type Ub₂ adopts an open conformation). The residual dipolar coupling (RDC) NMR experiments allowed me to calculate structural models of a Ub₂ mutant adopting a closed conformation at acidic pH with high salt. I will describe spin relaxation NMR and RDC experiments in more detail in chapter 3 materials and methods.

1.8 Specific aims

Although it had been shown that K48-linked Ub₂ binds to its binding partners, such as UBA2, in a sandwich-like mode at neutral pH [6], how UBA2 gets into the binding site of Ub₂ remains unknown. Most of K48-linked Ub₂ adopt closed conformation at neutral pH. The only way for UBA2 to bind K48-linked Ub₂ is through the open state of K48-linked Ub₂. I will test if the open conformation of K48-linked Ub₂ binds to UBA2 at acidic pH. I will perform titration of Ub₂/UBA2 and monitor it by NMR at acidic pH. The results and discussion are in chapter 4.

The K48-linked polyubiquitin chains are important signals for proteasomal degradation, and their recognition of ubiquitin binding partners is through the canonical hydrophobic patch formed by L8, I44, and V70. The K48-linked Ub₂ predominantly adopts the closed and open conformations at neutral and acidic

conditions, respectively. However, the mechanism of exchange between the open and closed conformations is still unknown. One of my aims is to study what is the driving force for opening the closed conformation. I introduced H68A, H68V, H68L, H68F and H68Y mutations in both ubiquitin domains of K48-linked Ub₂. The results and discussion are in chapter 5.

Many hypotheses proposed that ubiquitination promotes substrate unfolding, but experimental evidences are not clear. One of my aims is to use K48-linked Ub₂ as a model to test if the ubiquitination will undermine the stability of substrate by using NMR to monitor the H/D (Hydrogen/Deuterium) exchange rate. The result and discussion are in chapter 6.

The studies of free ubiquitin chains were done extensively but the study of K48-linked Ub₂ in an anchored form were neglected. One of my aims is to study the dynamics of K48-linked Ub₂ in an anchored form. I used ubiquitin mutant (L8A and I44A) as substrate because ubiquitin with simultaneous L8A and I44A mutations does not interact/form interface with another ubiquitin in an ubiquitin chain. The detail of this experiment and results are in chapter 7.

Chapter 2: Literature Review

2.1 Structures of Ub₁ and K48-linked Ub₂

2.1.1 Structures of Ub₁

The first structure of Ub₁ (PDB: 1UBQ) was determined in 1987 at 1.8 Å resolution by X-ray crystallographers Vijay-Kumar and Cook et al [64]. The structure showed that the ubiquitin is a compact and globular protein composed of five β-strands and one α-helix. One of the most important structural features of ubiquitin is that there is an extended hydrophobic surface flanked by the residues on the β-sheet (**Fig 2.1** PDB: 1D3Z). The study of alanine scanning mutations on ubiquitin surface residues shows that the residues on this hydrophobic surface and the C-terminal tail of ubiquitin are required for yeast cell viability [65]. The canonical hydrophobic patch, formed by residues L8, I44, and V70 shown in **Fig 2.1**, is important for proteasomal recognition. Almost all ubiquitin interacting and associated proteins bind to ubiquitin through this hydrophobic patch. I want to emphasize that H68 is located within this hydrophobic patch. There are 7 lysines on the ubiquitin surface.

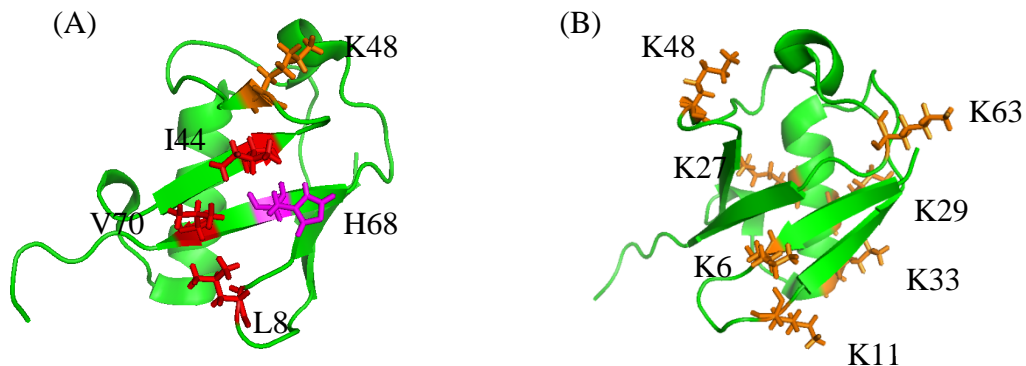


Fig 2.1 The structure of PDB: 1D3Z is shown in green. In (A) The residues show in red, orange or purple are hydrophobic patches (L8, I44 ad V70), K48, and H68 respectively. In (B) the residues colored in orange are all seven lysine residues on ubiquitin surface.

2.1.2 Structures of K48-linked Ub₂

In solution, the K48-linked Ub₂ can adopt closed and open conformations at neutral and acidic pH, respectively, based on NMR data as shown in **Fig 2.2** [1]. The X-ray crystal structure of Ub₂ (PDB: 1AAR) shown in **Fig 2.3 (A)** is in the closed state and this structure agrees well with the NMR data at neutral pH. This closed state structure provides a clear picture to understand the properties of Ub₂. The closed conformation of Ub₂ is an approximately 2-fold symmetric structure. The inter-domain interface is formed by the hydrophobic surface of each domain of Ub₂. The residues in the canonical hydrophobic patch (L8, I44, and V70) are buried at the interface, and hence not available for direct interactions with ubiquitin binding proteins. If this closed state, which is the predominant state in solution at neutral pH, the interaction between Ub₂ and ubiquitin-binding proteins will be hampered since the hydrophobic patches are sequestered. In fact, the open and closed conformations coexist and inter-convert in solution. Based on NMR data, 15% or less of Ub₂ adopts the open conformation at pH 6.8 [1].

Ironically, the crystal structure of the Ub₂ open conformation (PDB: 3NS8)[4], shown in **Fig 2.3 (B)**, was obtained at pH 7.5 whereas the crystal structure of the Ub₂ closed conformation structure (PDB: 1AAR), shown in **Fig 2.3 (A)**, was obtained at acidic pH (~4.5). Unlike the closed conformation, residues in the hydrophobic patch are exposed to solvent in the structure of the open conformation so that they are accessible to ubiquitin-binding proteins such as UBA2.

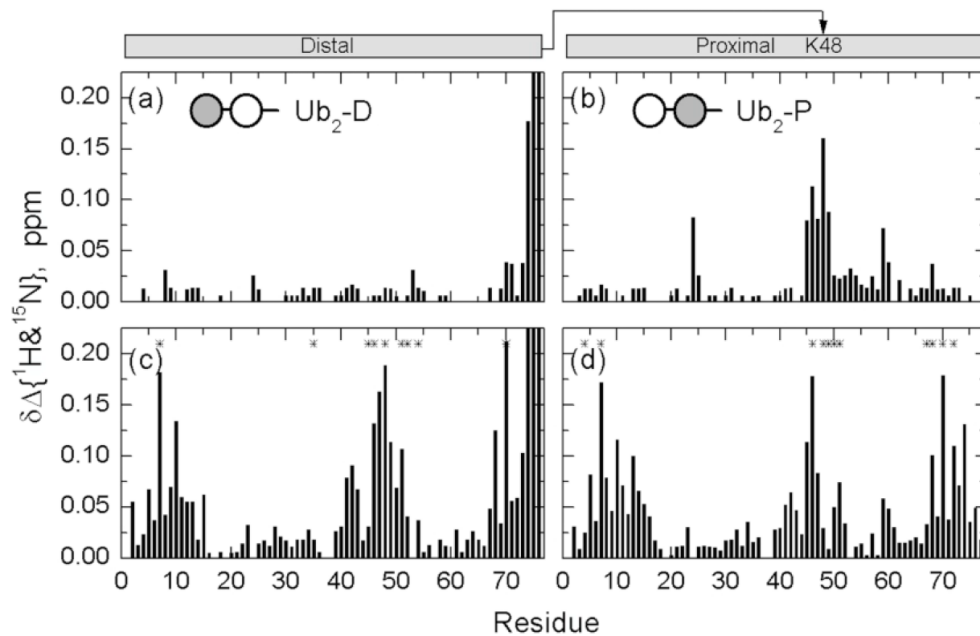


Fig 2.2 The CSPs in wild type Ub₂ compared to Ub₁ at pH 4.5 shown in (a), (b) and pH 6.8 shown in (c), (d). the Y axis represents combined amide CSP. X axis represents residue number. The figure was taken from [1].

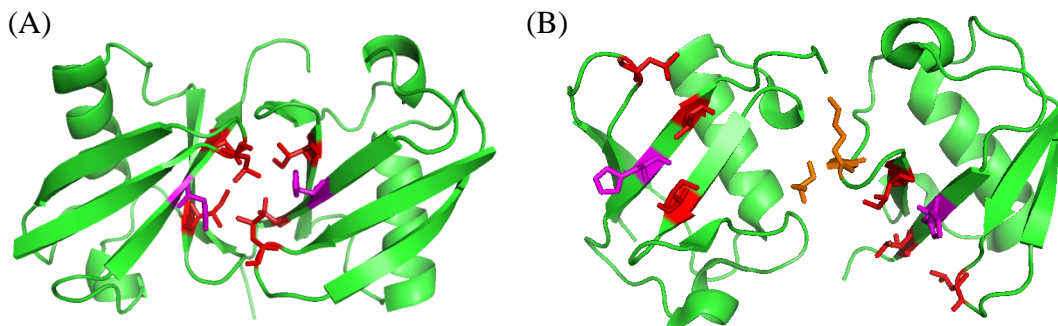


Fig 2.3 The Ub₂ structure of closed and open conformations shown in (A) and (B) respectively. (A) and (B) are the structures of PDB:1AAR and 3NS8, respectively. The residue H68 is colored in purple and the hydrophobic patch is colored in red.

2.2 The interaction of K48-linked Ub₂ and UBA2 at pH 6.8

K48-linked polyUb is an important signal for proteasomal degradation. It is believed that different linkages carry different signals. Some ubiquitin binding proteins are linkage specific, the documented examples include the selectivity of UBA2 of hHR23a for K48-linked polyUb [6] and the selectivity of the Rap80 for K63-linked polyUb [66]. UBA2 recognizes K48-linked polyUb chains in a “sandwich-like” binding mode. The dissociation constant K_d decreases from 400 ± 100 μ M (for Ub₁ and K63-linked Ub₂) to 18 ± 7 μ M (for K48-linked Ub₂) with the sandwich-like binding mode which is only available for K48-linked Ub₂. There are several important features of “the sandwich-like” binding mode. For example, the Ub-Ub linker region is involved in binding and the distal domain of Ub₂ shows a “lag phase” in binding for [UBA2]:[Ub₂] molar ratios less than 1. For UBA2, the sandwich like binding mode is clearly showed by the fact that the signals from two sides of UBA2 are perturbed simultaneously during titration.

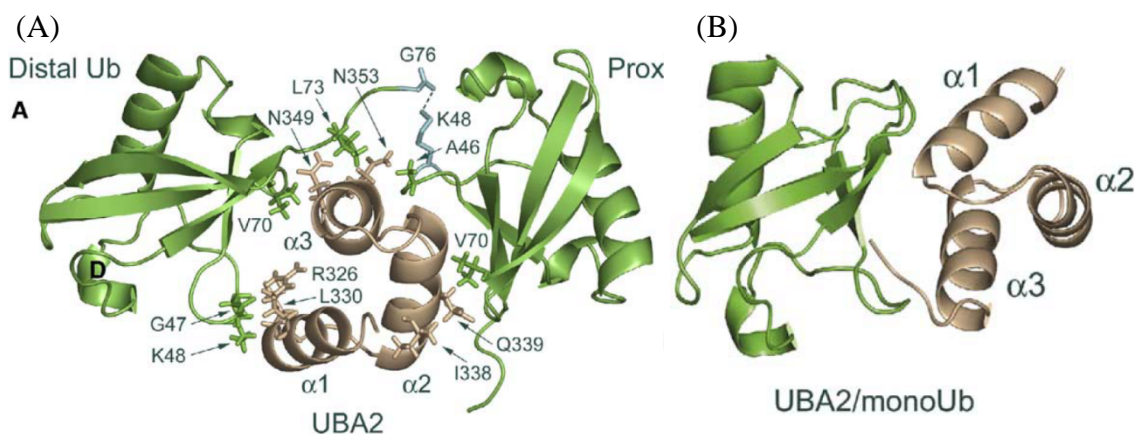


Fig 2.4 (A) represents the NMR-based structure model of UBA2 complex with K48-linked Ub₂ (PDB: 1ZO6) showing the sandwich-like binding mode. (B) represents the binding between Ub₁ and UBA2. The UBA2 is shown in brown. K48-linked Ub₂ and Ub₁ are shown in green. The figure is from [6].

Chapter 3: **Methods**

3.1 Protein expression and purification

3.1.1 Plasmid constructs, growth media and conditions

Plasmid constructs of all proteins used in this study were transformed into *E.coli* BL21(DE3) cells by heat shock. The plasmid constructs of K48R and D77 ubiquitin mutants (pET3a) and UBA2 (pGEX4-T2) were generously provided by Prof. Cecile Pickart (Johns Hopkins University). The additional H68A, H68V, H68L, H68F and H68Y mutations were introduced into K48R and D77 ubiquitin plasmid constructs separately by using Stratagene QuikChange™ Site-Directed Mutagenesis Kit. The final DNA plasmid construct of K48R+H68A, H68A+D77, K48R+H68V, H68V+D77, K48R+H68L, H68L+D77, K48R+H68F, H68F+D77, K48R+H68Y and H68Y+D77 were transformed separately into BL21(DE3) *E.coli* cells for protein over-expression.

Each 5mL starter culture with corresponding antibiotics was grown for 6-8 hours at 37°C to an O.D. 600 (optical density at 600nm wavelength) ~0.6 using single isolated colony from a fresh plate with the corresponding antibiotics. Cell culture for unlabelled protein was grown in the auto-inducing ZYP-5052 medium (contain 5g glycerol, 0.5g glucose(dextrose), 2g lactose, 10g tryptone, 5g yeast extract, 1mL of 1M MgSO₄•7H₂O, 3.3g (NH₄)₂SO₄, 6.8g KH₂PO₄, 7.1g Na₂HPO₄ per liter medium, pH adjusted by NaOH to 7.4) supplemented with ampicillin (100mg/L) and chloramphenicol (50 mg/L) at 37°C in a shaker incubator with continuous agitation at 220rpm overnight. For uniform ¹⁵N isotope incorporation in proteins, cell cultures

were grown in ZYP-5052 medium replacing $(\text{NH}_4)_2\text{SO}_4$ with $^{15}\text{NH}_4\text{Cl}$ (1 g/liter medium) and 2.84g Na_2SO_4 , such that $^{15}\text{NH}_4\text{Cl}$ provided the sole source of Nitrogen in the medium.

3.1.2 Purification of Ubiquitin

All cell pellets were frozen at -80°C for at least 30 minutes prior to lysis. Cells were resuspended in 30 mL lysis buffer (50 mM Tris pH 7.6, 0.02% Triton x100, 0.4 mg/mL lysozyme, protease inhibitors: 1 mM PMSF, 50 μM TLCK, 5 $\mu\text{g}/\text{mL}$ soybean trypsin inhibitor, 2.5 $\mu\text{g}/\text{mL}$ leupeptin, 20 $\mu\text{g}/\text{mL}$ DNaseI and 10 mM MgCl_2 were added to breakdown DNA) by pipetting the lysis buffer up and down. The cell suspension was centrifuged at 25,000 rpm for 25 minutes in an ultracentrifuge with a 45 Ti rotor. The supernatant was transferred to a 50 mL beaker on ice and stirred. 1~2% (v/v) undiluted 70% perchloric acid was added drop by drop to the supernatant. Most proteins except ubiquitin and lysozyme precipitated at this step. The milky solution was then ultra-centrifuged again at 25,000 rpm for 25 minutes in an ultracentrifuge with a 45 Ti rotor. The supernatant was dialyzed overnight at 4°C in 3 kDa MWCO (Molecular Weight Cut Off) dialysis tubing against 2 liters 50 mM ammonium acetate buffer at pH 4.5 overnight. The dialyzed sample was filtered by 0.45 μm syringe filter and then subjected to be purified by cation exchange chromatography on a 5 mL SP sepharose Fast Flow column (GE Healthcare). The column was pre-equilibrated with 50 mM ammonium acetate, pH 4.5, and ubiquitin was purified using a salt gradient (0%~20%B in 10 column volumes; the 1 mL/min flow rate; buffer A is 50 mM ammonium acetate and buffer B is 50mM ammonium acetate with 1M sodium chloride). The wild type ubiquitin and

other mutants were eluted around 14% buffer B. The purified protein was checked on a 15% sodium dodecyl sulfate (SDS) gel and concentrated using Amicon UF-4 centrifugal filter device with MWCO = 3 kDa and exchanged into the buffer (20mM sodium phosphate pH 6.8) used for most NMR experiments. Protein concentrations were determined by the absorbance at 280 nm ($\epsilon=0.16$ and 0.32 for 1 mg/mL for wild type and H68Y ubiquitin variant respectively) [67].

3.1.3 Synthesis and separation of Ub₂ chains

The segmental isotope labeling method was described by Pickart, C. M. [68]. I took advantage of ubiquitin K48R and D77 mutants served as blocks on distal and proximal domain of Ub₂ respectively to prevent from further elongation. K48-linked Ub₂ were synthesized through the E1/E2 reaction (1mM of each ubiquitin mutant, 2 mM ATP, 1 mM TCEP-HCl, 150 nM E1, 25 uM E2-25K and protein break down mix) in 50 mM Tris pH 8.0 buffer was incubated at 37°C for 4 hrs or 30°C overnight, I found that 30°C had a better yield. Protein break down mix (PBDM), an ATP regenerating system buffer, is composed of 5mM MgCl₂, 10 mM Creatine Phosphate, 1 U/mL Inorganic Phosphatase, 1 U/mL Creatine Phosphokinase.

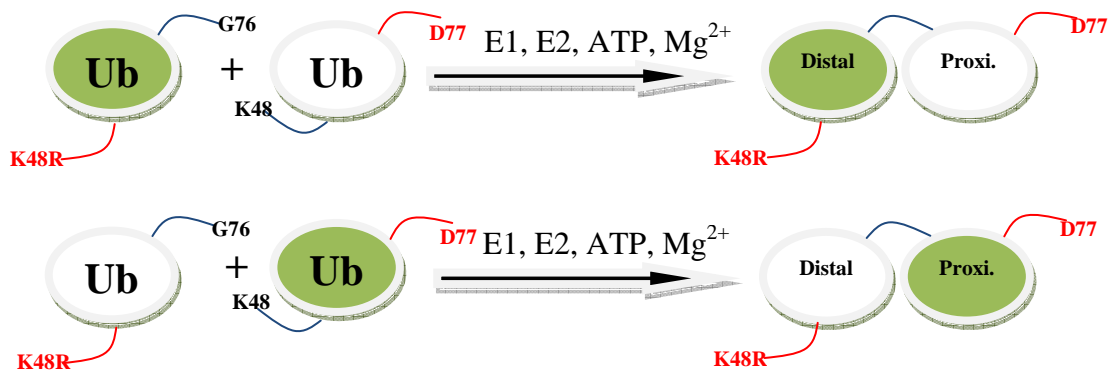


Fig 3.1.3 is the scheme which shows how the selective labeling on Ub₂ is achieved. The ubiquitins colored in green are ¹⁵N enriched ubiquitin (¹⁵N labeled) whereas the ubiquitins colored in white are ¹⁴N enriched ubiquitin (unlabeled). The carboxyl group of G76 from distal domain ubiquitin forms an isopeptide bond with the side chain of K48 from proximal domain ubiquitin by the help of E1, E2, ATP and cofactor Mg²⁺. The K48R and D77 mutations serve as the blocks to prevent further extension to higher polyubiquitin chains.

Ub₂ was then separated from Ub₁ using gel filtration column chromatography with 20 mM phosphate buffer at pH 6.8. Pure Ub₂ fractions were collected and verified by SDS-PAGE. If size exclusion column chromatography was not available, I separate Ub₂ from Ub₁ using a cation exchange column with step-gradient (Step I: 0%~15%B in 5 column volumes, Step II: 15%B for 5 column volumes, Step III: 15%~30% in 10 column volumes, buffer A and Buffer are the same as previously mentioned). Ub₂ usually is eluted in step III around 25~30%B.

3.1.4 Purification of UBA2 of hHR23a and E2-25K

Plasmids for GST-E2-25K (glutathione S-transferase-fused ubiquitin-conjugating enzyme E2-25K) and GST-UBA2 were generously provided by Prof. Cecile Pickart (Johns Hopkins University). E2-25k and UBA2 domain of hHR23A were expressed as GST-fused proteins in the media described above. Cell lysis was performed in PBS buffer, pH 7.4 complete with protease inhibitors, lysozyme and

Dnase I. The lysate was centrifuged and the soluble extract was filtered and loaded onto glutathione sepharose column pre-equilibrated with PBS buffer, pH 7.4. The unbound proteins were washed out with 6-8 column volumes of PBS buffer, and the fusion protein was eluted with 50 mM Tris pH 8.0, 10mM glutathione. GST-E2 was used as a fusion protein; however, the GST tag of UBA2 was cleaved using thrombin and separated UBA2 from GST tag protein by size exclusion column. The purity of the proteins was checked on 15% SDS polyacrylamide gels; GST-E2-25K and UBA2 were also concentrated using Amicon UF-4 centrifugal filter device and exchanged into their storage buffers (50 mM Tris pH 8.0 for GST-E2-25K, 20 mM phosphate pH 6.8 for UBA2). The protein concentrations were determined by absorbance at 280nm (for 1mg/mL concentrations, for UBA2 $\epsilon=0.198$, $\epsilon=1.7$ for GST-E2-25k).

3.1.5 Expression and Purification of E1

The plasmid construct of E1 used in ubiquitin dimer reactions was a gift from Prof. Cynthia Wolberger (Johns Hopkins University). The cells were streaked on a plate containing the antibiotics kanamycin (50 ug/mL, this antibiotic resistance is from the construct which is in pET28 vector) and chloramphenicol (50 ug/mL, this antibiotic resistance is from the Rosetta cells) and incubated at 37°C overnight. A single colony was inoculated in 5 mL LB as starter culture and incubated at 37°C overnight (~12 hrs). The starters were then transferred to a freshly prepared 1 L LB medium (pH 7.4 is adjusted by NaOH) and incubated at 37°C until O.D \approx 0.8. The culture was then induced with 1 mM IPTG at 20°C overnight. The cells were harvested and resuspended into lysis buffer (same as previously mentioned). The E1

was purified by using a nickel sepharose column. The purified E1 fraction was concentrated and exchange into 50 mM Tris pH 8.0 using an Amicon UF-4 centrifugal filter device.

3.2 NMR Methods

All NMR experiments were performed using standard pulse sequences on a Bruker 600 MHz spectrometer equipped with a cryoprobe. The sample temperature was 23°C. ^1H - ^{15}N correlation spectra such as SOFAST HMQC, spin relaxation experiments were acquired with the spectral widths of 7800 Hz and 2100 Hz for the ^1H and ^{15}N dimensions, respectively. A total of 256 t1 increments were collected with 2048 complex points in each. The spectra were processed using TopSpin (Bruker Biospin).

3.2.1 Chemical shift perturbation (CSP) surface mapping

The chemical shift perturbation surface mapping was used to map the interfaces between Ub domains of Ub₂. Backbone amide resonances in Ub₁ and individual Ub domains of Ub₂ were observed using ^1H - ^{15}N SOFAST HMQC. The combined amide CSP (chemical shift perturbation), $\Delta\delta_{\text{NH}}$, was calculated by **eq 1**.

$$\Delta^{(\text{D}),(\text{P})}\delta_{\text{NH}}^{(\text{pH } 4.5,6.8)} = \sqrt{\left(\text{Ub}_1\delta_{\text{H}}^{(\text{pH } 4.5,6.8)} - \text{Ub}_2^{(\text{D}),(\text{P})}\delta_{\text{H}}^{(\text{pH } 4.5,6.8)}\right)^2 + \left(\frac{\text{Ub}_1\delta_{\text{N}}^{(\text{pH } 4.5,6.8)} - \text{Ub}_2^{(\text{D}),(\text{P})}\delta_{\text{N}}^{(\text{pH } 4.5,6.8)}}{5}\right)^2}$$

eq (1)

in **eq (1)**, the $\delta_{\text{H}}^{(\text{pH } 4.5, 6.8)}$ and $\delta_{\text{N}}^{(\text{pH } 4.5, 6.8)}$ are the chemical shift (in proton and nitrogen respectively) of a signal in SOFAST HMQC spectra. The unit for combined amide CSP is ppm (part per million). The symbol of “Ub₂(D),(P)” in the upper left corner stands for distal or proximal domain of Ub₂. The symbol Ub₁ in the upper left corner stands for monoubiquitin.

The residues showing chemical shift perturbations are most likely to be involved in the formation of inter-domain interfaces in Ub₂. Because the NMR resonance signal from a nuclei is very sensitive to any change of its local chemical environment (such as protein binding, structural rearrangement). The temperature and the condition of solvent such as pH and salt also should be tightly controlled since any change of these parameters would contribute to the CSP. Bar graphs for each mutant were plotted using combined amide CSPs as y axis and sequential numbers of protein residues as x axis.

3.2.2 NMR pH titration experiments

To determine the pKa of the histidine side chain of Ub₁ and Ub₂, the combined ¹H-¹⁵N $\Delta\delta_{\text{NH}}$ was calculated using **eq (2)**. δ_{H} and δ_{N} are nitrogen and proton chemical shift respectively at particular pH. In **eq (3)**, “pH” stands for the pH condition of particular NMR sample. $\rho_{\text{protonated}}$ indicates the fraction of protonated histidine side chain. The pKa value can be determined by fitting pH and $\rho_{\text{protonated}}$ to **eq (3)**.

$$\Delta\delta_{\text{NH}} = \sqrt{(\delta_{\text{H}} - \delta_{\text{H}}^{\text{pH}7.6})^2 + \left(\frac{\delta_{\text{N}} - \delta_{\text{N}}^{\text{pH}7.6}}{5}\right)^2} \quad \text{eq (2)}$$

$$\Delta\delta_{\text{NH}}^{\text{total}} = \sqrt{(\delta_{\text{H}}^{\text{pH}2.8} - \delta_{\text{H}}^{\text{pH}7.6})^2 + \left(\frac{\delta_{\text{N}}^{\text{pH}2.8} - \delta_{\text{N}}^{\text{pH}7.6}}{5}\right)^2}$$

$$\frac{\Delta\delta_{\text{NH}}}{\Delta\delta_{\text{NH}}^{\text{total}}} = \rho_{\text{protonated}}$$

$$\rho_{\text{protonated}} + \rho_{\text{unprotonated}} = 1$$

$$pKa = pH - \log \frac{(\rho_{\text{unprotonated}})}{(\rho_{\text{protonated}})} \quad \text{eq (3)}$$

In the determination of the pH at which 50% of Ub₂ adopts open conformation, the combined CSP $\Delta\delta_{\text{NH}}$ between Ub₂ and Ub₁ at a particular pH was calculated using **eq (4)**. $\delta_{\text{H}}^{\text{Ub}1}$ and $\delta_{\text{N}}^{\text{Ub}1}$ are proton and nitrogen chemical shift respectively. ρ_{open} is fraction of Ub₂ at open state. The $pH_{50\% \text{ open}}$ can be determined by fitting the pH and ρ_{open} to **eq (5)**.

$$\Delta\delta_{\text{NH}} = \sqrt{(\delta_{\text{H}}^{\text{Ub}1} - \delta_{\text{H}}^{\text{Ub}2})^2 + \left(\frac{\delta_{\text{N}}^{\text{Ub}1} - \delta_{\text{N}}^{\text{Ub}2}}{5}\right)^2} \quad \text{eq (4)}$$

$$\Delta\delta_{\text{NH}}^{\text{total}} = \Delta\delta_{\text{NH}}^{\text{pH}7.6} - \Delta\delta_{\text{NH}}^{\text{pH}4.4}$$

$$\frac{\Delta\delta_{\text{NH}}}{\Delta\delta_{\text{NH}}^{\text{total}}} = \rho_{\text{closed}}$$

$$\rho_{\text{open}} + \rho_{\text{closed}} = 1$$

$$pH_{50\% \text{ open}} = pH - \log \frac{(\rho_{\text{closed}})}{(\rho_{\text{open}})} \quad \text{eq (5)}$$

3.2.3 NMR titration of UBA2 (hHR23a) with Ub₁ and Ub₂

For titrations performed at acidic pH, one of most difficult parts in this study is that the UBA2 is not stable (precipitates) at pH 4.5 at high protein concentration (2~5 mM). When the titration of ¹⁵N labeled Ub₁ or Ub₂ with unlabeled UBA2 was performed, the unlabeled UBA2 stock (2-5 mM) was prepared in 20 mM sodium phosphate buffer at pH 6.8. In total, 200 uL of UBA2 stock was added to the NMR sample of Ub₁ or Ub₂ which was prepared in 450 uL of 50 mM sodium acetate. A control experiment was performed (buffers contain no protein and ligand) to mimic the pH change upon adding 20 mM sodium phosphate to 50 mM sodium acetate to monitor any pH change upon titration. In this control experiment, verified by pH meter, the pH change upon adding 200 uL of 20 mM sodium phosphate buffer to 450 uL of 50 mM sodium acetate solution was very limited (at most 0.1 pH unit). The NMR spectra of Ub before and after the addition of the same amount (200 uL) of phosphate buffer alone (without UBA2) were almost identical. These control NMR experiments ensured that the changes in the spectra in the course of titrations were not from the change in the buffer. In the titrations of ¹⁵N UBA2 with unlabeled Ub₁ or Ub₂, all protein samples and stocks were prepared in the same buffer (50 mM sodium acetate, pH 4.5).

Solution of 0.5-1 mM ¹⁵N labeled Ub₂-distal and Ub₂-proximal samples were titrated with increasing amounts of an unlabeled UBA2 solution. Reverse titrations with ¹⁵N labeled UBA2 and unlabeled Ub₁ and Ub₂ were also performed in same way. The NMR titration experiments were performed as a series of ¹H-¹⁵N SOFAST HMQCs to monitor the binding of UBA2 to Ub₁ and Ub₂. Binding was monitored

through changes in the peak positions in the ^1H - ^{15}N SOFAST HMQC spectra.

Titration curves were continued until no or very little chemical shift changes were observed.

The binding affinities between UBA2 and Ub₁/Ub₂ were estimated from titration curves. The combined amide CSP $\Delta\delta_{\text{NH}}$ at particular titration point can be calculated using **eq (6)**.

$$\Delta\delta_{\text{NH}} = \sqrt{(\delta_{\text{H}} - \delta_{\text{H}}^{\text{free}})^2 + \left(\frac{\delta_{\text{N}} - \delta_{\text{N}}^{\text{free}}}{25}\right)^2} \quad \text{eq (6)}$$

$$\Delta\delta_{\text{NH}}^{\text{total}} = \sqrt{(\delta_{\text{H}}^{\text{fully-bound}} - \delta_{\text{H}}^{\text{free}})^2 + \left(\frac{\delta_{\text{N}}^{\text{fully-bound}} - \delta_{\text{N}}^{\text{free}}}{5}\right)^2}$$

$$\frac{\Delta\delta_{\text{NH}}}{\Delta\delta_{\text{NH}}^{\text{total}}} = \rho_{\text{bound}}$$

$$\rho_{\text{bound}} + \rho_{\text{free}} = 1$$

Here $\delta^{\text{fully-bound}}$ and δ^{free} are the chemical shifts corresponding to fully-bound (the end titration point) and free (no ligand added) states of the protein, respectively. δ_{H} and δ_{N} are proton and nitrogen chemical shifts, respectively, at a particular titration point. Since the combined amide CSP, $\Delta\delta_{\text{NH}}$, of Ub₂ proximal domain saturated at molar ratio = 1, it is reasonable to assume that the binding mode between UBA2 and Ub₂ is a 1:1 binding mode. In a 1:1 binding model,

$$\rho_{\text{bound}} = \frac{[\text{P}_t] + [\text{L}_t] + K_d - \sqrt{([\text{P}_t] + [\text{L}_t] + K_d)^2 - 4[\text{P}_t][\text{L}_t]}}{2[\text{P}_t]} \quad \text{eq (7)}$$

where $[P_t]$ and $[L_t]$ are the total molar concentrations of protein (^{15}N labeled Ub₁, Ub₂, or UBA2) and ligand (unlabeled Ub₁, Ub₂, or UBA2) respectively. The K_d is the apparent dissociation constant which can be determined by fitting **eq (7)**. Titration curves from residues showing a CSP of 0.1 ppm or greater were fit to **eq (7)** using an in-house program KdFit written in MATLAB [69]. For protein surface mapping upon ligand binding, the same method in section 3.2.1 was also used to map interaction surfaces between the UBA2 domain of hHR23A and Ub (Ub₁ and both distal and proximal domains of Ub₂). CSP bar graphs were plotted using combined amide CSPs. The residues showing broadening are indicated by long grey bars in the graph.

3.3 Introduction to RDC and Relaxation NMR experiments

The structures of Ub₂ and Ub₄ obtained from X-ray crystallography showed that the polyUb can adopt different conformations. This suggested that polyubiquitin chains are so flexible that the conformations observed in crystals could represent some bias due to lattice forces (crystal packing force). The conformations observed in the crystal structures represent only a small subset (or snapshots) of all the conformations that the chains could adopt in solution. The polyUb chain can adopt at least two conformations in solution from previous studies [1]. A comparison of the available solution and crystal structures of Ub₂ with Ub₁ shows the overall fold of each domain of Ub₂ is very similar to Ub₁. The residues showing structural rearrangement are involved in isopeptide bond linkage (the residues around K48 in

the proximal domain and the residues 72-76 in distal domain) and also those residues involved in forming inter-domain interactions if there are any.

The conventional NMR methods to determine structures of multi-domain proteins like Ub₂ or Ub₄ rely on the short distance constraints from NOEs (< 5 Å) observed by NMR. Structure determination of polyUb by NOE constraints is time-consuming. Two NMR approaches have been developed to provide long-range orientation information in large systems. It is reasonable to assume that there are no major structural rearrangements that occurred in both ubiquitin domains of Ub₂ on the RDC and relaxation time scale. Compared to traditional, NOE-based method, RDC and spin-relaxation are fast and simple methods for the determination of the relative orientation between distal and proximal domain.

3.3.1 Residual Dipolar Coupling (RDC)

The dipolar interaction between two nuclei in an external magnetic field is dependent on the angle of the inter-nuclear vector with respect to the external field. In isotropic solution, the protein tumbles freely so that the inter-nuclear vector in a protein samples all orientations with equal probability. Each dipolar interaction is averaged to zero in isotropic liquid. If the sampling of orientations is anisotropic, the protein will have some preferred orientations so that the dipolar interaction is not averaged to zero [40, 41]. In dilute liquid crystalline media (such as C12E5/hexanol), the measurable RDCs are about 0~25 Hz. The partial alignment of molecules in liquid crystals usually results from steric or electrostatic interactions between the molecules and the medium.

RDCs were measured in a weakly aligned liquid crystalline phase. The 2X stock of RDC medium was composed of 10% by weight polyethylene glycol PEG (C12E5) and n-hexanol (molar ratio 0.85). To prepare 150 uL 2X (10% Wt) RDC medium stock, 15 mg (mixture of PEG and hexanol) is required. PEG: 12.0384 uL, 1-n-hexanol: 4.18 uL, D2O: 10.5 uL [7%(v/v)D20], buffer: 124.5 uL are required to make 2X 150 uL RDC medium stock. The Ub₂ samples were added to 2X RDC medium stock in a 1:1 ratio (by volume) such that the final medium was a 5% C12E5 with 0.85 molar equivalents of n-hexanol [42]. The ¹⁵N-¹H IPAP-HSQC experiments [43] are performed to measure ¹H-¹⁵N couplings. Typically, 256 t1 increments were used. The RDCs were obtained from the difference in the ¹H-¹⁵N couplings observed in the buffer with aligned medium (anisotropic) and normal buffer (isotropic phase). The RDCs of each domain were used as restraints in HADDOCK 2.1 [70] structural calculations.

3.3.2 NMR Spin relaxation experiments (R_1 , R_2)

If the magnetic moment is rotated into the plane (x-y) perpendicular (90^0) to the applied field by means of a radio frequency pulse, the net nuclear spin magnetization in the z-direction $M_z(t)$ will relax back to its equilibrium value (M_0). This longitudinal relaxation is given the relationship:

$$M_z(t) = M_0(1 - e^{-R_1 t})$$

The net spin polarization is in the x-y plane transverse to the magnetic field of the spectrometer. This transverse magnetic moment will begin to relax towards zero because the precessing spins lose coherence with each other. This transverse relaxation is given by the relationship:

$$M_y(t) = M_0 \cos(\omega_0 t) e^{-R_2 t}$$

$$M_x(t) = M_0 \sin(\omega_0 t) e^{-R_2 t}$$

The unit for rate constant R is 1/second. ¹⁵N transverse and longitudinal (R_1) relaxation rate constants (R_1 and R_2) were obtained by least-square fitting of peak intensities in the corresponding series of 2D spectra to a single exponential decay.

$$I(t) = I_{(0)} e^{-Rt}$$

where $I_{(t)}$ is the intensity of a peak at a particular time t; R is the relaxation rate constant (R_1 or R_2). $I_{(0)}$ is the intensity of a peak at time t = 0. The 2D planes for these ¹⁵N relaxation experiments were acquired with the spectrum width 7.2 kHz and 2 kHz in the ¹H and ¹⁵N dimensions respectively. For each 2D plane, 128 increments in nitrogen were collected. Each increment consists of 1024 complex points.

¹⁵N longitudinal relaxation rates (R_1) are sensitive to the overall tumbling rate.

$$R_1 = 3d^2 \frac{S^2 \tau_c}{(1 + \omega^2 \tau_c^2)}$$

S^2 is the order parameter and d^2 is the dipolar contribution to R_1 . τ_c is the overall tumbling time of the protein. τ_c can be expressed by the Stokes-Einstein-Debye relationship,

$$\tau_c = \frac{\eta V}{kT}$$

η is the viscosity of the medium and V is the volume which is proportional to the molecular weight (MW) of the protein:

$$V = \rho * MW$$

where ρ is density. In general, the larger proteins have shorter R_1 and greater R_2 .

Chapter 4: Interaction between open state of Ub₂ and UBA2

4.1 Introduction

At near physiological pH (pH 6.8), the predominant conformation of K48-linked Ub₂ in solution is the closed conformation according to NMR studies [1]. The structures of Ub₂ in the closed conformation were first solved by X-ray crystallography (PDB:1AAR shown in **Fig 4.1(A)**) and also supported by NMR data [1]. The closed conformation is stabilized mainly by the inter-domain interface between distal and proximal domains [6]. This interface is mainly stabilized by the hydrophobic interaction between the hydrophobic patches (L8, I44, and V70) from both domains of Ub₂. Most ubiquitin interacting proteins bind to same hydrophobic patch. On the other hand, the predominant ensemble of Ub₂ structures in solution at acidic pH (pH 4.5) are open conformations in which no non-covalent inter-domain interaction between the two domains in Ub₂ was detected by NMR. The structures of Ub₂ in the open state were recently solved by X-ray crystallography such as PDB:3NS8 shown in **Fig 4.1(B)** [4] and PDB:3AUL [71]. It is important to verify if the open state of Ub₂ still preserves the ability to bind to ubiquitin interaction protein. I used one of ubiquitin interacting protein, UBA2 (Ubiquitin Associated 2), to study this.

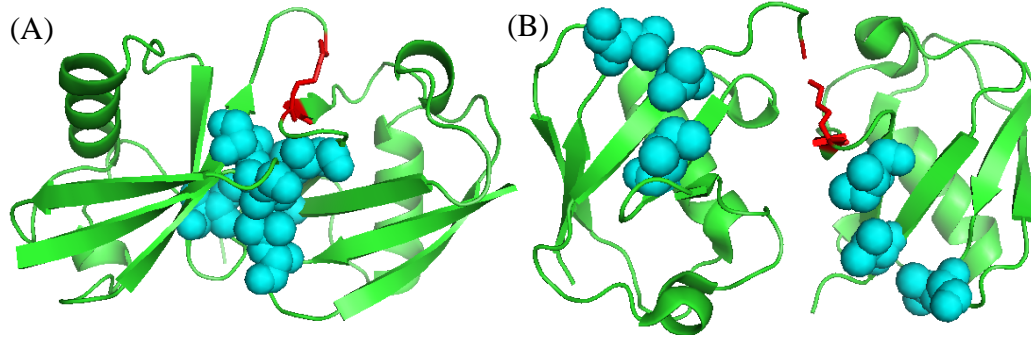


Fig 4.1 (A) shows the structure of the closed state Ub₂ (PDB:1AAR) [4]. (B) shows the structure of an open state Ub₂ (PDB:3NS8). L8, I44, and V70 are shown as cyan spheres. The linker region is shown as red stick.

UBA2 domain is a part of hHR23a (human Homolog of RAD23a) as shown in **Fig 4.1 (C)**. UBA2 binds preferentially to K48-linked polyubiquitin chains [6] and has a lower affinity to K63-linked polyUb [69]. hHR23a was originally identified as an important factor involved in the recognition of DNA lesions via its XPC domain and it was also found to play a central role in targeting ubiquitinated proteins for proteasomal degradation. It was found that hHR23a is capable of simultaneously binding the 26S proteasome and polyubiquitinated substrates via UBL and UBA domain, respectively. This allows hHR23a to deliver ubiquitinated proteins to the proteasome [6, 72-75]. The UBA2 was shown to bind Ub₂ in a sandwich-like mode at neutral pH. This sandwich binding mode is unique for K48-linked Ub₂ to interact with UBA2 as shown in **Fig 4.1 (D)**. Obviously, there are several interesting questions to ask. The first question is that whether if the Ub₂ is capable of binding UBA2 in the open state. The second question is if Ub₂ can bind UBA2 in a similar sandwich-like mode at acidic pH.

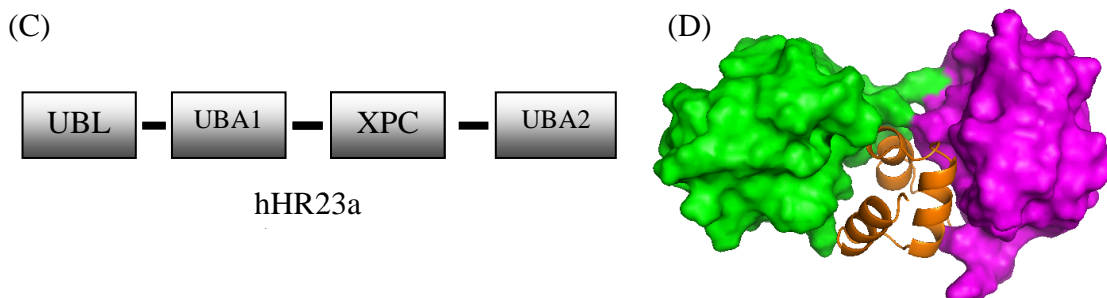


Fig 4.1 (C) is the cartoon presentation of hHR23a. UBL (Ubiquitin Like) domain is in the N-terminal of hHR23a. UBA1 is the first UBA domain after UBL domain. UBA2 is located in the C-terminal of hHR23a. XPC is the XPC binding domain. (D) is showing the sandwich binding mode from the NMR model of PDB:1ZO6. The distal and proximal domains are colored in green and magenta respectively. The UBA2 domain is shown in orange ribbon.

4.2 Interaction of UBA2 and Ub₁ at pH 4.5

Before characterizing the interaction between UBA2 and K48-linked Ub₂, I characterized the binding between UBA2 and Ub₁. The main reason for this experiment is that there is no study of the interaction between ubiquitin and UBA2 or other ubiquitin binding proteins at acidic pH to date. Second, is to confirm that the binding between UBA2 and Ub₂ is not affected by pH variations. This experiment served as a valuable control experiment to ensure that a change, if there is any, in Ub₂ binding to UBA2 is not caused by pH variation.

In order to observe proteins in NMR studies, ¹⁵N-NH₄Cl was introduced during protein expression to produce ¹⁵N enriched protein because the natural abundance of ¹⁵N is only 0.37%. All amide functional groups will be uniformly labeled with ¹⁵N. In the NMR titration studies, only one protein at a time is labeled to reduce the spectral complexity. In the ¹⁵N labeled Ub₁ titration with unlabeled UBA2 shown in **Fig 4.2 (A)**, it showed that Ub₁ is capable of binding UBA2 via its hydrophobic patch. In the ¹⁵N labeled UBA2 titration with unlabeled Ub₂ shown in **Fig 4.2 (B)**, the spectral perturbations observed involve the loop connecting helices 1 and 2 (residues 330-

332) and the N-terminus of helix 3 (residues 348-352) – the “canonical” Ub-binding surface on the UBAs [6, 69, 76-78]. After the titration data from UBA2 is analyzed with a one-to-one binding model, the interaction between UBA2 and Ub₁ is shown to be relatively weak (average $K_d = 215 \pm 35M$). This observed weak interaction between K48-linked Ub₂ and UBA2 at pH 4.5 is similar to what previously reported at neutral pH [69, 76]. All these results indicate that the Ub₁ and UBA2 interaction at pH 4.5 is similar to that at neutral pH.

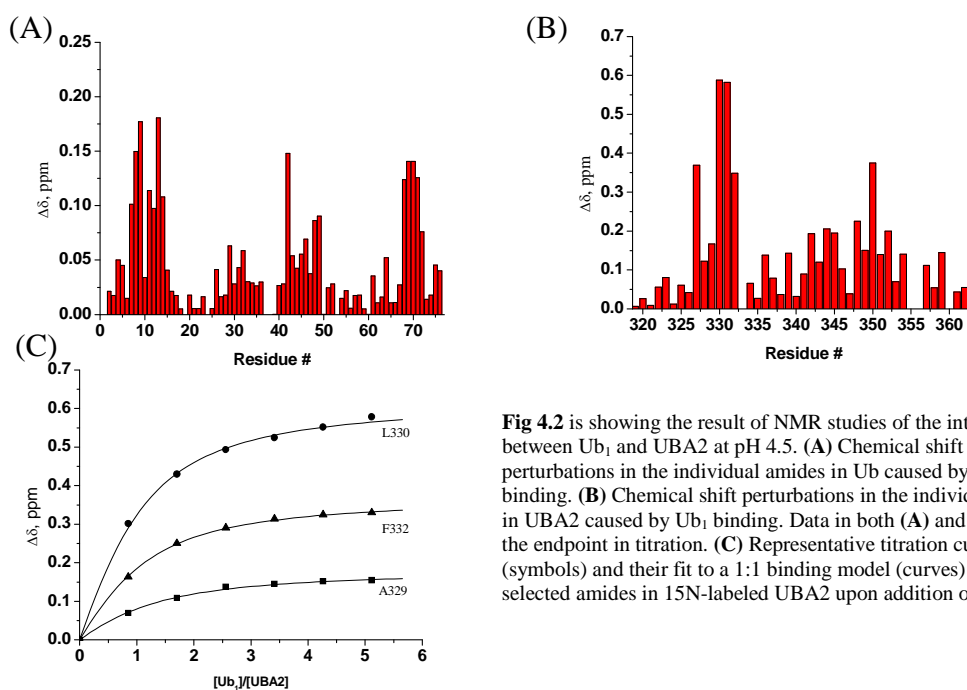


Fig 4.2 is showing the result of NMR studies of the interaction between Ub₁ and UBA2 at pH 4.5. **(A)** Chemical shift perturbations in the individual amides in Ub caused by UBA2 binding. **(B)** Chemical shift perturbations in the individual amides in UBA2 caused by Ub₁ binding. Data in both **(A)** and **(B)** are at the endpoint in titration. **(C)** Representative titration curves (symbols) and their fit to a 1:1 binding model (curves) for selected amides in ¹⁵N-labeled UBA2 upon addition of Ub₁.

4.3 Interaction of UBA2 and Ub₂ at pH 4.5

The UBA2 not only binds to K48-linked Ub₂ (natively adopts a closed conformation) but also binds to K63-linked Ub₂ (natively adopts an open conformation) at neutral pH. The interaction between UBA2 and K63-linked Ub₂ is much weaker than that between UBA2 and K48-linked Ub₂ because the binding sites

for UBA2 on K63-linked Ub₂ function as two independent binding sites whereas the binding sites for UBA2 on K48-linked Ub₂ function as a single binding site for UBA2. In order to elucidate the binding mode between the open conformation of K48-linked Ub₂ and UBA2, I performed NMR titration studies at pH 4.5 because K48-linked Ub₂ adopt open conformation predominantly. In order to reduce the spectral complexity, I synthesized Ub₂ which contains only one ¹⁵N labeled domain *in vitro* with E1 and E2-25K (see Section 3.1.3 for more detail).

The results of NMR titration studies of UBA2 and Ub₂ are summarized in **Fig 4.3 (A) - (E)**. Unlike UBA2 binding to Ub₁ (shown in **Fig 4.2 (A) - (C)** previously) and K63-linked Ub₂ [69], the distal and proximal domain behaved differently upon titration by adding unlabeled UBA2. The proximal domain showed spectral perturbations in the hydrophobic patch in early titration points ($[UBA2] / [Ub_2] = 0.1 \sim 1$). The CSPs from proximal domain saturated at the $[UBA2] / [Ub_2] = 1$. This suggests that UBA2 bind strongly to proximal domain with 1:1 stoichiometry. Although the K_d from fitting the stoichiometric binding curve is not reliable, it still provides a K_d value to compare with K_d from the UBA2-Ub₁ titration. Fitting the titration curves (**Fig. 4.3 (E)**) yielded K_d values in the micromolar range (1.3 ± 0.9 uM). The increase in the binding affinity for Ub₂ is at least two order of magnitude compared to Ub₁. Similar observations are also seen at neutral pH [6, 79]. This indicates that hHR23a UBA2 still retains its selectivity for the K48-linkage at acidic conditions. Unlike the proximal domain, the NMR titration studies of the distal domain showed very little changes at the beginning of titration. The CSPs of distal domain slowly increased upon adding unlabeled UBA2 to ¹⁵N distal domain labeled

Ub₂. The CSPs of distal domain do not reach saturation at the endpoint of titration ([UBA2] / [Ub₂] = 2.7). This suggests that UBA2 binding to the distal domain is significantly weaker than the binding to the proximal domain. Such differential UBA2 binding abilities for the distal and proximal domains in K48-linked Ub₂ is fully consistent with the observation at neutral conditions (pH 6.8) [6]. On top of that, the perturbation from NMR amide signal of the isopeptide saturated at [UBA2] / [Ub₂] = 1 (The isopeptide bond will be ¹⁵N labeled only if the proximal domain of Ub₂ is ¹⁵N labeled). This indicated that the linker between the distal and proximal domains is directly involved in UBA2 binding. Although the distal domain showed little perturbation in early titration steps, the signals in distal domain such as T7 and V70 attenuated in early titration points and the NMR amide signals from I44 and the C-terminal residues attenuated at end point ([UBA2] / [Ub₂] = 2.7).

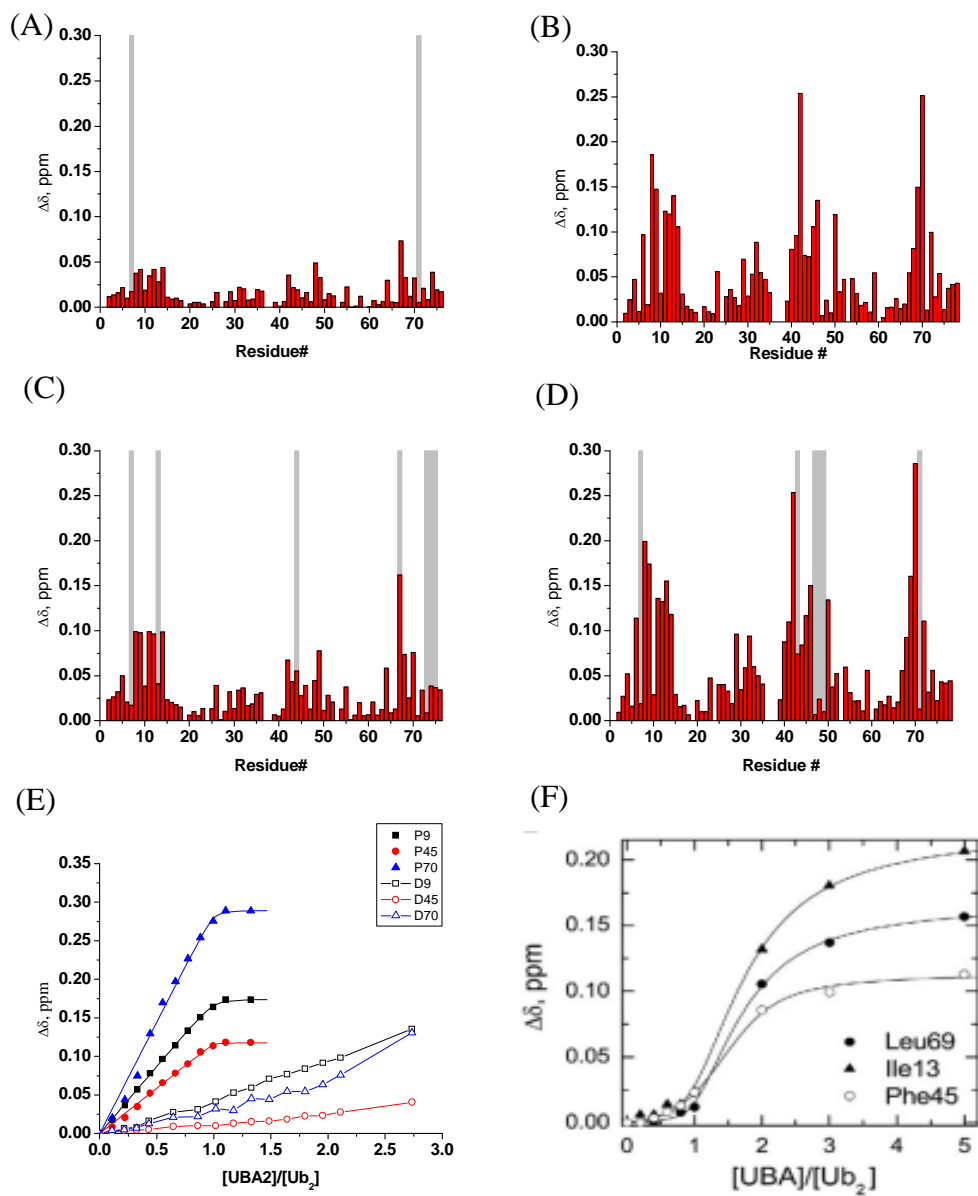
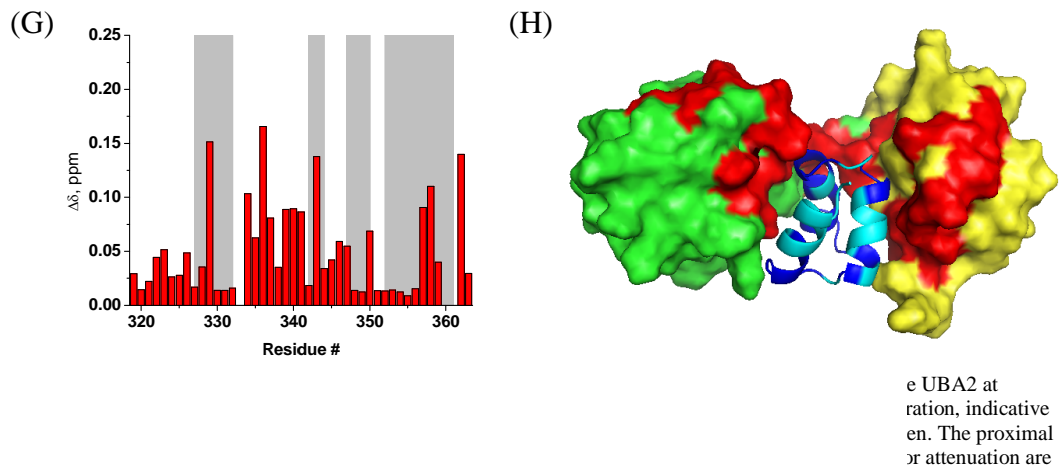


Fig 4.3 NMR analysis of K48-linked Ub₂ binding to UBA2 at pH 4.5. Spectral perturbations in backbone amides in the distal domain shown in (A) and (C) at [UBA2]/[Ub₂]=1 and 2.7 respectively. The spectral perturbations proximal domain shown in (B) and (D) at [UBA2]/[Ub₂]=1 and 1.32 respectively. (E) Representative binding curves for the proximal Ub (solid symbols) and the distal Ub (open symbols) upon UBA2 titration. The lines for the proximal-Ub data represent the results of fitting the data to a 1:1 binding model (assuming that binding to the distal Ub is negligible at these steps), while the lines for the distal data merely connect the data points. The dissociation constant for the proximal Ub obtained from this fit was $K_d = 1.6 \pm 0.9$ μ M (averaged over 11 residues). (F) is the titration curve of Ub₂ in distal domain at neutral pH [6].

I also monitored UBA2 domain binding by observing ^{15}N labeled UBA2. The NMR titration studies of ^{15}N -labeled UBA2 upon adding unlabeled Ub₁ stock suggest that there are more UBA2 residues affected compared to UBA2/Ub₁ binding. I found that there are strong signal attenuations in helix 2 located on the “backside” of UBA2. This pattern of binding is characteristic of the sandwich binding mode at neutral pH [6]. It is noteworthy that many UBA2 signals are significantly attenuated in early titration points ($[\text{Ub}_2] / [\text{UBA2}] = 0.2$). The signal broadening (or attenuation) in NMR is an indication of intermediate or slow exchange on the NMR time scale. The signal attenuations imply that the binding between UBA2 and Ub₂ has slow off-rates indicating tighter binding.



I also performed NMR spin-relaxation experiments to measure ^{15}N R_1 ($1/T_1$) and R_2 ($1/T_2$) which are sensitive indicators of the size of the complex. In general, the larger proteins tumble slower in solution and the smaller proteins tumble faster; this results in longer and shorter, respectively, longitudinal relaxation time T_1

whereas it is totally opposite for transverse relaxation time T_2 . The transverse relaxation time of amide protons ($^1\text{H } T_2$) showed a decrease from ~50 ms for free Ub_1 to 28.5 ms for the $\text{Ub}_1/\text{UBA2}$ complex. This agreed with the 1:1 stoichiometry of binding. In the NMR titration studies with ^{15}N UBA2, the $^1\text{H } T_2$ decreased from ~25 ms for free Ub_2 to 16.8 ms for $\text{UBA2}/\text{Ub}_2$ complex at the 1.1:1 molar ratio. This suggests that one UBA2 molecule is bound to Ub_2 at acidic pH. The longitudinal ^{15}N relaxation time (T_1) measured from the ^{15}N distal Ub_2 at the endpoint of titration ($[\text{UBA2}] / [\text{Ub}_2] = 2.7$) increased from 699 ± 38 ms (for the free Ub_2) to $T_1 = 961 \pm 49$ ms. The expected molecular weights of 1:1 and 2:1 UBA2: Ub_2 complexes are 23.2 and 29.2 kDa respectively. The T_1 measured at the endpoint of titration (molar ratio=2.7) is 961 ± 49 ms. The calculated molecular weight of the $\text{UBA2}/\text{Ub}_2$ complex from the T_1 is 26 ± 2 kDa [6]. This indicates that more than one UBA2 could bind Ub_2 at acidic pH. The second UBA2 binding to the distal domain of K48-linked Ub_2 was also observed in the previous NMR titration of $\text{Ub}_2/\text{UBA2}$ at neutral pH [6].

4.4 Discussion

First, I showed that the interaction of $\text{UBA2}-\text{Ub}_1$ at acidic pH is similar to that at neutral pH. Ubiquitin is very stable from pH 2 to 10, however UBA2 seems to be unstable at acidic pH. I originally thought that the interaction may be affected by the change in pH (from 6.8 to 4.5). I was surprised that the change in pH (more than two pH units) does not significantly change the interaction of UBA2 with Ub_1 . This result may reveal that the interaction between UBA2 and Ub_1 is mainly a hydrophobic interaction which is also not greatly affected by change in pH. This finding also

allows me to explore the interaction of UBA2-Ub₂ without worrying about the effect from pH change.

The structures of K48-linked Ub₂ determined by X-ray crystallography at pH 7.5 and pH 4.5 represent open and closed conformations, respectively [80]. Ironically, the predominant conformations of K48-linked Ub₂ in solution at neutral and acidic pH are closed and open conformations, respectively, as shown by NMR [1]. Although the structures of K48-linked Ub₂ determined by X-ray and NMR at similar pH show different conformations, the closed conformation of Ub₂ by X-ray at acidic pH agrees well with the one at neutral pH by NMR. The intrinsic flexibility of Ub₂ allows it to adopt two states at the same pH in solution. It is also reasonable to treat the open conformation observed in the crystal structure as a single snapshot from the ensemble of probably many open conformations. From the open-conformation X-ray structure, it appears that the Ub hydrophobic patch is exposed to the solvent and available for binding to any ubiquitin binding protein.

I also showed that the open state of K48-linked Ub₂ is capable of binding the UBA2 domain of hHR23a in a similar sandwich-like mode as the closed state. Also the binding affinity between the open state of Ub₂ and UBA2 is comparable to that between the closed state of Ub₂ and UBA2. Furthermore, the UBA2 binding to the open state of Ub₂ is much tighter than to Ub₁ because the interaction with the linker region is involved. This indicates that UBA2 also retains its selectivity for K48 linkage even at acidic pH (open state of Ub₂).

I propose that the UBA2-Ub₂ binding mode could be explained by a conformation selection mechanism. For the ensemble of all available Ub₂

conformations coexisting in solution, including the open and closed states, a ligand such as UBA2 selects the open conformation to form the tightly-bound sandwich-like complex. At neutral pH, the open state is estimated to be about 15-20% populated [81]. Even though the open state is less populated at physiological pH, a fast equilibrium exchange within the conformational ensemble of Ub₂ would shift the equilibrium toward open conformations, thus facilitating further UBA2 binding.

The results and the model I proposed could explain why K48-linked Ub₂ can bind to UBA2 when most of binding sites on Ub₂ are not available and sequestered at pH 6.8. This study mainly focuses on open state of K48-linked Ub₂. It would really be interesting, at least for me, to study the binding between UBA2 and the completely closed state of K48-linked Ub₂ (such as cyclic Ub₂).

Chapter 5: Roles of H68 in conformation exchange in Ub₂

5.1 Introduction

Solution NMR studies showed that K48-linked Ub₂ predominantly adopts a closed conformation at neutral pH. The inter-domain interface is formed by the hydrophobic patches from both domains of Ub₂. The closed conformation is mainly stabilized by its inter-domain hydrophobic interaction. On the other hand, the open conformations of K48-linked Ub₂ have no inter-domain interface and are predominant at acidic pH. In solution, the open and closed conformations of Ub₂ coexist and interconvert. The pH can affect the equilibrium of the open and closed state of Ub₂. I proposed that H68 is the key residue for opening the closed conformation based on several facts.

First, there is only one histidine (H68) in ubiquitin which is also well conserved among eukaryotes. Second, H68 is located in the center of the canonical hydrophobic patch (L8, I44, and V70) which contributes to the stability of the closed conformation. Third, the side chain of histidine can carry a positive charge once it gets protonated at acidic pH, as shown in **Fig 5.1**. Forth, the general pKa value (about 6) of histidine's side chain is coincidentally in the range between pH 4.5 and 6.8. Last but not least, the distance between the side chains of two histidines from the two domains of Ub₂ in the closed state is about 9 Å (PDB: 1AAR). The energy of repulsion between two domains is estimated to be about 9.44 kcal/mol in the closed conformation, assuming that the dielectric constant at the inter-domain interface is 4.

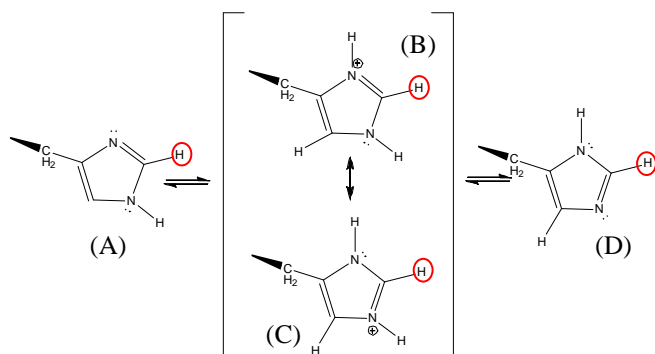


Fig 5.1 The diagram represents the side chain of histidine. (A) and (D) represent the unprotonated side chain of histidine. (A) and (D) are tautomer forms of unprotonated side chain of histidine. (B) and (C) represent the protonated side chain of histidine. (B) and (C) are resonance structures of protonated side chain of histidine. I performed the HSQC experiments which focuses on the proton circled in red. This proton does not easily exchange with solvent.

5.2 Monitoring the pKa of H68 and distribution of open and closed states in Ub₁ and Ub₂

5.2.1 Motivations

Although the pKa of histidine's side chain is generally about 6, the pKa of it in a protein could largely deviate from 6. NMR is an ideal tool and maybe the only method to measure any change in chemical environment of each residue including the change in the charge state of a side chain. I performed a series of ¹H-¹⁵N SOFAST HMQC experiments to measure the pKa of histidine in Ub₁ and Ub₂ by targeting the signal (shown in Fig 5.1) from H68's side chain (imidazole ring) directly. The result is shown in **Fig 5.2.2**. I also monitored the NMR signals of each amide signal (Ub₁ and Ub₂) from the protein backbone at various pH values. This allowed me to calculate the distribution of open and closed states by comparing the CSP between Ub₁ and Ub₂ at various pH values (see section 3.2.1). There are three specific aims in this study.

1: What is the pKa of H68's side chain in ubiquitin?

- 2: Is there a large difference in pKa of the H68 side chain between Ub₁ and Ub₂?
- 3: What is the pH when the populations of K48-linked Ub₂ in open and closed states are equal? Is this pH similar to the pI of ubiquitin or pKa of H68 side chain?

5.2.2 The distribution of open and closed states of Ub₂ and the pKa of H68 in Ub₁ and Ub₂

There was a technical issue for me to detect the signal of H68's side chain using NMR. The folded-in peaks from backbone amides interfere with the signals from H68's side chain in the SOFAST HMQC spectrum. I had tried several ways to avoid folded-in peaks from backbone amides including using 99% D₂O instead of 5% D₂O (for lock purpose in NMR). I found that the signals from backbone amides can be suppressed by using 99% D₂O because the proton of amide ¹H-N will exchange into ²H-N, hence become invisible in the ¹H NMR spectrum. Although this solution was practical and used extensively, it also created several inconveniences such as the conversion of pD to pH and in preparation of NMR samples for these experiments which required lyophilization. I overcame the problem by greatly increasing the spectral width in the nitrogen dimension in ¹H-¹⁵N SOFAST HMQC experiments so that the peaks from backbone amides stayed where they should be instead of folding in and did not interfere with the signal of H68's side chain. The only drawback of this method was that I had to increase the number of increments in the nitrogen dimension to achieve a reasonable resolution. The estimated time for a typical SOFAST HMQC experiment with reasonable resolution was about 45 minutes per experiment with a

0.5 mM sample, which is acceptable and realistic. The result of this experiment is processed and shown in **Fig 5.2.2**.

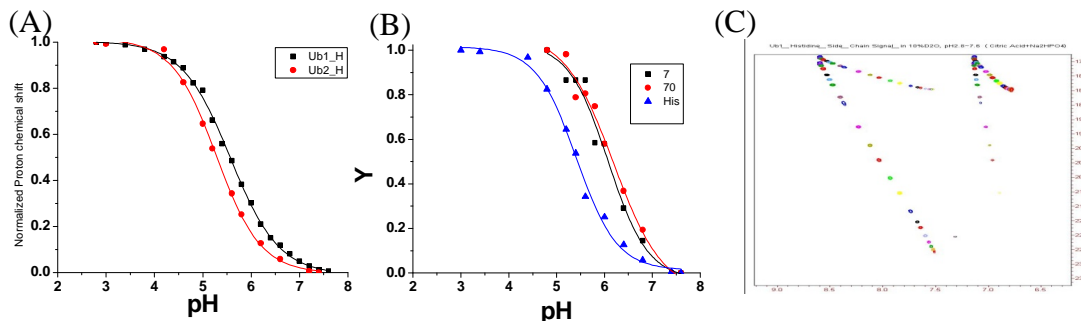


Fig 5.2.2 NMR of the signals of H68's side chain. In (A), Y axis is normalized proton chemical shift. The pKa of H68 in Ub₁ (shown in black) is 5.565 (5.524~5.606) and the pKa of H68 in Ub₂ (shown in red) is 5.478(5.421~5.535). In (B), the blue curve represents the fitting curve of NMR signals from H68's side chain in Ub₂ same as the red curve in (A). The black squares and red circles represent the NMR signals of amide protons from residues Thr7 and Val70 in Ub₂ respectively (the normalized combined CSP between Ub₁ and Ub₂ is shown on Y axis). The 50% Ub₂ adopting the open conformation happens at pH 6.074 (5.859~6.290) and 6.189 (6.003~6.375) for residues Thr7 and Val70, respectively. (C) is the overlay of NMR spectrum of the H68's side chain at different pH to show how the NMR signal from H68's side chain was measured.

5.2.3 Discussion

Originally, I thought that the histidine in Ub₂ may have a higher pKa than the histidine of Ub₁ because Ub₂ had a second ubiquitin domain compared to Ub₁. If the presence of a second ubiquitin domain – through the interdomain contact – blocks the histidine from access to the solvent, the pKa of histidine in Ub₂ should be higher than in Ub₁. From the results, I concluded that there is no major difference in the pKa of histidine between Ub₁ and Ub₂ as shown in **Fig 5.2.2 (A)**. I also showed that the pKa of H68's side chain in ubiquitin is about 5.5 which is similar to the pKa of free histidine. This indicated that the solvent accessibility of H68's side chain in Ub₂ is not blocked by the presence of the second ubiquitin domain. This result strongly supports that the open and closed conformations of Ub₂ are inter-exchangeable.

I also calculated the distribution of the open and closed conformations by monitoring the amide signals of Ub₂ and Ub₁. The result, as shown in **Fig 5.2.2 (B)**, shows that 50% of Ub₂ adopts the open conformation at pH 6. If I compare this pH value with the pKa (5.5) of H68's side chain, there is a 0.5 pH unit increase. Here, I want to point out that 50% of H68's side chains are protonated (positive-charged) at pH = pKa. If histidine is the only factor for opening the closed conformation, I would not be able to observe a 0.5 pH unit increase. In fact, if I check the distribution of the open conformation at pH 5.5 in **Fig 5.2.2 (B)**, nearly 75% of Ub₂ adopts the open conformation. It is reasonable to hypothesize that there are other factors and repulsions besides point-to-point charge repulsion which is the result of positive charges on H68's side chains in the two domains. I think other repulsions such as bulk-charge field repulsion may contribute to the force for opening the closed conformation.

If I take the point-to-point charge interaction into consideration, about 10% of histidine side chains are charged at pH6.56 according to **Fig 5.2.2 (A)**, so that the pH for equally-populated open and closed states of Ub₂ should be higher than 6.56. In fact, open and closed states of Ub₂ are equally-populated at pH 6 according to Fig5.2.1B instead of pH 6.56. It is reasonable to hypothesize that it is the inter-domain hydrophobic interactions that bring the pH from 6.56 to 6 because the structure of the closed conformation (PDB:1AAR) shows that the inter-domain interface is mainly stabilized by the hydrophobic interaction between two ubiquitin domains. Based on the facts above, I proposed that there are at least three major interactions which mediate the distribution of open and closed states. They are bulk

charge field effect (bulk charge of ubiquitin), point-to-point charge effect (the point charge on the side chain of histidine) and inter-domain hydrophobic interaction. I will further examine these interactions in following sections.

5.3 The effect of H68 mutations on open and closed states of Ub₂

5.3.1 Introduction

H68 is located in the inter-domain interface of closed conformation Ub₂. If a side chain of histidine is protonated, it will carry a positive charge. In my hypothesis, the electrostatic repulsion between the positive charges on the side chains of the two histidines will destabilize the closed conformation and force it to open. The shift from open state to closed state in Ub₂ was observed between pH 4.5 and 6.8 in previous NMR studies. The pKa of H68 in ubiquitin measured (about 5.5) falls in the range between pH 4.5 and 6.8. This implies that the distribution of open and closed conformations is highly correlated with the charge state of histidine side chains. I removed the positive charge on the histidine side chain by mutating H68 to H68A, H68V, H68F, and H68Y. I need to clarify the naming system to avoid misunderstanding. The Ub₂ constructs having H68 mutations in both domains are named double mutants, such as H68A double mutant, H68L double mutant, H68F double mutant, and H68Y double mutant. The Ub₂ constructs having the H68 mutation in only one of two domains are named half mutants. For example, the distal half H68Y mutant of Ub₂ means that the H68Y mutation only exists in distal domain of Ub₂ and the proximal domain of Ub₂ has H68 instead of H68Y.

5.3.2 H68A double mutant

The result of H68A double mutant in **Fig 5.3.2** showed there is no inter-domain interface formed at both neutral and acidic pH. This suggested that the H68 residue may be important for the integrity of the hydrophobic patch. However, H68 is not considered a key residue for maintaining the integrity of the Ub hydrophobic patch and the H68A mutation *in vivo* is not a lethal mutation in yeast [65].

Furthermore, H68A mutation does not affect ubiquitin chain synthesis *in vitro*. To my surprise, all these facts suggest that H68A should be a mild mutation for ubiquitin but the H68A mutant lost the ability to form the inter-domain interface. If I compare alanine with histidine, the side chain of alanine is much smaller than that of histidine. The replacement of histidine with alanine may create a large cavity around residue 68 if there is no structural rearrangement. In order to stabilize the structure, the ubiquitin should undergo local structural rearrangement around residue 68 to minimize the cavity which could disrupt the integrity of the hydrophobic patch in the H68A double mutant. It is known that the mutations in hydrophobic patch residues can disrupt the hydrophobic patch such as L8A, I44A, and V70A [82]. The current study is the first time that H68 was found to be important for maintaining the integrity of the hydrophobic patch. I proposed that the integrity of the hydrophobic patch will be restored if I increase the size of the side chain at residue 68 using H68V, H68F, or H68Y mutations.

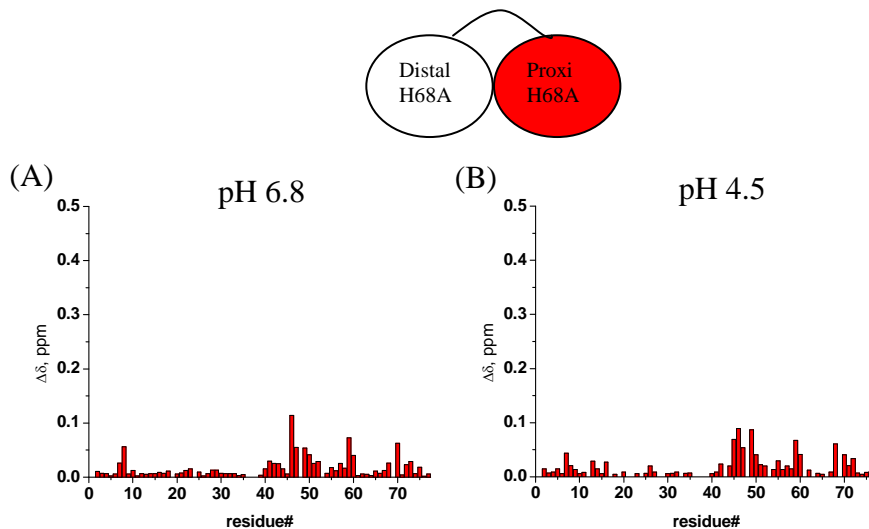


Fig 5.3.2 The CSP between Ub₁ and Ub₂ at pH 6.8 with 20 mM phosphate buffer is shown as (A) and pH 4.5 with 50 mM NaAc buffer shown as (B). For H68A double mutant Ub₂, the distal domain contains K48R and H68A mutations and the proximal domain contains H68A and D77 mutations. Only the proximal domain is ¹⁵N-labeled. The cartoon of top represents the Ub₂ construct used in this study. The mutations in H68 for each Ub unit are indicated. The Ub unit (in this case proximal) that is ¹⁵N-labeled is colored red. A similar schematics is used in the subsequent figures, where applicable.

5.3.3 H68V and H68L double mutants

When I increased the length of side chain at residue 68 by mutating H68 to H68V, H68L, H68F, and H68Y, the interface between the two domains at pH 6.8 gradually restored among those mutants (as shown in **Fig 5.3.3 (A)**, **Fig 5.3.3 (C)**, **Fig 5.3.4 (A)** and **Fig 5.3.5(A)**). The result for the H68V mutant in Fig5.3.3A suggests that the side chain of valine is large enough to prevent hydrophobic patch packing from forming a large cavity in it so that the change of hydrophobic patch packing is greatly reduced and the inter-domain interface of Ub₂ is formed at neutral pH. The H68V double mutant showed that the size of the H68's side chain is crucial for maintaining the integrity of hydrophobic patch packing and also the side chain of valine is large enough to avoid disruption of proper hydrophobic packing at neutral pH. The results for H68L double mutant in **Fig 5.3.3 (C)** and **(D)** also show the

similar phenomenon as H68V. The results for H68F and H68Y double mutants also strongly support this idea shown in Fig5.3.4A, Fig5.3.5A and Fig5.3.6A.

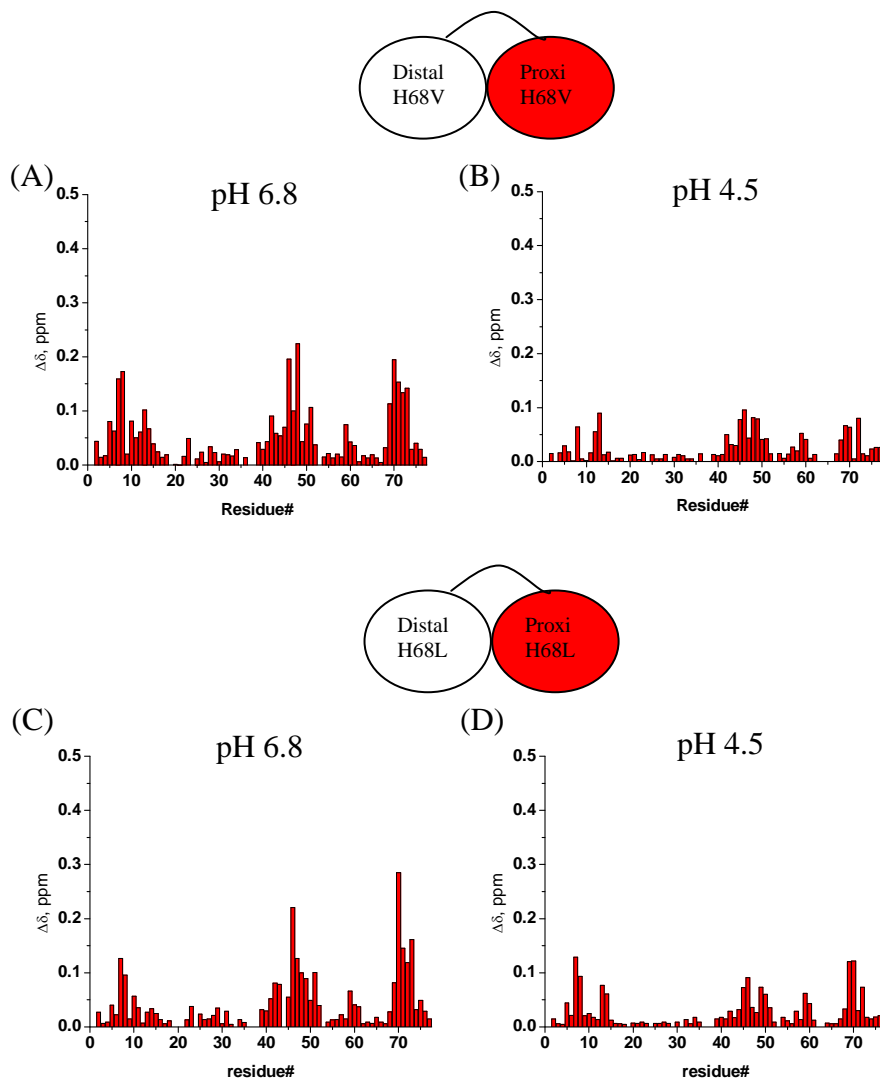


Fig 5.3.3 The CSP between Ub₁ and Ub₂ at pH 6.8 and pH 4.5 is shown as (A)(C) and (B)(D) respectively. For H68V double mutant and H68L double mutant are shown as (A)(B) and (C)(D) respectively. The distal domain contains K48R and H68V/H68L mutations and the proximal domain contains H68V/H68L and D77 mutations. Only proximal domain is ¹⁵N-labeled.

If one looks at the result for H68V double mutant at acidic pH, one may be puzzled why most Ub₂ adopts the open conformation since there is no point-to-point charge interaction in this mutant. Actually, this result happens to reveal the bulk

charge field effect between the two ubiquitin domains. As I mentioned earlier, the ubiquitin can carry a bulk positive charge at acidic pH because the pI of ubiquitin is 6.56. I think the bulk charge field effect is stronger than the inter-domain hydrophobic interaction in the case of H68V and H68L double mutant at acidic pH. I proposed the inter-domain hydrophobic interaction will overcome the bulk charge field effect at acidic pH and bring Ub₂ to form a closed conformation at acidic pH if I further increase the size of the side chain at residue 68 since the size of the valine or leucine side chain in is still much smaller than histidine's.

5.3.4 H68F and H68Y double mutant

In the result of H68F and H68Y double mutant at acidic pH as shown in **Fig 5.3.4 (B)**, **Fig 5.3.5 (B)** and **Fig 5.3.6 (B)**, most Ub₂ of H68F and H68Y double mutant can adopt the closed conformation at acidic pH. This shows that the inter-domain hydrophobic interactions of H68F and H68Y double mutant are stronger than the bulk charge field effect so that they can bring the two ubiquitin domains together to form a closed conformation at acidic pH. I think this is reasonable because the size of the side chain in histidine, phenylalanine, and tyrosine are comparable. Unlike the H68V mutant, these mutations (H68F and H68Y) would not create a large cavity around residue 68 which could undermine the integrity of hydrophobic patch packing. Furthermore, if you compare the magnitude of CSPs in H68Y double mutant with other double mutants, you may be surprised by the magnitude of CSPs in H68Y double mutant because they are much greater than for any other mutants. Although the larger magnitude of CSPs cannot be directly translated into the stronger inter-

domain interaction, it is still a good indication of that. I showed that the H68F and H68Y mutants may have nearly the same (H68F) or even better (H68Y) hydrophobic patch packing for inter-domain hydrophobic interaction. The NMR relaxation data supports that the H68Y double mutant forms a more rigid (tighter) closed conformation than wild type Ub₂.

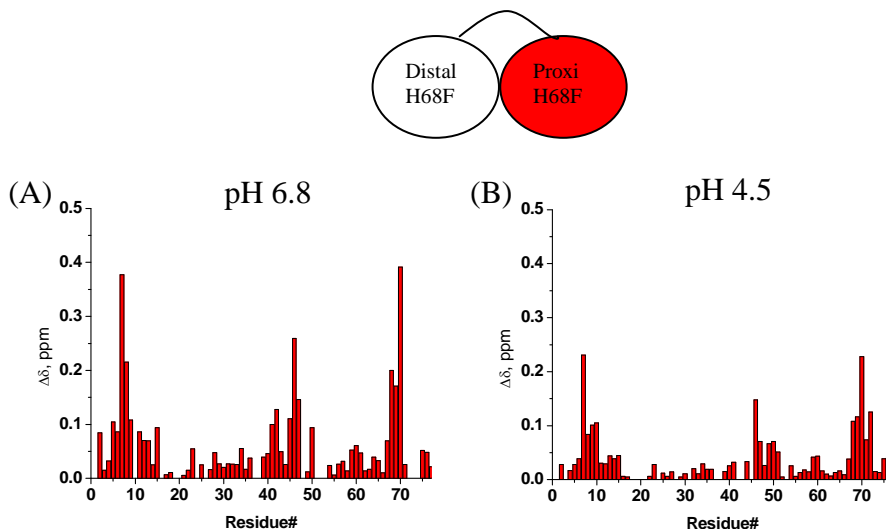


Fig 5.3.4 The CSP between Ub₁ and Ub₂ at pH 6.8 with 20 mM phosphate buffer is shown as (A) and pH 4.5 with 50 mM NaAc buffer shown as (B). For H68F double mutant Ub₂, the distal domain contains K48R and H68F mutations and the proximal domain contains H68F and D77 mutations. Only proximal domain is ¹⁵N-labeled.

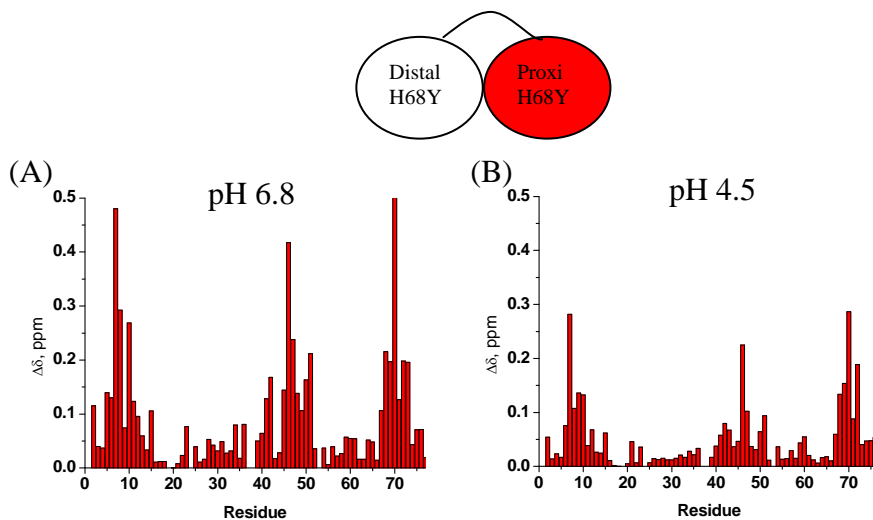


Fig 5.3.5 The CSP between Ub₁ and Ub₂ at pH 6.8 with 20 mM phosphate buffer is shown as (A) and pH 4.5 with 50 mM NaAc buffer shown as (B). For H68Y double mutant Ub₂, the distal domain contains K48R and H68Y mutations and the proximal domain contains H68Y and D77 mutations. Only proximal domain is ¹⁵N-labeled.

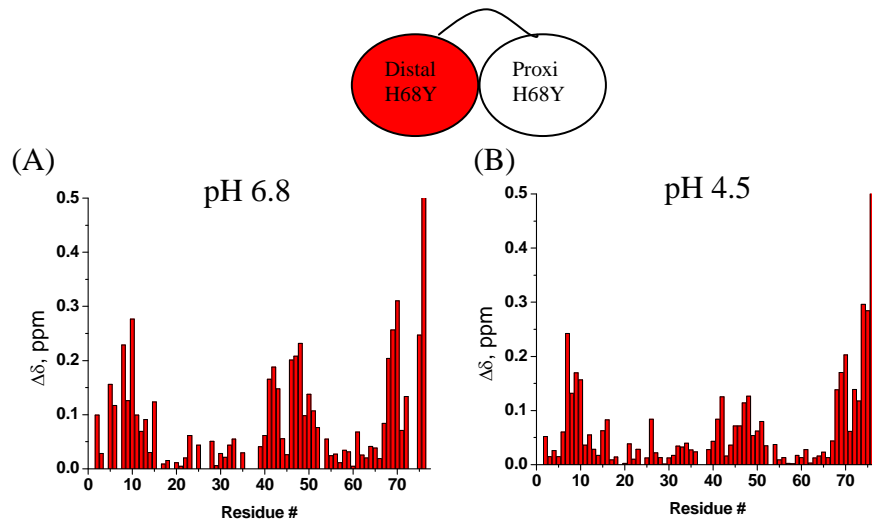


Fig 5.3.6 The CSP between Ub₁ and Ub₂ at pH 6.8 with 20 mM phosphate buffer is shown as (A) and pH 4.5 with 50 mM NaAc buffer shown as (B). For H68Y double mutant Ub₂, the distal domain contains K48R and H68Y mutations and the proximal domain contains H68Y and D77 mutations. Only distal domain is ¹⁵N-labeled.

5.3.5 Relaxation data of H68Y double mutant

From NMR R_1 and R_2 relaxation data of H68Y double mutant Ub₂, both domains of H68Y double mutant have a lower R_1 and higher R_2 compared to wild type at neutral and acidic pH. In general, a protein with a lower R_1 and higher R_2 has larger molecular weight or the larger volume however this is not true in this case based on two facts. First, the H68Y double mutant of Ub₂ has an almost identical molecular weight to wild type Ub₂. Second, the H68Y double mutant of Ub₂ forms a closed conformation at both acidic and neutral pH based on CSP data (**Fig 5.3.5 and 5.3.6**). Furthermore, the closed conformation of H68Y double mutant and wild type is very similar because the CSPs between both H68Y double mutant and wild type Ub₂ with their respective Ub₁ are very similar. I proposed that the H68Y double mutant with a lower R_1 and higher R_2 results from the H68Y double mutant Ub₂ forming a more rigid closed conformation than wild type. The significantly larger CSPs

observed in the H68Y double mutant at neutral pH (Fig 5.3.5 and 5.3.6) also supports this idea.

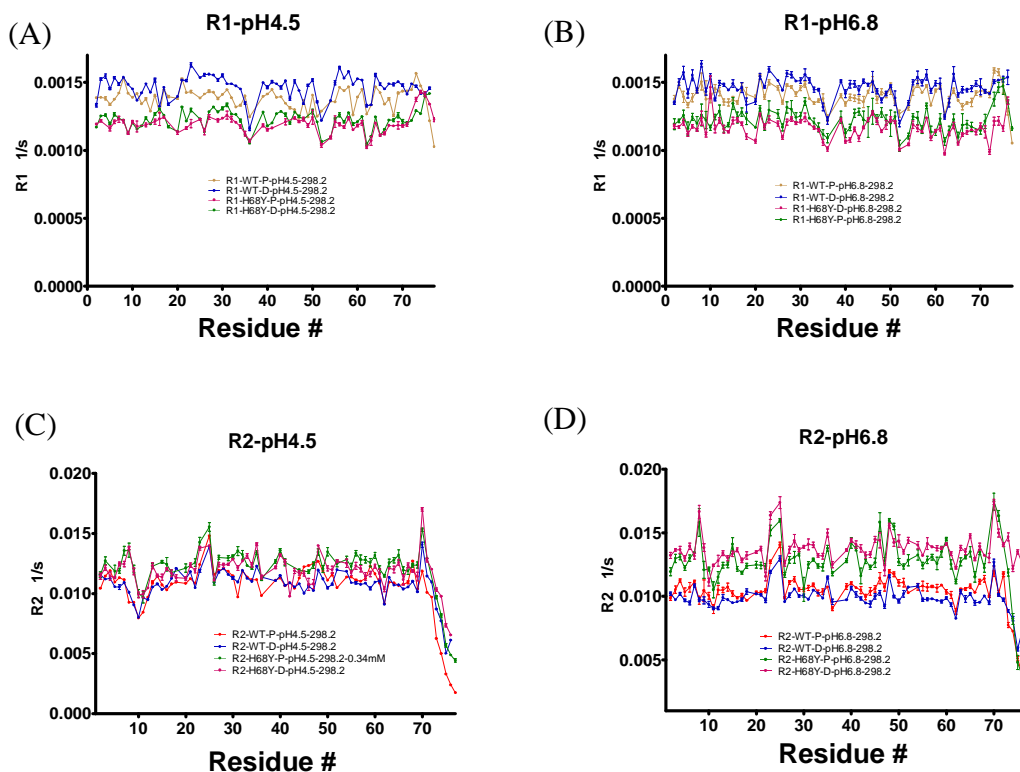


Fig 5.3.7 The comparisons of R₁ and R₂ between H68Y double mutant and wild type Ub₂. (A) and (C) are the comparisons of R₁ at pH 6.8 and 4.5 respectively. The proximal and distal domains of wild type Ub₂ are showed in yellow and blue respectively. The proximal and distal domains of H68Y double mutant Ub₂ are showed in green and red respectively. (B) and (D) are the comparisons of R₂ at pH 6.8 and 4.5 respectively. The proximal and distal domains of wild type Ub₂ are showed in red and blue respectively. The proximal and distal domains of H68Y double mutant Ub₂ are showed in green and purple respectively.

5.3.6 Interaction of H68Y and H68F double mutants with UBA2

I confirmed that both H68Y and H68F can form the closed conformation at neutral pH and acidic pH in the earlier section. Although these mutations do not interfere with the recognition of E1 and E2-25K conjugating enzyme, judging by the fact that chain synthesis is not reduced, their recognition of other ubiquitin binding

proteins are still unknown. I performed titration of ^{15}N labeled H68F double mutant with UBA2 in order to examine the recognition at acidic pH, as shown in **Fig 5.3.8 (A)**. The titration of UBA2 and wild type Ub₂ at acidic pH, detailed in chapter-4, provides a good reference to compare. The results show that the Ub₂ of the H68F double mutation retains its recognition of UBA2. Interestingly, during the titration, there are more residues attenuated in H68F double mutant compared to those in wild type (**Fig 4.3 (D)**). The UBA2 binds to Ub₂ of H68F double mutant in a similar “sandwich like” mode because I found that the C-terminal residues in the distal domain are involved in binding (distal domain data is not shown).

I also performed titration of ^{15}N labeled H68Y double mutant with unlabeled UBA2 at neutral pH to study the interaction between H68Y double mutant and UBA2. The results show that the Ub₂ of the H68Y double mutation retains its recognition of UBA2. In **Fig 5.3.8 (B)**, it clearly showed that the UBA2 binds to Ub₂ of H68Y double mutant via the canonical hydrophobic patch in the distal domain. Furthermore, the C-terminal residues of the distal domain also showed strong attenuations indicating the “sandwich like” binding mode is also retained in H68Y double mutant.

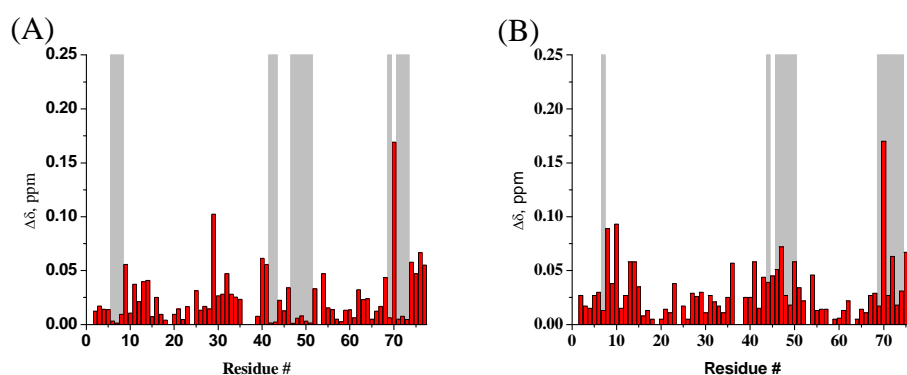


Fig 5.3.8 the titration results of H68F and H68Y double mutant. **(A)** shows the binding between ^{15}N labeled proximal domain of H68F double mutant and UBA2 at pH 4.5. **(B)** shows the binding between ^{15}N labeled distal domain of H68Y double mutant and UBA2 at pH 6.8. The residues which are attenuated upon titration are showed in long grey bar.

5.4 The single-charge effect on open and closed conformations of Ub₂

5.4.1 Introduction

In section 5.3, I showed that H68 is important for the open and closed conformations. The results of the H68Y and H68F double mutants clearly showed that if there is no point-to-point charge repulsion in Ub₂ such as H68F and H68Y double mutants, the Ub₂ of these mutants can adopt a closed conformation even at acidic pH because the hydrophobic interactions between the two domains of H68Y double mutant are capable of overcoming the bulk charge field repulsion at acidic pH. It is interesting to examine the effect of point-to-bulk charge repulsion by using half H68Y mutants. In the half H68Y mutants of Ub₂, only one H68Y mutation exists in Ub₂ for example the distal half H68Y mutant Ub₂ contains K48R and H68Y mutations in distal domain and only a D77 mutation in proximal domain. The ubiquitin domain that contains the H68Y mutation will lose its positive charge on the side chain at residue 68 but it still can carry a bulk positive charge at acidic pH. On the other hand, the wild type domain retains its positive charge on the H68 side chain.

5.4.2 Half H68Y mutants and the point-to-bulk charge repulsion

The results from half H68Y mutants showed that it could form the inter-domain interface at neutral pH but the interface is disrupted at acidic pH (as shown in **Fig 5.4.1, 5.4.2, 5.4.3 and 5.4.4**). The Ub₂ of the half H68Y mutant behaved like wild type Ub₂. No matter if the histidine only exists in either the distal or proximal domain; the Ub₂ of half H68Y mutants can adopt the closed conformation at neutral

pH and shift to an open conformation at acidic pH. This finding shows the point-to-bulk charge repulsions are strong enough for the closed conformation to open.

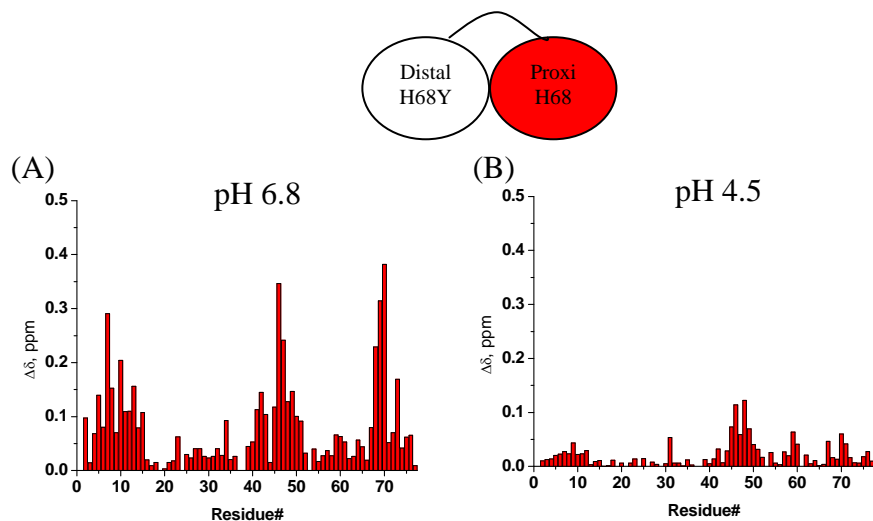


Fig 5.4.1 The CSP between Ub₁ and Ub₂ at pH 6.8 with 20 mM phosphate buffer is shown as (A) and pH 4.5 with 50 mM NaAc buffer shown as (B). For this H68Y half mutant Ub₂, the distal domain contains K48R and H68Y mutations and the proximal domain contains only D77 mutation. Only proximal domain is ¹⁵N-labeled.

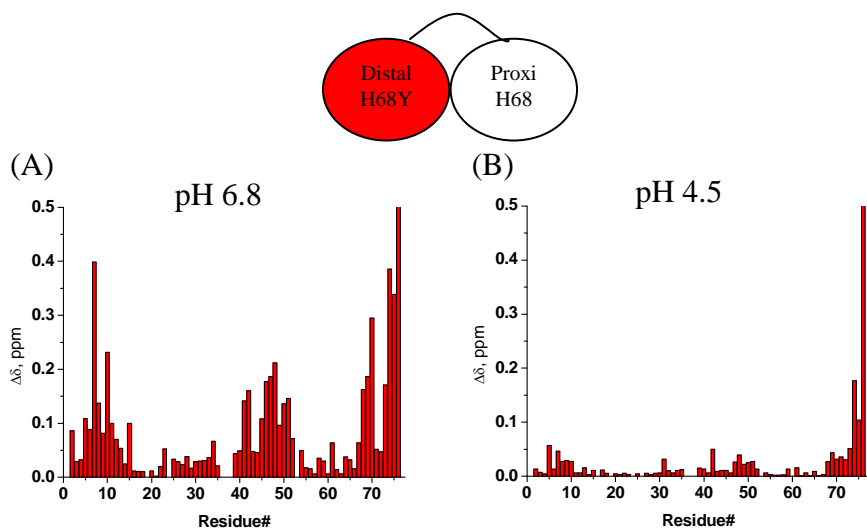


Fig 5.4.2 The CSP between Ub₁ and Ub₂ at pH 6.8 with 20 mM phosphate buffer is shown as (A) and pH 4.5 with 50 mM NaAc buffer shown as (B). For this H68Y half mutant Ub₂, the distal domain contains K48R and H68Y mutations and the proximal domain contains only D77 mutation. Only distal domain is ¹⁵N-labeled.

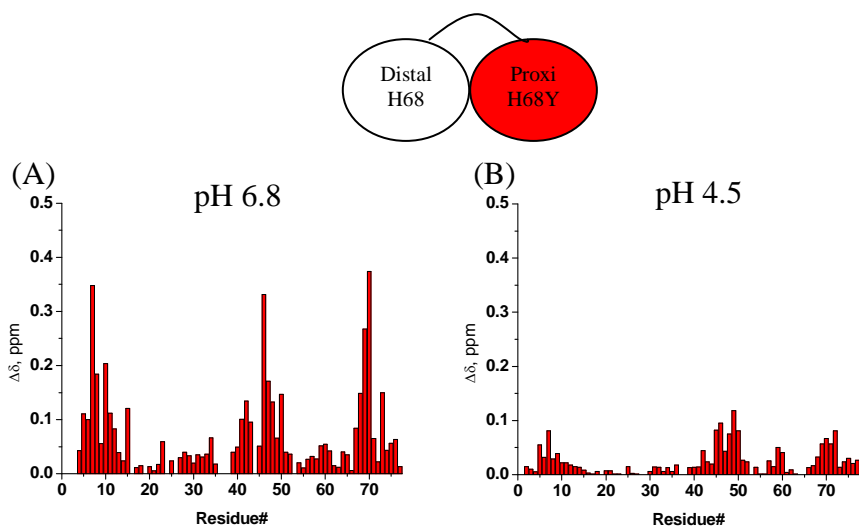


Fig 5.4.3 The CSP between Ub₁ and Ub₂ at pH 6.8 with 20 mM phosphate buffer is shown as (A) and pH 4.5 with 50mM NaAc buffer shown as (B). For this H68Y half mutant Ub₂, the distal domain contains only K48R mutation and the proximal domain contains H68Y and D77 mutation. Only proximal domain is ¹⁵N-labeled.

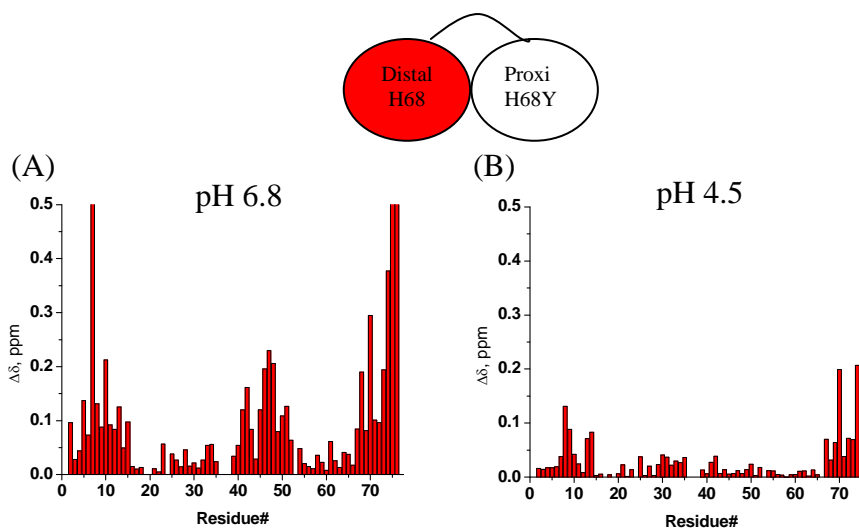


Fig 5.4.4 The CSP between Ub₁ and Ub₂ at pH 6.8 with 20mM phosphate buffer is shown as (A) and pH 4.5 with 50mM NaAc buffer shown as (B). For this H68Y half mutant Ub₂, the distal domain contains K48R mutation and the proximal domain contains H68Y and D77 mutation. Only distal domain is ¹⁵N-labeled.

5.5 Exploring the salt effects on the half H68Y mutant and wild type of Ub₂

5.5.1 Introduction

It is very clear that the charge repulsion served as the driving force for Ub₂ to open the closed conformation. In order to examine the strength of this charge repulsion, I put wild type and the half H68Y mutant of Ub₂ in high salt condition to test if high salt could screen these charge repulsions including point-to-bulk and point-to-point charge repulsions. A well-known issue with NMR is that samples with high salt concentrations will significantly increase the pulse length which can prohibit their uses in NMR. In general, a sample with 200 mM salt concentration can easily drive the proton 90⁰ pulse length to 16 us and more, however, a proton 90⁰ pulse length for a normal NMR sample with 20-50 mM salt is about 9-12 μs. In order to avoid this problem, one can use a shape tube or a thinner NMR tube (3 mm in diameter) to perform NMR experiments.

5.5.2 The salt effects on half H68Y mutant and wild type at 0.5 M and 1 M NaCl

I found that the half H68Y mutant of Ub₂ can form the closed conformation at pH 4.5 with high salt (0.5 M NaCl), as shown in **Fig 5.5.2** and **Fig 5.5.3**, however, the wild type Ub₂ only showed marginal CSPs at these conditions. This suggests that point-to-bulk charge repulsions can be screened by 0.5 M NaCl. On the other hand, the results from wild type Ub₂ show that the point-to-point charge repulsions are so

strong that even 1 M NaCl could not screen them. These results support my hypothesis that it is very unfavorable for Ub₂ to adopt a closed conformation at acidic pH because the two positive point charges are close to each other in space. From these results I conclude that the point-to-point charge repulsion is the strongest charge repulsion because even 1 M NaCl is not enough to screen it. Although the point-to-bulk charge repulsions are weaker than point-to-point charge repulsion, they are still strong enough to open the closed conformation at acidic pH, based on the results from half H68Y mutant at low salt condition. Although the bulk charge field repulsions are the weakest repulsions, they also contribute to the force needed to open the closed conformation, based on the results from H68V double mutant at acidic pH.

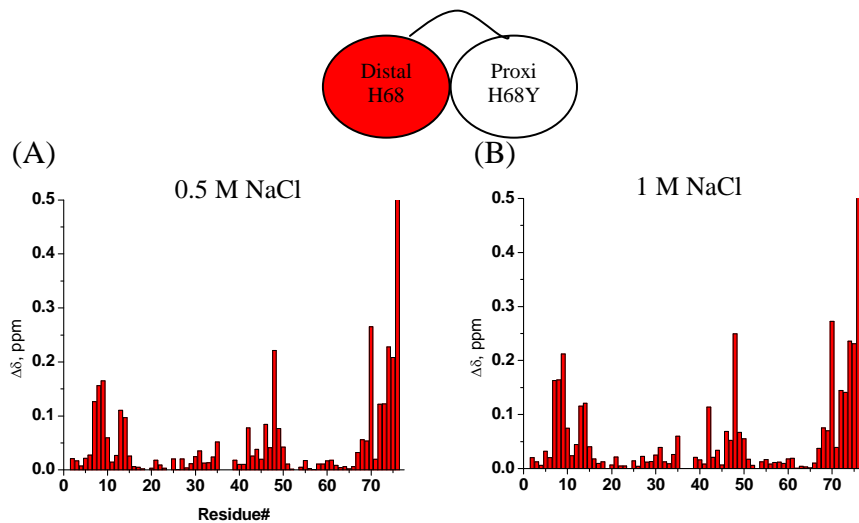


Fig 5.5.2 The CSP between Ub₁ and Ub₂ at pH 4.5 with 50 mM NaAc buffer plus 0.5 M NaCl and 1 M NaCl are shown in (A) and (B) respectively. For this H68Y half mutant Ub₂, the distal domain contains only K48R mutation and the proximal domain contains H68Y and D77 mutation. Only Distal domain is ¹⁵N-labeled.

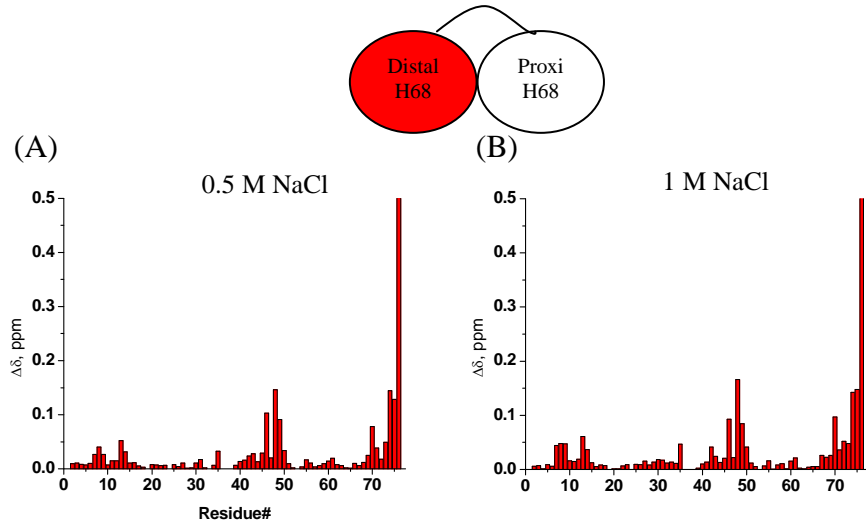


Fig 5.5.3 The CSP between Ub₁ and Ub₂ at pH 4.5 with 50 mM NaAc buffer plus 0.5 M NaCl and 1 M NaCl are shown in (A) and (B) respectively. For this wild type Ub₂, the distal domain contains only K48R mutation and the proximal domain contains only D77 mutation. Only distal domain is ¹⁵N-labeled.

5.6 The structure of half H68Y mutant Ub₂ at pH 4.5 with 0.5 M NaCl

Although the structure of PDB: 1AAR clearly defines the closed conformation of Ub₂ and the data from solution NMR at neutral pH agrees well with it, the available open conformation structures were solved by X-ray crystallography and they may not represent the full picture of the open conformation in solution. Unlike the closed state of Ub₂, the open state is an ensemble of open conformations which is defined by no inter-domain interface between two domains. The intrinsic flexibility of Ub₂ in the open state may cause difficulties to obtain “the structure in the open state” of Ub₂. I had tried to obtain an average structure of the open state for wild type Ub₂ at acidic pH by using RDCs, but the initial attempt was unsuccessful. I knew that the half H68Y mutant of Ub₂ can form the closed conformation at acidic pH with high salt so that it is highly possible to obtain the closed conformation structure.

Since this structure will not be as stable as wild type in neutral pH because there are bulk-to-bulk and point-to-bulk charge repulsions that exist between the two domains. This structure can be treated as the pre-open conformation of Ub₂ which serves as an intermediate structure between the open and closed conformations.

I performed HADDOCK 2.1 structural calculations by using the constraint of RDCs and CSPs to generate the NMR model which is shown in **Fig 5.6.1 (A)**. The calculated structure agreed well with RDCs (correlation coefficient = 0.998 and $\chi^2 = 0.024$) and had a RMSD (root-mean-square deviation) for the overall lowest-energy structure of $0.8 \pm 0.5\text{\AA}$. When I aligned this Ub₂ structure with PDB: 1AAR by fixing the distal domain, I observed a 30-degree rotation in proximal domain. If this structure represents the pre-open conformation, it is clear that the Ub₂ will open by twisting instead of directly pulling away (see **Fig 5.6.2**). It is also highly possible for Ub₂ to adopt the pre-open conformation before a fully-open state.

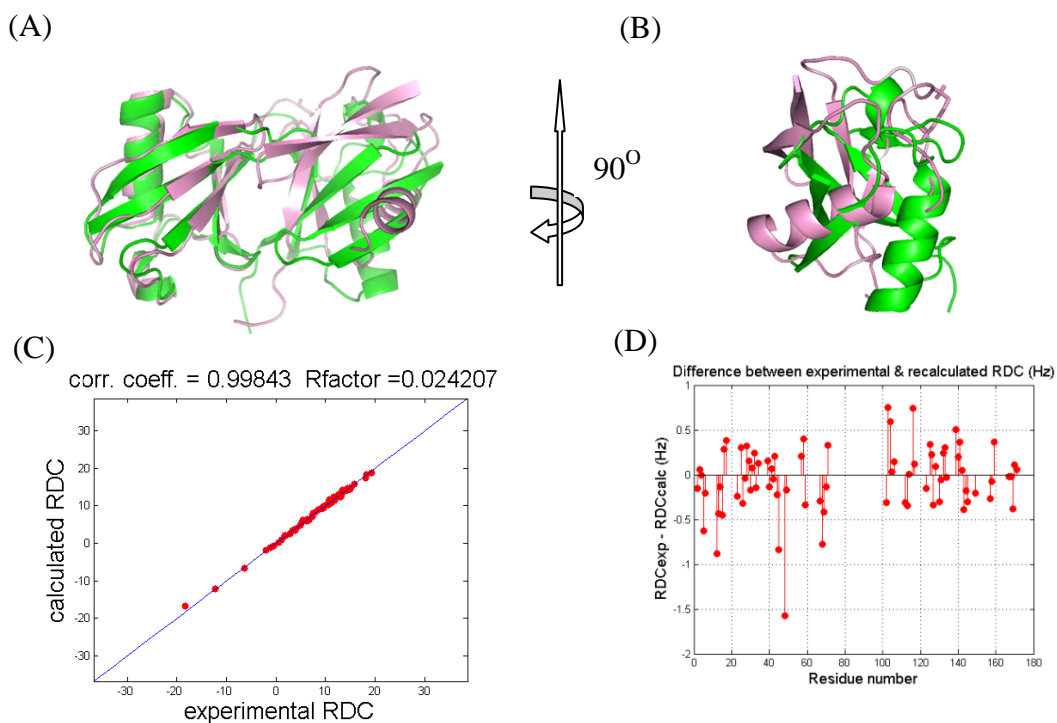


Fig 5.6.1 The NMR model of pre-open state. (A) and (B) show the overlay of 1AAR and pre-open state Ub₂ structure. NMR model of pre-open state and 1AAR are shown in pink and green respectively. This NMR model has a RMSD of the overall lowest energy structure (0.8 +/- 0.5Å). (C) and (D) show that the NMR model agrees well with RDCs.

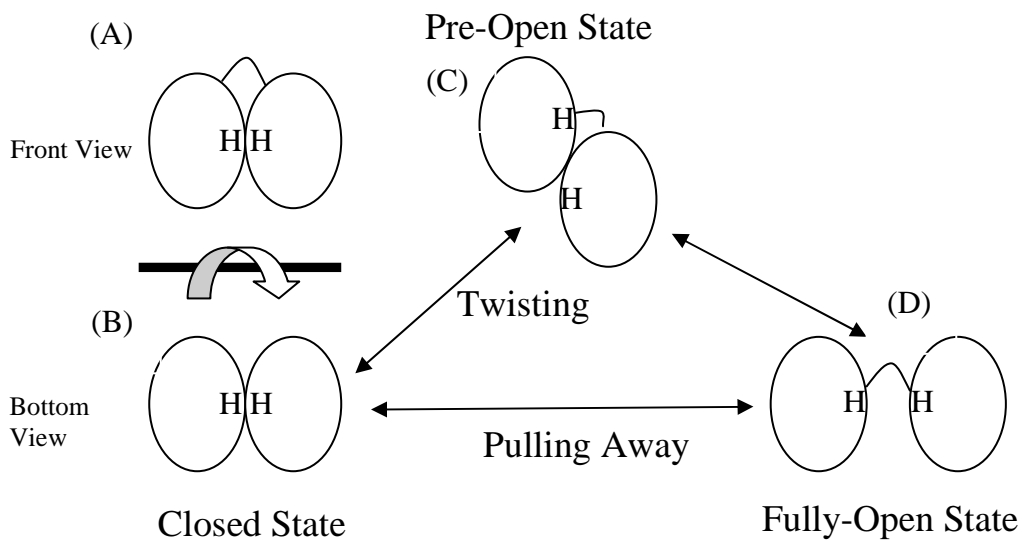


Fig 5.6.2 The proposed mechanism of opening the closed conformation of Ub₂. (A) and (B) are the front and bottom view of a closed conformation Ub₂. The (C) and (D) present pre-open state and fully-open state of Ub₂ respectively. The closed state of Ub₂ can undergo two-steps pathway including twisting steps (B) to (C) or one step pathway involving pulling away the ubiquitin from each other.

5.7 Summary

I have shown that there is no major difference in the pKa of histidine between Ub₁ and Ub₂ in Fig 5.2.2 (A). I also showed that the pKa of histidine's side chain in ubiquitin is about 5.5, which is similar to what was reported previously [83]. I also showed that the solvent accessibility of H68's side chain in Ub₂ is not blocked by the presence of the second ubiquitin domain. The result, as shown in Fig 5.2.2 (B), indicates that the open and closed states are equally populated at pH 6. I showed that there are at least four major interactions to control the distribution of the open and closed states. They are bulk charge field repulsion, point-to-point charge repulsion, point-to-bulk charge repulsion, and inter-domain hydrophobic interaction. I concluded that the point-to-point charge repulsion is the strongest and the point-to-bulk charge repulsions are weaker than point-to-point charge repulsion and the bulk charge field repulsions are the weakest repulsions. I revealed the bulk charge field repulsion between the two ubiquitin domains by using H68V double mutant. This weak bulk charge field repulsion contributes the force for opening the closed conformation. I also showed, using half H68Y mutant, that the point-to-bulk charge repulsions are sufficiently strong to open the closed conformation. The point-to-bulk charge repulsions can be minimized by 0.5 M NaCl but the point-to-point charges repulsions are too strong to screen them even by 1 M NaCl. I found that the H68 residue is important to maintain the integrity of the hydrophobic patch. I also showed that the H68Y double mutant can form a more rigid closed conformation than wild type ubiquitin by NMR relaxation data and the significantly larger CSPs observed in H68Y double mutant. I performed the titrations of H68 double mutants with UBA2 to

show the Ub₂ of double mutants retain a similar “sandwich like” binding mode. I also showed that the half mutant behaved like wild type Ub₂. I was able to calculate the NMR model of the pre-open state of Ub₂ by using RDCs and CSPs. If the structure of half H68Y mutant at acidic pH with high salt represents the pre-open conformation, it is clear that the closed conformation of Ub₂ will be opened by twisting instead of pulling away. The half H68Y mutant has weaker electrostatic repulsion than wild type ubiquitin at acidic pH condition. On top of that, I also put half H68Y mutant at high salt condition to shield/screen the electrostatic repulsion between two domains. Putting half H68Y mutant in high salt condition may also strengthen the hydrophobic interaction between two domains. All of these factors above allow me having a stable pre-open state to obtain the structure of it. This structure of pre-open state suggests that Ub₂ adopt pre-open conformation before fully-open states. This pre-open state is also supported by other studies[81].

Chapter 6: The hydrogen-deuterium (H-D) exchange studies of Ub₂ and Ub₁ at pH5.5

6.1 Introduction

Amide hydrogens in the protein backbone can exchange with protons from water in solution. The half-times of the amide hydrogen exchange can range from seconds, minutes, and days and even years. The residues involved in a hydrogen bond or that are buried in the core of the protein will show a slower exchange rate. In H-D exchange experiments, the backbone amide H-D exchange is monitored by a series of ¹H-¹⁵N SOFAST HMQC spectra after a rapid change of solvent (from H₂O to D₂O). The H-D exchange experiments can be started by using various techniques such as re-dissolving a lyophilized sample in D₂O or diluting a sample into D₂O. I tried both ways and found that the dilution method give me a more stable result.

The ubiquitination was proposed to have a role in partially unfolding a substrate. The K48-linked Ub₂ can be used as a mimic of a mono-ubiquitinated Ub₁ see **Fig 6.1** for detail. In this mimic, the proximal and the distal domains of Ub₂ can be treated as a substrate and an ubiquitin which is ligated to the substrate, respectively. If ubiquitination indeed unfolds and destabilizes the substrate, the H-D exchange rate of an ubiquitinated substrate will be faster than the rate of a free substrate. In other words, I should be able to observe a faster H-D exchange rate in the Ub₂ proximal domain compared to Ub₁. I also expect to find that the H-D exchange rate between the distal domain of Ub₂ and Ub₁ are comparable.

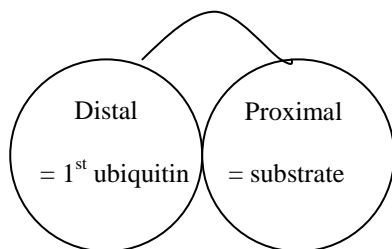


Fig 6.1 represents the K48-linked Ub₂. It can be used as a mimic of mono-ubiquitinated substrate (ubiquitin).

6.2 The results of H-D exchange at pH 5.5

The selected results were processed and shown in **Fig 6.2**. The full results are in Appendices. The residues showing the faster exchange rates for distal of Ub₂ than Ub₁ are 31, 32, 34, 35, and 36 and they are localized in the end of a long helix as shown in Fig 6.3. Both distal and proximal domains of Ub₂ show a slower exchange rate than Ub₁ at residue 48. Most residues showed the similar exchange rates among Ub₁ and Ub₂. The results indicated that the residues in the end of the helix in the distal domain are destabilized by ubiquitination. In other words, the result suggests that ubiquitination destabilizes ubiquitin itself instead of the substrate. This contradicts to what I expected.

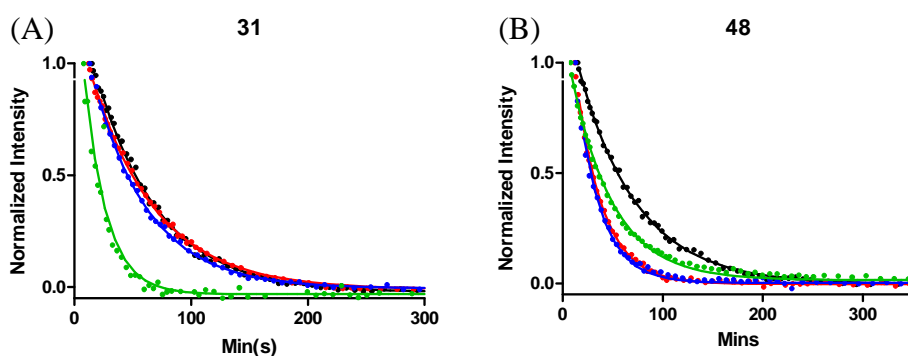


Fig 6.2 The results of H-D exchange. (A) and (B) represent residues 31 and 48 respectively. The curves colored in black or green represent the data from proximal and distal domain of Ub₂ respectively. The curves colored in red or blue represent the data of Ub₁ in two separated experiments to ensure the reliability of H-D exchange experiment.

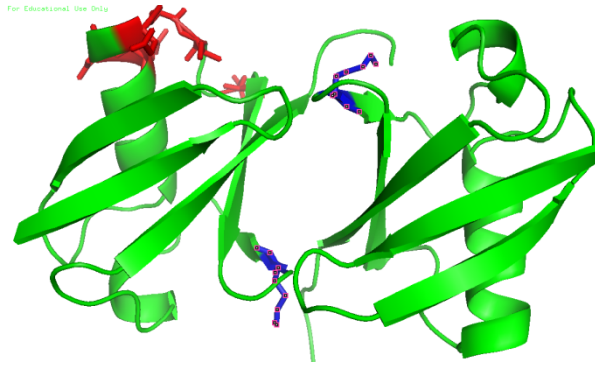


Fig 6.3 The residues affected by ubiquitination. The structure of PDB:1AAR is shown in green. The residues showing faster exchange rates than Ub₁ are colored in red. The residues showing slower exchange rates than Ub₁ are colored in blue. The distal and proximal domains are shown in left and right respectively.

Chapter 7: The dynamics of K48-linked Ub₂ in an anchored form

7.1 Introduction

After the polyUb chains are ligated to a substrate, the polyUb chains will be recognized by their binding partners. The interactions between free polyUb chains and their binding partners have been extensively explored in the past; however no one used NMR to monitor the change in the interaction between substrate-ligated polyUb chains and their binding partners.

A K48-linked Ub₃ can be used as a mimic of a substrate-ligated Ub₂. In this mimic, the two most distal domains of ubiquitin are wild type ubiquitins but the most proximal domain contains L8A and I44A mutations. Since the L8A and I44A mutations are shown to disrupt the hydrophobic patch interactions, the most proximal domain cannot form an interface with other ubiquitins in this Ub₃ construct.

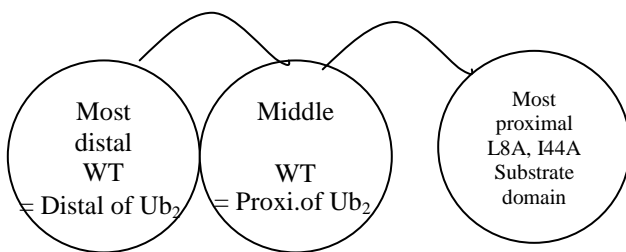


Fig 6.1 represents the K48-linked Ub₃. It can be used as a mimic of a substrate-ligated Ub₂. The most distal domain of Ub₃ is equivalent to the distal domain of Ub₂. The middle domain of Ub₃ is equivalent to the proximal domain of Ub₂. The most proximal domain of Ub₃ is equivalent to the substrate.

7.2 The results

The results from Fig 7.2.5 show that there is no interaction between the substrate domain and other domains of Ub₃. This confirmed that it is reasonable to assume that the property of the ubiquitin with L8A and I44A is similar to the substrate which does not interact with other ubiquitins. The results from Fig 7.2.1, Fig 7.2.2, Fig 7.2.3, and Fig 7.2.4 show that the substrate-ligated Ub₂ behaves like free Ub₂ because it can adopt the open and closed conformations at acidic and neutral pH respectively. There is no major change in dynamics. The results from Fig 7.2.6 also show that its ability to bind UBA2 is retained in the substrate-ligated Ub₂.

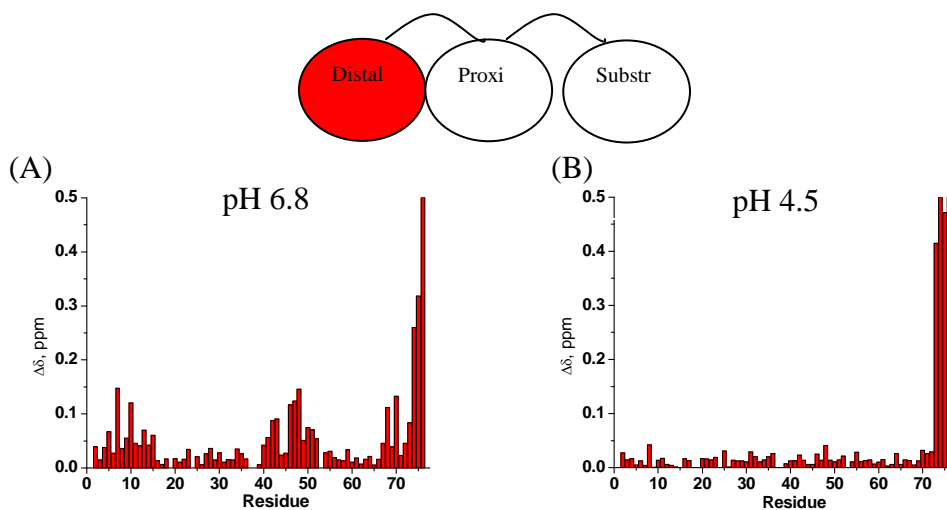


Fig 7.2.1 The CSP between Ub₁ and Ub₃ at pH 6.8 with 20 mM Sodium Phosphate buffer is shown in (A) and pH 4.5 with 50 mM Sodium Acetate buffer is shown in (B). In this Ub₃ construct, all linkage is K48-linked. The distal domain of Ub₃ contains only K48R mutation and the proximal domain has no mutation. The substrate which is Ub contains L8A, I44A and D77 mutation. Only distal domain is ¹⁵N-labeled.

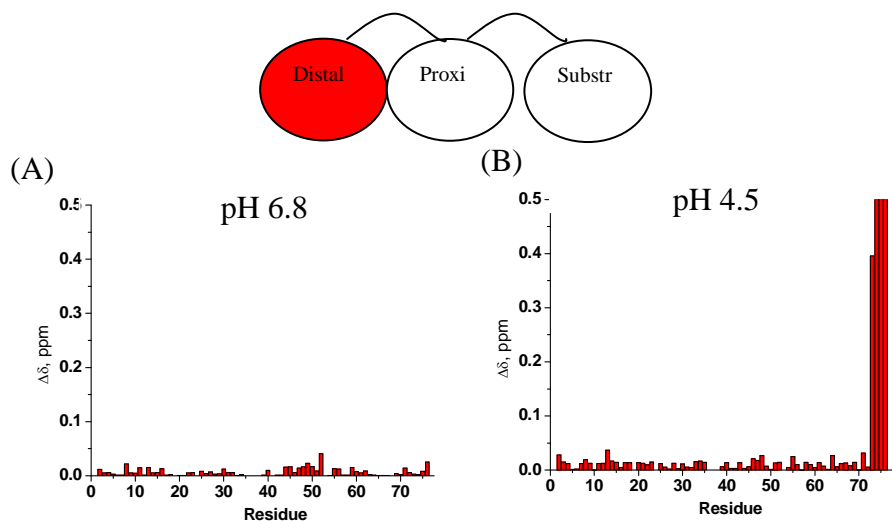


Fig 7.2.2 The CSP between Ub₂ and Ub₃ at pH 6.8 with 20 mM Sodium Phosphate buffer is shown in (A) and pH 4.5 with 50 mM Sodium Acetate buffer is shown in (B). In this Ub₃ construct, all linkage is K48-linked. The distal domain of Ub₃ contains only K48R mutation and the proximal domain has no mutation. The substrate which is Ub₁ contains L8A, I44A and D77 mutation. Only distal domain is ¹⁵N-labeled.

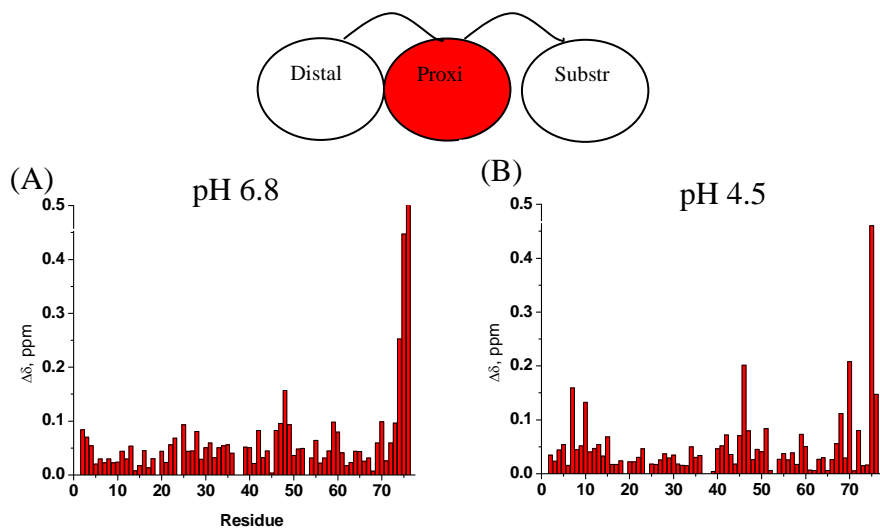


Fig 7.2.3 The CSP between Ub₁ and Ub₃ at pH 6.8 with 20 mM Sodium Phosphate buffer is shown in (A) and pH 4.5 with 50 mM Sodium Acetate buffer is shown in (B). In this Ub₃ construct, all linkage is K48-linked. The distal domain of Ub₃ contains only K48R mutation and the proximal domain has no mutation. The substrate which is Ub₁ contains L8A, I44A and D77 mutation. Only proximal domain is ¹⁵N-labeled.

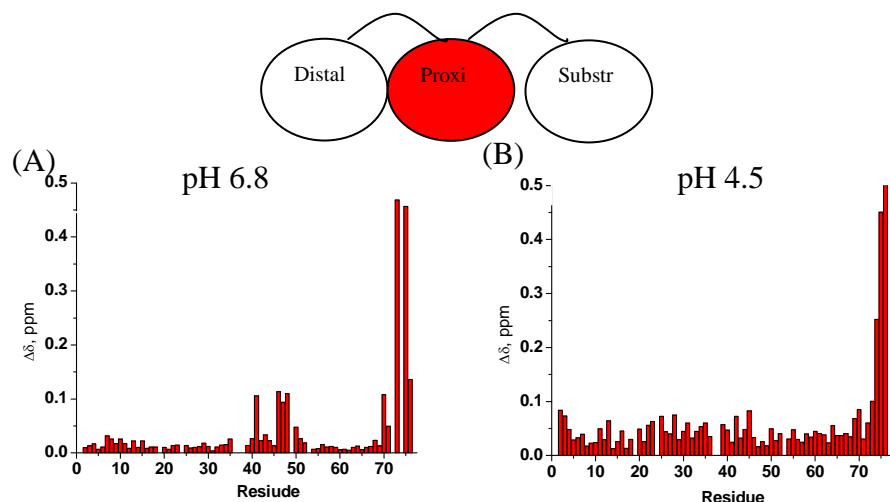


Fig 7.2.4 The CSP between Ub₂ and Ub₃ at pH 6.8 with 20 mM Sodium Phosphate buffer is shown in **(A)** and pH 4.5 with 50 mM Sodium Acetate buffer is shown in **(B)**. In this Ub₃ construct, all linkage is K48-linked. The distal domain of Ub₃ contains only K48R mutation and the proximal domain has no mutation. The substrate which is Ub₁ contains L8A, I44A and D77 mutation. Only proximal domain is ¹⁵N-labeled.

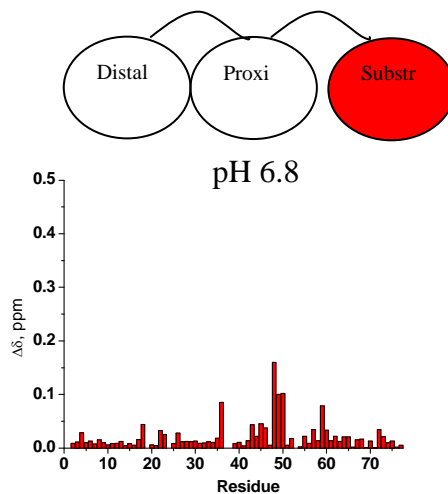


Fig 7.2.5 The CSP between Ub₁ and Ub₃ is measured at pH 6.8 with 20 mM sodium phosphate buffer. In this Ub₃ construct, all linkage is K48-linked. The distal domain of Ub₃ contains only K48R mutation and the proximal domain has no mutation. The substrate which is Ub₁ contains L8A, I44A and D77 mutation. Only the substrate domain is ¹⁵N-labeled.

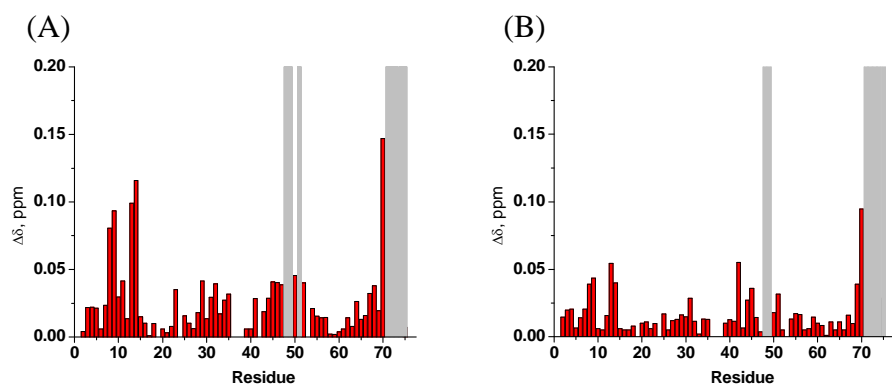


Fig 7.2.6 The CSPs upon the titration of UBA2 are shown in red. The residues shown in vertical grey bar represent the signals are strongly attenuated. (A) shows ^{15}N -labeled distal domain of substrate-attached Ub_2 at $[\text{UBA2}]/[\text{Ub}_3]=2.0$. (B) shows ^{15}N -labeled proximal domain of substrate-attached Ub_2 at $[\text{UBA2}]/[\text{Ub}_3]=1.5$

Chapter 8: Studies of the most proximal domain in K48-linked Ub₅ and of OTU1's binding surface on Ub₂

8.1 The penta-ubiquitin (Ub₅)

The K48-linked tetra-ubiquitin structures are available by NMR and X-ray[84-86]. In the following I call the most distal domain as the 1st ubiquitin and, correspondingly, the most proximal domain as the 4th ubiquitin. In one of the Ub₄ structures, the 1st ubiquitin forms an interface with the 2nd ubiquitin and the 3rd ubiquitin could form an interface with the 4th ubiquitin at neutral pH. In another Ub₄ structure, the 1st ubiquitin forms an interface with the 3rd ubiquitin and the 2nd ubiquitin forms an interface with the 4th ubiquitin at neutral pH. It would be interesting to determine if the 5th ubiquitin could interact with other ubiquitins.

It is time-consuming to synthesize selectively labeled Ub₅ in a traditional way because it involves several steps to de-block K48C and D77 as mentioned in [68]. I made the most proximal domain labeled in Ub₅ by mixing the unlabeled K48R Ub₁, unlabeled K48-linked wild type Ub₃ and ¹⁵N labeled D77 Ub₁. The unlabeled Ub₃ can be easily synthesized by using only unlabeled wild type Ub₁ in chain synthesis *in vitro*. The products of that will be Ub₂, Ub₃, Ub₄, and longer. They can be separated by gel filtration column chromatography. The results in **Fig 8.1** show that the most proximal of Ub₅ could form the inter-domain interface with another ubiquitin in Ub₅ but the interacting partner is still unknown.

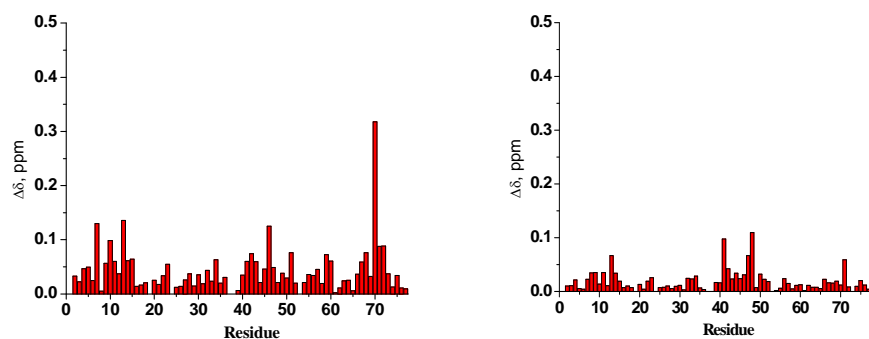


Fig 8.1 The CSPs between Ub₁ and Ub₅ is obtained at pH 6.8 with 20 mM sodium phosphate buffer. In this Ub₅ construct, all linkages are K48-linked. Only the most proximal domain of Ub₅ is ¹⁵N-labeled and contains only a D77 mutation. The most distal domain contains only a K48R mutation. **(A)** is the CSPs between Ub₁ and most proximal domain of Ub₅. **(B)** is the CSPs between the proximal domain of Ub₂ and the most proximal domain of Ub₅

8.2 Elucidating the OTU1 binding surface on Ub₂

Otubain 1 is a cysteine deubiquitinating enzyme (DUB) and is highly linkage-specific for K48-linked polyUb with no activity detectable for K6, K11 and K29-linked polyUb. The cleavage is not limited to either end of a polyubiquitin chain. Both free and substrate-ligated polyUb can be degraded into Ub₁. I used unlabeled Otu1 and ¹⁵N labeled K48-linked Ub₂ to map the Otu1 binding surface on Ub₂. The Otu1 used in NMR titration studies was inactive to avoid cleavage during titration by mutating the active site cysteine. The Otu1 variant was provided by Prof. Wolberger's lab. This study was published in 2009, *JMB*, 386(4): 1011-1023. [3]

Otu1 binds the distal and proximal domains of Ub₂ simultaneously via canonical hydrophobic patches on both ubiquitin domains. The titration results indicated the binding between Otu1 and ubiquitin was in the slow exchange regime because many peaks attenuated during the titration. The results are shown in **Fig 8.2**.

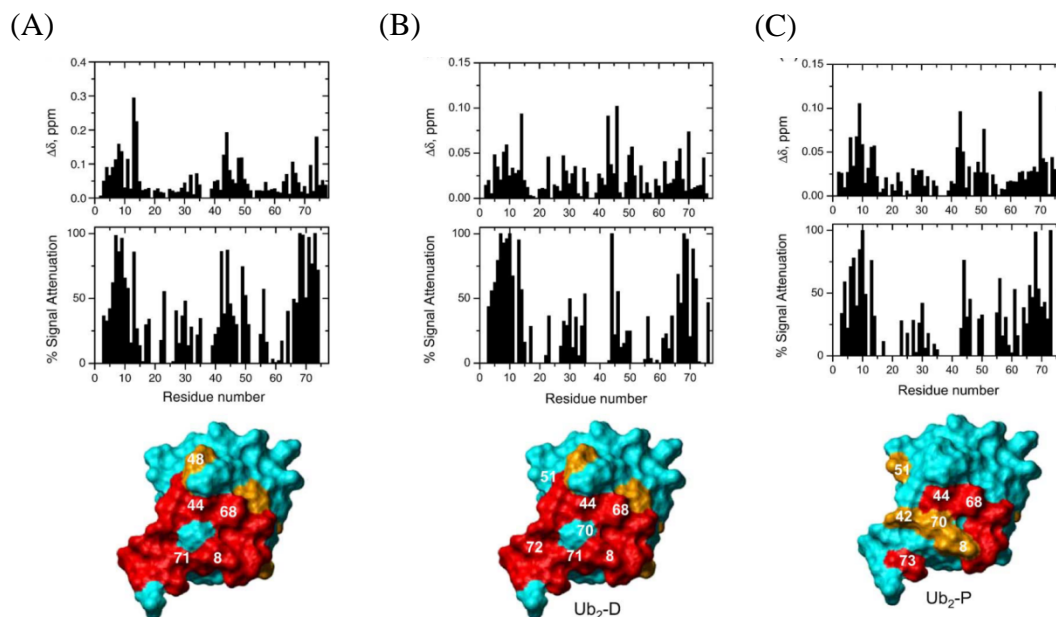


Fig 8.2 NMR CSP maps of the human Otu1 binding interface on the two domains in K48-linked Ub₂. (A) Ub₁ (B) distal domain of K48-linked Ub₂; and (C) proximal domain of K48-linked Ub₂. The CSP and signal attenuations at the endpoint of titration shows in upper panels and the middle panels show respectively. The lower panels show the cartoon representations of the binding surfaces on ubiquitin. The residues colored in orange have a $\Delta\delta_{\text{NH}} > 0.05$ ppm and the residues colored in red show more than 60% attenuation. The figures are from published paper [3].

Chapter 9: Summary of my studies and future directions

I studied the open conformation of K48-linked ubiquitin chain recognition by the UBA2 of hHR23a which is a K48-specific receptor at acid pH. I found that the linkage specific feature and sandwich like binding mode are preserved in the open conformation. One of the main difficulties in this study was to overcome the instability of high concentration of UBA2 at acidic pH. My solution to it may help other research with similar problems.

I also found that the driving forces controlling the equilibrium between the open and closed conformations of K48-linked Ub₂ are mainly electrostatic repulsions and hydrophobic interactions. The protonation state of H68's side chain is crucial to

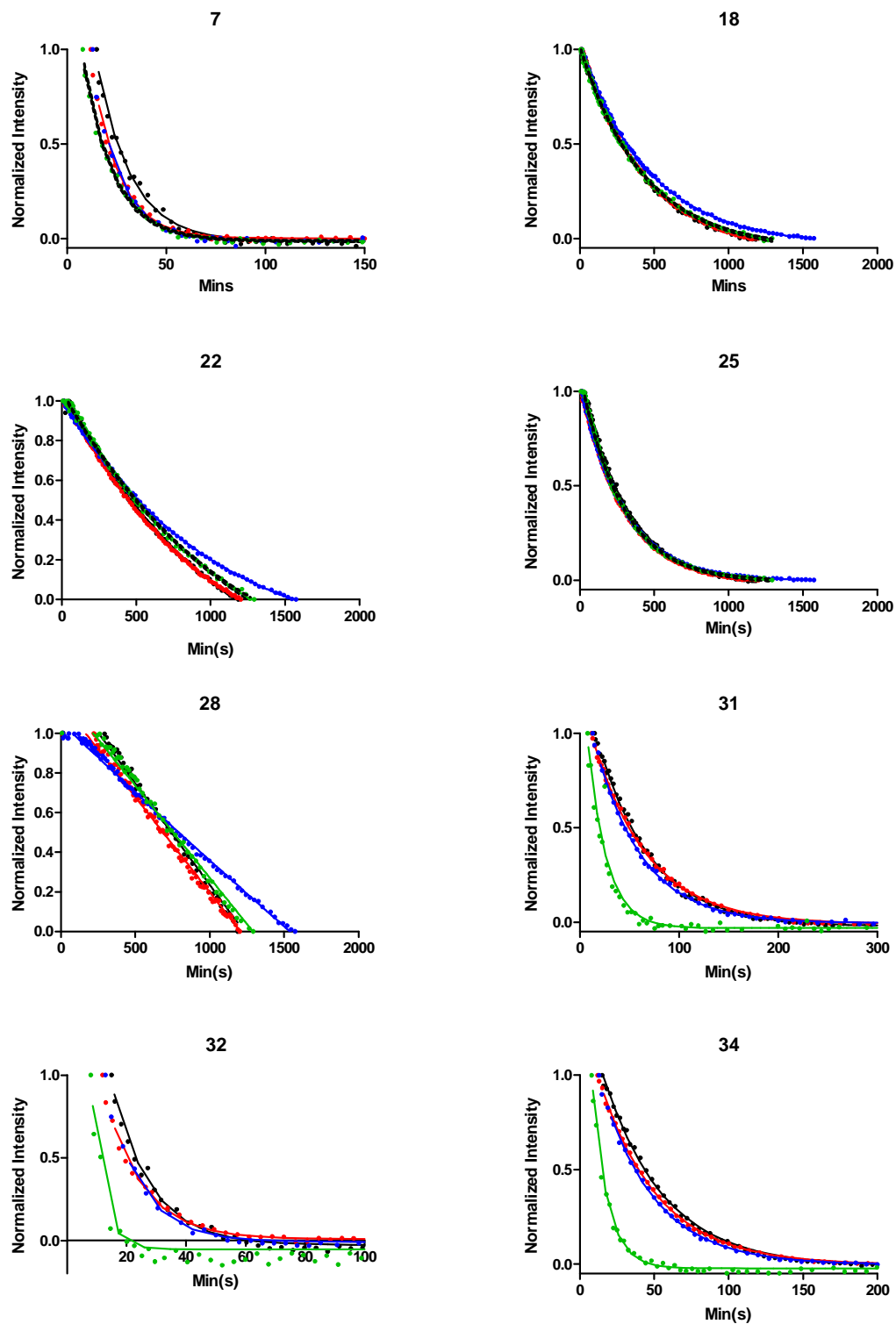
control the open and closed conformation exchange. This is the first time that H68 is found to play an important role in ubiquitin conformation exchange. H68V double mutant of K48-linked Ub₂ revealed that the bulk charge field repulsion between two domains do play a role in opening the closed conformation of Ub₂. H68Y and H68F double mutant of K48-linked Ub₂ shows that the K48-linked Ub₂ can remain adopting closed conformation at acidic pH condition if H68 is replaced by tyrosine or phenylalanine. The fact that H68Y double mutant binds UBA2 at acidic pH like wild type diubiquitin indicates that H68Y mutation does not disrupt the Ub₂ recognition of UBA2. Unlike previous attempts to lock Ub₂ in closed state at acidic pH by using linker[87] or without linker[88] to make cyclic Ub₂, I made this possible by alleviating electrostatic repulsion. This mutant can be used as a tool to study if the disassembly of K48-linked Ub₂ by K48-specific DUBs (de ubiquitinating enzymes) is affected by the interactions between the two ubiquitin domains in Ub₂. Overall these results highlight the complexity of intermolecular interactions that control the conformational equilibrium in a polyubiquitin chain and are likely responsible for the ability of these chains to act as versatile cellular signals.

The half H68Y mutant of K48-linked Ub₂ at high salt allowed me to capture the pre-open state of K48-linked Ub₂. This pre-open state structure provides the clue to understand the opening the closed conformation. This finding suggests that the opening of closed conformation is through twisting instead of pulling away.

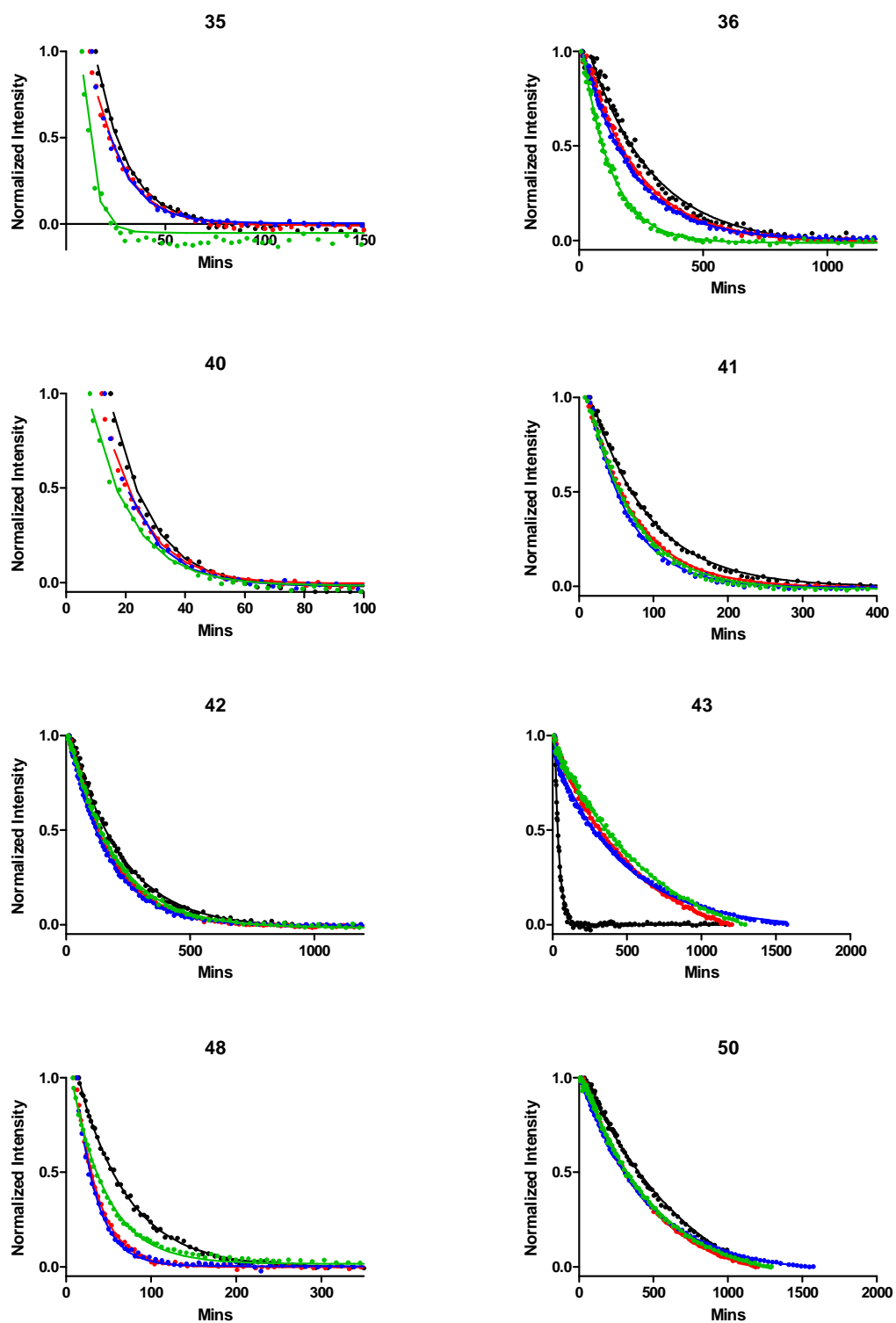
In H/D exchange experiment on diubiquitin, the proximal ubiquitin shows no major difference in stability from distal ubiquitin. The reason may be that the ubiquitin is a small and very stable protein. I think if one can try to use a bigger

protein such as UBCH5b or use less stable protein such as ubiquitin with destabilizing core mutations such as I13S, I30S, L43A, L67S, or L69S ubiquitin variants. The ability to destabilize substrate may be able to be detected.

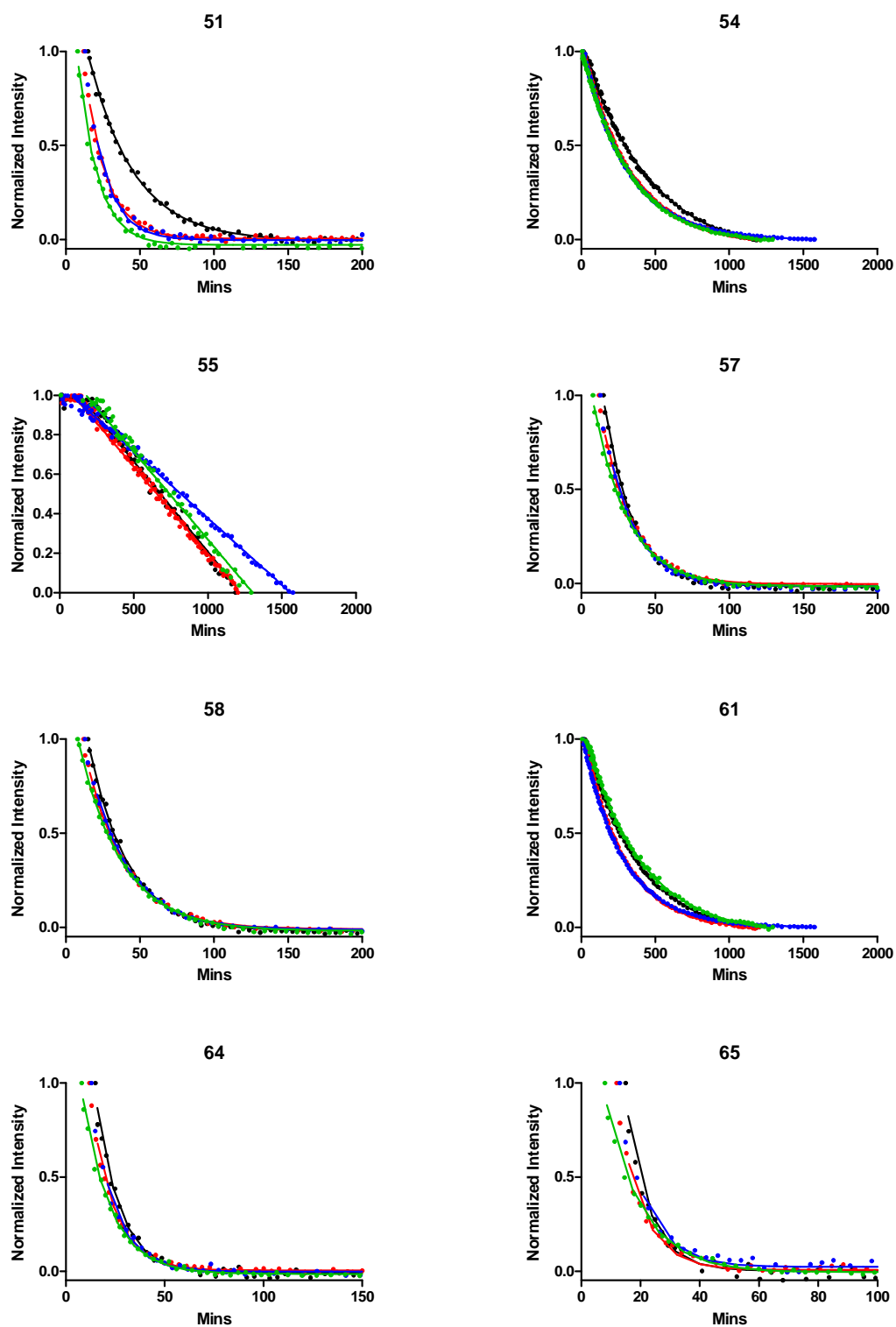
Appendix



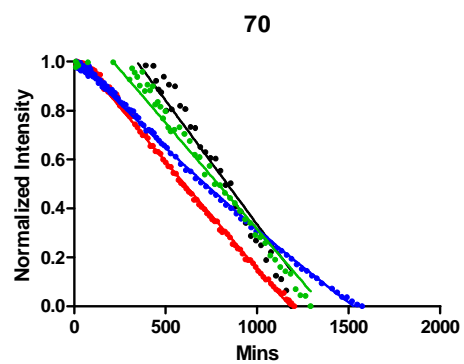
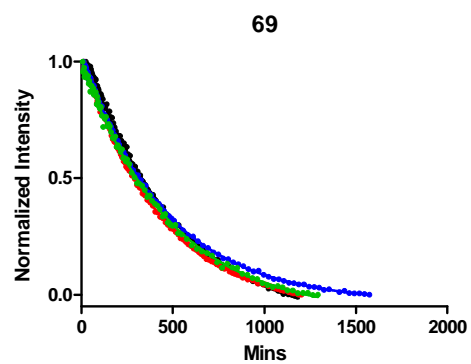
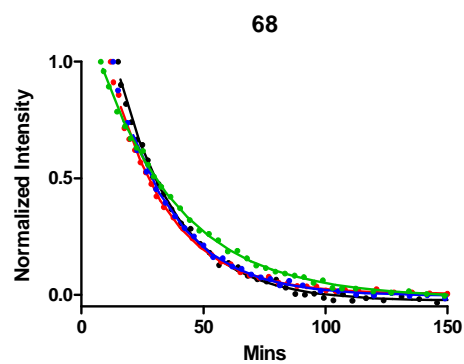
The full results of H-D exchange experiments. The curves colored in black or green represent the data from proximal and distal domain of Ub₂ respectively. The curves colored in red or blue represent the data of Ub₁ in two separated experiments to ensure the reliability of H-D exchange experiment. Residue numbers are indicated on top of each plot.



The full results of H-D exchange experiments. The curves colored in black or green represent the data from proximal and distal domain of Ub₂ respectively. The curves colored in red or blue represent the data of Ub₁ in two separated experiments to ensure the reliability of H-D exchange experiment. Residue numbers are indicated on top of each plot.



The full results of H-D exchange experiments. The curves colored in black or green represent the data from proximal and distal domain of Ub₂ respectively. The curves colored in red or blue represent the data of Ub₁ in two separated experiments to ensure the reliability of H-D exchange experiment. Residue numbers are indicated on top of each plot.



The full results of H-D exchange experiments. The curves colored in black or green represent the data from proximal and distal domain of Ub₂ respectively. The curves colored in red or blue represent the data of Ub₁ in two separated experiments to ensure the reliability of H-D exchange experiment. Residue numbers are indicated on top of each plot.

References

1. Varadan, R., et al., *Structural properties of polyubiquitin chains in solution*. J Mol Biol, 2002. **324**(4): p. 637-47.
2. Weissman, A.M., N. Shabek, and A. Ciechanover, *The predator becomes the prey: regulating the ubiquitin system by ubiquitylation and degradation*. Nat Rev Mol Cell Biol, 2011. **12**(9): p. 605-20.
3. Wang, T., et al., *Evidence for bidentate substrate binding as the basis for the K48 linkage specificity of otubain 1*. J Mol Biol, 2009. **386**(4): p. 1011-23.
4. Lai, M.Y., et al., *Structural and biochemical studies of the open state of Lys48-linked diubiquitin*. Biochim Biophys Acta, 2012.
5. Pickart, C.M. and M.J. Eddins, *Ubiquitin: structures, functions, mechanisms*. Biochim Biophys Acta, 2004. **1695**(1-3): p. 55-72.
6. Varadan, R., et al., *Structural determinants for selective recognition of a Lys48-linked polyubiquitin chain by a UBA domain*. Mol Cell, 2005. **18**(6): p. 687-98.
7. Schoenheimer, R., *The Dynamic State of Body Constituents*. Harvard University Press , Cambridge, MA., 1942: p. 78 PP.
8. Ciechanover, A., Hod, Y., and Hershko, A., *A heat-stable polypeptide component of an ATP-dependent proteolytic system from reticulocytes*. Biochem. Biophys. Res. Commun, 1978. **81**: p. 1100-1105.
9. Hershko, A., et al., *Proposed role of ATP in protein breakdown: conjugation of protein with multiple chains of the polypeptide of ATP-dependent proteolysis*. Proc Natl Acad Sci U S A, 1980. **77**(4): p. 1783-6.

10. Ciechanover, A., et al., *ATP-dependent conjugation of reticulocyte proteins with the polypeptide required for protein degradation*. Proc Natl Acad Sci U S A, 1980. **77**(3): p. 1365-8.
11. van Wijk, S.J. and H.T. Timmers, *The family of ubiquitin-conjugating enzymes (E2s): deciding between life and death of proteins*. FASEB J, 2010. **24**(4): p. 981-93.
12. Ye, Y. and M. Rape, *Building ubiquitin chains: E2 enzymes at work*. Nat Rev Mol Cell Biol, 2009. **10**(11): p. 755-64.
13. Naujokat, C. and T. Saric, *Concise review: role and function of the ubiquitin-proteasome system in mammalian stem and progenitor cells*. Stem Cells, 2007. **25**(10): p. 2408-18.
14. Pickart, C.M., *Mechanisms underlying ubiquitination*. Annu Rev Biochem, 2001. **70**: p. 503-33.
15. Nandi, D., et al., *The ubiquitin-proteasome system*. J Biosci, 2006. **31**(1): p. 137-55.
16. Welchman, R.L., C. Gordon, and R.J. Mayer, *Ubiquitin and ubiquitin-like proteins as multifunctional signals*. Nat Rev Mol Cell Biol, 2005. **6**(8): p. 599-609.
17. Baek, K.H., *Conjugation and deconjugation of ubiquitin regulating the destiny of proteins*. Exp Mol Med, 2003. **35**(1): p. 1-7.
18. Hershko, A., et al., *Components of ubiquitin-protein ligase system. Resolution, affinity purification, and role in protein breakdown*. J Biol Chem, 1983. **258**(13): p. 8206-14.

19. Kirkin, V. and I. Dikic, *Ubiquitin networks in cancer*. *Curr Opin Genet Dev*, 2011. **21**(1): p. 21-8.
20. Behrends, C. and J.W. Harper, *Constructing and decoding unconventional ubiquitin chains*. *Nat Struct Mol Biol*, 2011. **18**(5): p. 520-8.
21. Saeki, Y., et al., *Lysine 63-linked polyubiquitin chain may serve as a targeting signal for the 26S proteasome*. *Embo J*, 2009. **28**(4): p. 359-71.
22. Ramaekers, C.H. and B.G. Wouters, *Regulatory functions of ubiquitin in diverse DNA damage responses*. *Curr Mol Med*, 2011. **11**(2): p. 152-69.
23. Ramadan, K. and M. Meerang, *Degradation-linked ubiquitin signal and proteasome are integral components of DNA double strand break repair: New perspectives for anti-cancer therapy*. *FEBS Lett*, 2011. **585**(18): p. 2868-75.
24. Al-Hakim, A., et al., *The ubiquitous role of ubiquitin in the DNA damage response*. *DNA Repair (Amst)*, 2010. **9**(12): p. 1229-40.
25. Vlachostergios, P.J., et al., *The ubiquitin-proteasome system in cancer, a major player in DNA repair. Part I: post-translational regulation*. *J Cell Mol Med*, 2009. **13**(9B): p. 3006-18.
26. Daulny, A. and W.P. Tansey, *Damage control: DNA repair, transcription, and the ubiquitin-proteasome system*. *DNA Repair (Amst)*, 2009. **8**(4): p. 444-8.
27. Sugasawa, K., *UV-induced ubiquitylation of XPC complex, the UV-DDB-ubiquitin ligase complex, and DNA repair*. *J Mol Histol*, 2006. **37**(5-7): p. 189-202.

28. Goldberg, A.L., et al., *The importance of the proteasome and subsequent proteolytic steps in the generation of antigenic peptides*. Mol Immunol, 2002. **39**(3-4): p. 147-64.
29. Kisselev, A.F., et al., *The sizes of peptides generated from protein by mammalian 26 and 20 S proteasomes. Implications for understanding the degradative mechanism and antigen presentation*. J Biol Chem, 1999. **274**(6): p. 3363-71.
30. Groll, M., et al., *Structure of 20S proteasome from yeast at 2.4 Å resolution*. Nature, 1997. **386**(6624): p. 463-71.
31. Forster, A., et al., *The 1.9 Å structure of a proteasome-11S activator complex and implications for proteasome-PAN/PA700 interactions*. Mol Cell, 2005. **18**(5): p. 589-99.
32. Smith, D.M., et al., *Docking of the proteasomal ATPases' carboxyl termini in the 20S proteasome's alpha ring opens the gate for substrate entry*. Mol Cell, 2007. **27**(5): p. 731-44.
33. Rabl, J., et al., *Mechanism of gate opening in the 20S proteasome by the proteasomal ATPases*. Mol Cell, 2008. **30**(3): p. 360-8.
34. Walz, J., et al., *26S proteasome structure revealed by three-dimensional electron microscopy*. J Struct Biol, 1998. **121**(1): p. 19-29.
35. Glickman, M.H., et al., *A subcomplex of the proteasome regulatory particle required for ubiquitin-conjugate degradation and related to the COP9-signalosome and eIF3*. Cell, 1998. **94**(5): p. 615-23.

36. Schreiner, P., et al., *Ubiquitin docking at the proteasome through a novel pleckstrin-homology domain interaction*. Nature, 2008. **453**(7194): p. 548-52.
37. Husnjak, K., et al., *Proteasome subunit Rpn13 is a novel ubiquitin receptor*. Nature, 2008. **453**(7194): p. 481-8.
38. Mayor, T., et al., *Quantitative profiling of ubiquitylated proteins reveals proteasome substrates and the substrate repertoire influenced by the Rpn10 receptor pathway*. Mol Cell Proteomics, 2007. **6**(11): p. 1885-95.
39. Verma, R., et al., *Multiubiquitin chain receptors define a layer of substrate selectivity in the ubiquitin-proteasome system*. Cell, 2004. **118**(1): p. 99-110.
40. Elsasser, S., et al., *Rad23 and Rpn10 serve as alternative ubiquitin receptors for the proteasome*. J Biol Chem, 2004. **279**(26): p. 26817-22.
41. Elsasser, S., et al., *Proteasome subunit Rpn1 binds ubiquitin-like protein domains*. Nat Cell Biol, 2002. **4**(9): p. 725-30.
42. Fu, H., et al., *Multiubiquitin chain binding and protein degradation are mediated by distinct domains within the 26 S proteasome subunit Mcb1*. J Biol Chem, 1998. **273**(4): p. 1970-81.
43. van Nocker, S., et al., *The multiubiquitin-chain-binding protein Mcb1 is a component of the 26S proteasome in Saccharomyces cerevisiae and plays a nonessential, substrate-specific role in protein turnover*. Mol Cell Biol, 1996. **16**(11): p. 6020-8.
44. Deveraux, Q., et al., *A 26 S protease subunit that binds ubiquitin conjugates*. J Biol Chem, 1994. **269**(10): p. 7059-61.

45. Groll, M., et al., *A gated channel into the proteasome core particle*. Nat Struct Biol, 2000. **7**(11): p. 1062-7.
46. Whitby, F.G., et al., *Structural basis for the activation of 20S proteasomes by 11S regulators*. Nature, 2000. **408**(6808): p. 115-20.
47. Kohler, A., et al., *The axial channel of the proteasome core particle is gated by the Rpt2 ATPase and controls both substrate entry and product release*. Mol Cell, 2001. **7**(6): p. 1143-52.
48. Smith, D.M., et al., *ATP binding to PAN or the 26S ATPases causes association with the 20S proteasome, gate opening, and translocation of unfolded proteins*. Mol Cell, 2005. **20**(5): p. 687-98.
49. Gallery, M., et al., *The JAMM motif of human deubiquitinase Pohl1 is essential for cell viability*. Mol Cancer Ther, 2007. **6**(1): p. 262-8.
50. Maytal-Kivity, V., et al., *MPN+, a putative catalytic motif found in a subset of MPN domain proteins from eukaryotes and prokaryotes, is critical for Rpn11 function*. BMC Biochem, 2002. **3**: p. 28.
51. Verma, R., et al., *Role of Rpn11 metalloprotease in deubiquitination and degradation by the 26S proteasome*. Science, 2002. **298**(5593): p. 611-5.
52. Yao, T. and R.E. Cohen, *A cryptic protease couples deubiquitination and degradation by the proteasome*. Nature, 2002. **419**(6905): p. 403-7.
53. Finley, D., *Recognition and processing of ubiquitin-protein conjugates by the proteasome*. Annu Rev Biochem, 2009. **78**: p. 477-513.
54. Hershko, A. and A. Ciechanover, *The ubiquitin system*. Annu Rev Biochem, 1998. **67**: p. 425-79.

55. Raasi, S. and D.H. Wolf, *Ubiquitin receptors and ERAD: a network of pathways to the proteasome*. Semin Cell Dev Biol, 2007. **18**(6): p. 780-91.
56. Bays, N.W., et al., *HRD4/NPL4 is required for the proteasomal processing of ubiquitinated ER proteins*. Mol Biol Cell, 2001. **12**(12): p. 4114-28.
57. Muratani, M. and W.P. Tansey, *How the ubiquitin-proteasome system controls transcription*. Nat Rev Mol Cell Biol, 2003. **4**(3): p. 192-201.
58. Matunis, M.J., *On the road to repair: PCNA encounters SUMO and ubiquitin modifications*. Mol Cell, 2002. **10**(3): p. 441-2.
59. Aguilar, R.C. and B. Wendland, *Ubiquitin: not just for proteasomes anymore*. Curr Opin Cell Biol, 2003. **15**(2): p. 184-90.
60. Willis, M.S., et al., *Sent to destroy: the ubiquitin proteasome system regulates cell signaling and protein quality control in cardiovascular development and disease*. Circ Res, 2010. **106**(3): p. 463-78.
61. Hofmann, K., *Ubiquitin-binding domains and their role in the DNA damage response*. DNA Repair (Amst), 2009. **8**(4): p. 544-56.
62. O'Connell, B.C. and J.W. Harper, *Ubiquitin proteasome system (UPS): what can chromatin do for you?* Curr Opin Cell Biol, 2007. **19**(2): p. 206-14.
63. Osley, M.A., *H2B ubiquitylation: the end is in sight*. Biochim Biophys Acta, 2004. **1677**(1-3): p. 74-8.
64. Vijay-Kumar, S., C.E. Bugg, and W.J. Cook, *Structure of ubiquitin refined at 1.8 Å resolution*. J Mol Biol, 1987. **194**(3): p. 531-44.
65. Sloper-Mould, K.E., et al., *Distinct functional surface regions on ubiquitin*. J Biol Chem, 2001. **276**(32): p. 30483-9.

66. Sims, J.J. and R.E. Cohen, *Linkage-specific avidity defines the lysine 63-linked polyubiquitin-binding preference of rap80*. Mol Cell, 2009. **33**(6): p. 775-83.
67. Wilkins, M.R., et al., *Protein identification and analysis tools in the ExPASy server*. Methods Mol Biol, 1999. **112**: p. 531-52.
68. Pickart, C.M. and S. Raasi, *Controlled synthesis of polyubiquitin chains*. Methods Enzymol, 2005. **399**: p. 21-36.
69. Varadan, R., et al., *Solution conformation of Lys63-linked di-ubiquitin chain provides clues to functional diversity of polyubiquitin signaling*. J Biol Chem, 2004. **279**: p. 7055-7063.
70. Dominguez, C., R. Boelens, and A.M. Bonvin, *HADDOCK: a protein-protein docking approach based on biochemical or biophysical information*. J Am Chem Soc, 2003. **125**(7): p. 1731-7.
71. Hosszu, L.L., et al., *The H187R mutation of the human prion protein induces conversion of recombinant prion protein to the PrP(Sc)-like form*. Biochemistry, 2010. **49**(40): p. 8729-38.
72. Sugasawa, K., et al., *Two human homologs of Rad23 are functionally interchangeable in complex formation and stimulation of XPC repair activity*. Mol Cell Biol, 1997. **17**(12): p. 6924-31.
73. Raasi, S. and C.M. Pickart, *Rad23 ubiquitin-associated domains (UBA) inhibit 26 S proteasome-catalyzed proteolysis by sequestering lysine 48-linked polyubiquitin chains*. J Biol Chem, 2003. **278**(11): p. 8951-9.

74. Wang, Q., et al., *Ubiquitin recognition by the DNA repair protein hHR23a*. *Biochemistry*, 2003. **42**(46): p. 13529-35.
75. Raasi, S., et al., *Binding of polyubiquitin chains to ubiquitin-associated (UBA) domains of HHR23A*. *J Mol Biol*, 2004. **341**(5): p. 1367-79.
76. Ryu, K.S., et al., *Binding surface mapping of intra and inter domain interactions among hHR23B, ubiquitin and poly ubiquitin binding site 2 of S5a*. *J Biol Chem*, 2003. **278**(38): p. 36621-7.
77. Mueller, T.D., M. Kamionka, and J. Feigon, *Specificity of the interaction between ubiquitin-associated domains and ubiquitin*. *J Biol Chem*, 2004. **279**(12): p. 11926-36.
78. Zhang, D., S. Raasi, and D. Fushman, *Affinity makes the difference: nonselective interaction of the UBA domain of Ubiquilin-1 with monomeric ubiquitin and polyubiquitin chains*. *J Mol Biol*, 2008. **377**(1): p. 162-80.
79. Raasi, S., et al., *Diverse polyubiquitin interaction properties of ubiquitin-associated domains*. *Nat Struct Mol Biol*, 2005. **12**(8): p. 708-14.
80. Cook, W.J., et al., *Structure of a diubiquitin conjugate and a model for interaction with ubiquitin conjugating enzyme (E2)*. *J Biol Chem.*, 1992. **267**: p. 16467-71.
81. Ryabov, Y. and D. Fushman, *Interdomain mobility in di-ubiquitin revealed by NMR*. *Proteins*, 2006. **63**(4): p. 787-96.
82. Beal, R., et al., *Surface hydrophobic residues of multiubiquitin chains essential for proteolytic targeting*. *Proc Natl Acad Sci U S A*, 1996. **93**(2): p. 861-6.

83. Fujiwara, K., et al., *Structure of the ubiquitin-interacting motif of S5a bound to the ubiquitin-like domain of HR23B*. J Biol Chem, 2004. **279**(6): p. 4760-7.
84. Cook, W.J., et al., *Structure of tetraubiquitin shows how multiubiquitin chains can be formed*. J Mol Biol, 1994. **236**(2): p. 601-9.
85. Phillips, C.L., et al., *Structure of a new crystal form of tetraubiquitin*. Acta Crystallogr D Biol Crystallogr, 2001. **57**(Pt 2): p. 341-4.
86. Eddins, M.J., et al., *Crystal structure and solution NMR studies of Lys48-linked tetraubiquitin at neutral pH*. J Mol Biol, 2007. **367**(1): p. 204-11.
87. Dickinson, B.C., R. Varadan, and D. Fushman, *Effects of cyclization on conformational dynamics and binding properties of Lys48-linked di-ubiquitin*. Protein Sci, 2007. **16**(3): p. 369-78.
88. Hirano, T., et al., *Conformational dynamics of wild-type Lys-48-linked diubiquitin in solution*. J Biol Chem, 2011. **286**(43): p. 37496-502.